



Università degli Studi di Cagliari

PHD in Molecular and Translational Medicine

Cycle XXXI

**Metabolic dependencies and alterations of papillary
thyroid carcinoma cell lines**

Scientific Disciplinary Sector

MED-05

PhD Student:

Laura Tronci

Coordinator of the PhD Programme

Prof. Amedeo Columbano

Supervisor

Prof. Luigi Atzori

Final exam. Academic Year 2017 – 2018

Thesis defence: January-February 2019 Session

To my Parents....

*We must have perseverance
and above all confidence in ourselves.*

*We must believe that
we are gifted for something
and that this thing must be attained.*

Marie Skłodowska-Curie

Index

Acknowledgements	6
Abstract	7
List of Figures	9
List of Tables	11
List of Abbreviations	12
I. Introduction	16
<i>Thyroid Cancer</i>	17
<i>Papillary thyroid carcinoma.</i>	17
<input type="checkbox"/> BRAF	19
<input type="checkbox"/> RAS	20
<input type="checkbox"/> RET/PTC	20
<input type="checkbox"/> PAX8/PPARG	21
<input type="checkbox"/> TERT	21
<input type="checkbox"/> TP53	21
<i>Cancer cells metabolism.</i>	23
<input type="checkbox"/> Aerobic Glycolysis	25
<input type="checkbox"/> Tricarboxylic acid (TCA) cycle	26
<input type="checkbox"/> Glutaminolysis	27
<input type="checkbox"/> Pentose phosphate pathways	28
<input type="checkbox"/> Lipid metabolism	29
<input type="checkbox"/> Redox Balance	30
<i>Thyroid cancer metabolism.</i>	33
<i>Cancer stem cells (CSCs)</i>	36
<i>Targeting cancer cells metabolism: Vitamin C anti-tumoral effects</i>	41
<i>Metabolomics</i>	45
<input type="checkbox"/> The metabolomic approach	45
<input type="checkbox"/> Metabolomics in thyroid cancer research	48
II. Aim of the Project	51
III. Materials and methods	54
<i>Cell culture and treatment</i>	55
<i>Sphere formation assay</i>	57
<i>Evaluation of Cytotoxicity</i>	59
<i>Reactive Oxygen Species (ROS) Assay</i>	60

<i>Determination of intracellular aminothiol levels.</i>	61
<i>Protein extraction and quantification</i>	62
<i>Immunoblotting</i>	63
<i>Immunofluorescence</i>	65
<i>Glucose uptake assay.</i>	66
<i>Glucose Addiction Assay.</i>	67
<i>Apoptosis Analysis: Flow Cytometric Analysis with Annexin V/Propidium Iodide staining</i>	68
<i>Sample preparation for metabolomics analysis</i>	69
<i>Ultra high performance liquid chromatography-tandem mass spectrometry analysis.</i>	70
<i>Gas chromatography-mass spectrometry analysis.</i>	73
<i>Nuclear magnetic resonance spectroscopy: ¹H-NMR.</i>	74
<i>Statistical Analysis</i>	76
<input type="checkbox"/> <i>Multivariate statistical analysis</i>	76
<input type="checkbox"/> <i>Univariate statistical analysis</i>	76
IV. Results	78
Part one: Metabolic and redox reprogramming in PTC-derived cell lines	78
<i>Bioenergetic metabolic changes in PTC-derived cell lines.</i>	79
<i>Glucose and lactate exchange across the membrane of PTC-derived cells</i>	83
<i>Redox status in PTC-derived cell lines</i>	89
IV. Results	94
Part two: Metabolomic alterations in CSCs-like in thyrospheres derived from PTC-cell lines	94
<i>Thyrospheres Forming Assay and stemness profile</i>	95
<i>Multivariate statistical analysis of GC-MS metabolomics profile of thyrosphere and adherent cells.</i>	98
<i>Metabolic comparison between B-CPAP adherent cells and thyrospheres</i>	101
<i>Metabolic comparison between TPC-1 adherent and thyrospheres.</i>	103
<i>Metabolic comparison between Nthy-ori3-1 adherent cells and thyrosphere.</i>	104
<i>Metabolomic comparison between B-CPAP, TPC-1 and Nthy-ori3-1 thyrospheres</i>	105
IV. Results	108
Part three: Anti-tumoral effects and metabolic reprogramming Vitamin C-induced	108
<i>Citotoxicity Vitamin C-induced in PTC-derived cell lines.</i>	109
<i>Oxidative stress and aminothiols modulation by vitamin C</i>	111
<i>Metabolic effect induced by Vitamin C treatment in PTC-derived cell lines.</i>	114
<i>Preliminary results: detection of apoptosis or necrosis induced by Vitamin C treatment.</i>	118
V. Discussion	121
<i>Metabolic and redox reprogramming in PTC-derived cell lines.</i>	122

<i>Metabolomic alterations in CSCs-like in thyrospheres derived from PTC-cell lines.</i>	128
<i>Anti-tumoral effects and metabolic reprogramming Vitamin C-induced.</i>	131
VI. Conclusion	135
VII.	Bibliography
138	
Appendix: Publications and Presentations	168

Acknowledgements

I gratefully acknowledge the support and guidance of my supervisor, Prof. Luigi Atzori, for his scientific support, for all the advices, and for teaching me to challenge myself.

I would like to express my gratitude to my teammates, in the Clinical Metabolomic Group, especially Federica and Maria Laura for listening, giving me words of encouragement, for helping me survive all the stress during my Ph.D and for all the fun we have had in the last three years.

I also would like to acknowledge Prof. Roberta Vanni, Dr. Paola Caria, who so generously contributed to the work presented in this thesis, and Dr. Monica Deiana for her scientific support.

My sincere thanks also goes to Prof. Julian Griffin, who provided me the opportunity to join their team in the University of Cambridge as visiting student, and who gave access to the laboratory and research facilities.

Last but not the least, I would like to thank my family: my Mom and Dad, my sister and my little niece, for the continuous support during my studies, for their patience, for their unconditional love and care, no matter my reached goals. Without their precious support it would not be possible become what I am becoming.

Profound gratitude goes also to Adriano, for have been always next to me, sharing positive and negative moments, for his immense support, for always have believed in me, even more than I have believed in myself.

Abstract

Thyroid cancer is the most common endocrine malignancy and among the major types, papillary thyroid carcinoma (PTC) represents 90% of all thyroid carcinomas. Several studies have identified in PTC recurrent somatic genetic alterations in known oncogenes (i.e., *BRAF*, *RAS* and *RET*). Recently, *hTERT* promoter mutations have been observed in approximately 11% of PTC with aggressive behavior, and together with other genetic mutations, like *TP53* mutations, have been associated with aggressive forms of PTC. Cancer cells show profound metabolic alterations and a perturbed redox homeostasis, allowing them to meet the metabolic and biosynthetic needs. Redox state, which, together with altered metabolism, is considered a hallmark of cancer cells, is closely dependent on various metabolic pathways, resulting in a crosstalk between metabolism and redox homeostasis. Currently, cancer research and the evaluation of targetable features, have met a new challenge, due to the heterogeneity of tumor and the different cell populations behaviour within the tumor mass. Indeed, PTCs, as most tumors, are constituted by a subset of cells, cancer stem cells (CSCs), which are crucially involved in tumor progression and recurrence more than the differentiated tumor cells. CSCs exhibit a distinct metabolic phenotype, supporting tumor growth and survival, but how they adapt their metabolism to the cancer process is still unclear, and no data are yet available for PTC. Understanding this metabolic remodeling and dependence is essential to elucidate the fundamental mechanisms of tumorigenesis as well as to find new therapeutic strategies, targeting cancer metabolism. Among all the possible anti-tumoral compounds, high-dose of vitamin C has been showed to exhibit cytotoxic effect in cancer cells, primarily mediated by pro-oxidant and metabolic effects. However, the exact role of vitamin C in the metabolic perturbation and its potential use as a therapy target in cancer treatment and prevention in PTC is still poorly understood and require further studies.

This study aimed to investigate the metabolic alterations and redox status of PTC-derived cell lines in association with the different genetic backgrounds, underlying the metabolic dependencies of PTC differentiated and CSCs cells. Furthermore, vitamin C has been used as anti-tumoral compound, in order to clarify the anti-cancer mechanism and to better understand the metabolic sensitivity of PTC-derived cells.

A targeted and untargeted metabolomic approach has been used to investigate the metabolic profile of PTC-derived cells, while molecular analysis, such as immunoglotting, immunofluorescence, fluorimetric assays have been used to better understand the mechanism beyond the metabolic alterations. This approach has led to the understanding of the metabolic features and their association with redox balance and genotypes in PTC-derived differentiated and stem cells. Furthermore, beside the known oxidative effect of vitamin C, our analyses have elucidated its effect in the alteration of the metabolism, consequently affecting the cancer cell survival. Our data demonstrated that PTC-derived cells, particularly B-CPAP cells, harboring *BRAF*, *TP53* and *hTERT* mutation, displayed the most perturbed metabolism and altered redox homeostasis, as reported by changes in metabolites and carriers involved in energetic pathways, and by changes in antioxidants, ROS and electron carriers levels. According to the fundamental role of metabolic alterations in CSCs, our findings reported variations in metabolic pathways, particularly in glycolytic and TCA cycle metabolites in thyrospheres, containing CSCs, compared to non-cancer stem-like cell and in thyrospheres versus parental cells. Finally, our data highlighted the sensitivity of PTC-derived cells to the vitamin C and its anti-tumoral mechanism by modulating metabolism and redox balance reciprocally.

Taken together, our study demonstrated the pivotal role of the metabolism and redox homostasis regulations in PTC biology, and, consequently their role as promising therapeutic and diagnostic features. Overall, we underlined the interplay among oncogenic, metabolic and redox events in cancer development, progression and survival, pinpointing the need for a better understanding of the metabolic complexity and plasticity in cancer cells.

List of Figures

Figure 1. Relative frequency of the main variants of papillary carcinoma in the United States

Figure 2. Hallmarks of cancer

Figure 3. Models of Carcinogenesis

Figure 4. Metabostemness hypothesis for the tumor heterogeneity and the origin of CSCs.

Figure 5. Scheme of a general cell metabolomics workflow

Figure 6. Multivariate statistical analysis of PTC-derived and control cells

Figure 7. Energetic metabolites in PTC-derived cell lines

Figure 8. Relative glucose uptake and extracellular lactate level

Figure 9. Expression of GLUT-1, MCT-4 in thyroid cells

Figure 10. Glucose starvation assay

Figure 11. Redox control in human thyroid cell lines

Figure 12. Expression of glutamate-cysteine ligase and glutaminase 1

Figure 13. Thyrospheres forming assay

Figure 14. Multivariate statistical analysis of thyrospheres and adherent thyroid cell lines

Figure 15 Metabolomic changes in B-CPAP derived thyrosphere and adherent cells.

Figure 16. Metabolomic changes of TPC1 derived thyrosphere and adherent cells

Figure 17. Metabolomic changes in Nthy-ori3-1 derived thyrosphere and adherent cells

Figure 18. Metabolomic changes between B-CPAP, TPC-1 and Nthy-ori3-1 derived thyrosphere cells

Figure 19. Summary of the metabolic variations and pathways resulting from the comparison between B-CPAP, TPC-1 and Nthy-ori3-1 thyrosphere cells

Figure 20. Effects of vitamin C in cell viability

Figure 21. ROS production vitamin C-induced in thyroid cell lines

Figure 22. Antioxidants ratio modulation vitamin C-induced

Figure 23. Metabolic alterations in glycolysis and TCA cycle vitamin C-induced

Figure 24. Changes in Nicotinamide and NAD⁺ levels vitamin C-induced

Figure 25. Relative glucose uptake after vitamin C treatment

Figure 26. Representative scatterplots of flow cytometric analysis of apoptotic/necrotic cells

Figure 27. Vitamin C metabolic effects

List of Tables

Table 1. Frequency of genetic alterations in commonly mutated genes across the spectrum of PTC

Table 2. Citotoxicity of vitamin C in cancer cells

Table 3. Thyroid cell lines, tissue origins and genetic background

Table 4. Functional parameters and stemness markers of thyrospheres

Table 5. Antibodies List

Table 6. UHPLC/MS-MS detected compound with calculated masses, mass fragments, polarity and column.

Table 7. GC/MS identified metabolites with masses (m/z) and retention time (RT).

Table 8. Statistical analysis results of glucose starvation assay

Table 9. Multivariate stastical analysis parameters

List of Abbreviations

¹H-NMR: Nuclear magnetic resonance

2-NBDG: 2-[N-(7-nitrobenz-2-oxa-1, 3-diazol-4-yl) amino]-2-deoxy-D-glucose

3PG: 3-phosphoglycerate

ATC: anaplastic thyroid carcinoma

bFGF: basic fibroblastic growth factor

BSA: bovine serum albumin

CAFs: cancer associated fibroblasts

CE-MS: capillary electrophoresis-mass spectrometer

CSC: cancer stem cells

CV-PTC: classical variant papillary thyroid carcinoma

DAHP: dihydroxyacetone phosphate

DCF: 2',7'-dichlorofluorescein

DHA: dehydroascorbic acid

DMEM: Dulbecco's Modified Eagle's Medium

DMSO: dimethyl sulfoxide

ECD: electrochemical detector

EGF: epidermal growth factor

EI: electron ionization

EMT: epithelial-mesenchymal transition

ENO- α : enolase α

F6P: fructose-6-phosphate

FAO: fatty acid oxidation

FBS: fetal bovine serum

FH: fumarate dehydrogenase

FNAB: fine needle aspiration biopsy

FT-ICR: Fourier transform ion cyclotron resonance

FTC: follicular thyroid carcinoma

FV-PTC: follicular variant papillary thyroid carcinoma

G6P: glucose-6-phosphate
G6PD: glucose-6-phosphate dehydrogenase
GAP: glyceraldehyde-3-phosphate
GAPDH: glyceraldehyde phosphate dehydrogenase
GCL: glutamate cysteine ligase
GC-MS: gas chromatography-mass spectrometer
GLS1: glutaminase 1
GLS2: glutaminase 2
GLUT1: glucose transporter 1
GPX: glutathione peroxidase
GR: glutathione reductase
GSH: glutathione reduced
GSSG: glutathione oxidized
H₂-DCFDA: 2',7'-dichlorofluorescein diacetate
HIF: hypoxia-inducible factor
HILIC: hydrophilic interaction liquid chromatography
HK1: hexokinase 1
HPLC: high performance liquid chromatography
IC₅₀: half-maximal inhibitory concentration
IDH: isocitrate dehydrogenase
iPC: induced pluripotent stem cells
KEAP1: Kelch-like ECH-associated protein 1
KH II: hexokinase II
LC-MS: liquid chromatography-mass spectrometer
LDH-A: lactate dehydrogenase
MAPK: mitogen activated protein kinase
MCT4: Monocarboxylate transporter 4
ME1: malic enzyme 1
MS: mass spectrometry
MTC: medullary thyroid carcinoma

MTT: ((3-(4,5-dimethylthiazol-2-yl)-2,5-diphenyltetrazolium bromide

NAC: N-acetyl-cysteine

NAD⁺: nicotinamide adeninedinucleotide

NADP⁺:nicotinamide adeninedinucleotide phosphate

NADPH: nicotinamide adenin dinucleatide phosphate

NMR: nuclear magnetic resonance

NNT: normal thyroid tissue

NRF2: nuclear factor (erythroid-derived 2)-like 2

OXPPOS: oxidative phosphorylation

PBS: phosphate buffer saline

PCA: principal component analysis

PDK:pyruvate dehydrogenase kinase

PDTC poorly differentiated thyroid carcinoma

PEP: phosphoenolpyruvate

PFK-1: Phosphofructokinase 1

PFKFB3: 6-phosphofructo-2-kinase/fructose-2,6-biphosphatase 3

PGK-1: Phosphoglycerate Kinase 1

PI: Propidium Iodide

PK-M2: Pyruvate kinase isozymes M2

PLS-DA: partial least square-discriminant analysis

PPP: pentose phosphate pathway

PRXs: peroxiredoxin

PTC: Papillary thyroid carcinoma

ROS: reactive oxygen species

SDH: succinate dehydrogenase

SFM: serum-free medium

SRM: selected reaction monitoring

SVCTs: sodium-ascorbate co-transporters

TBH: tert-Butyl hydriperoxide

TC: thyroid carcinoma

TCA: tricarboxylic acid cycle

TCV-PTC: tall cell variant papillary thyroid carcinoma

TERT: telomerase reverse transcriptase

TFA: trifluoroacetic acid

TOF: time-of-flight

TOMM20: translocase of outer mitochondrial membrane 20

TrX: thioredoxin

TSP: 3,3,3-trimethylsilylpropionate

UHPLC-MS: ultra high performance liquid chromatography-mass spectrometry

VHL: Von Hippel-Lindau

VIP: variable importance in projection list

WT: wild type

α KG: alpha ketoglutaric acid

I. Introduction

Thyroid Cancer

Thyroid cancer (TC) is the most frequent endocrine cancer, with an increasing incidence worldwide in the last decades (El-Naggar et al. 2017). TC originates in the thyroid gland from two different cell types: follicular cells, which are epithelial and the majority of thyroid cells, and parafollicular cells (Colin et al. 2013). Those carcinomas derived from epithelial cells, can be classified in four major types, based on cellular morphology and histological architecture: papillary (PTC), follicular (FTC) poorly differentiated (PDTC), and anaplastic (ATC). On the contrary, carcinomas originating from parafollicular cells are medullary thyroid carcinomas (MTC) (Ciavardelli et al. 2017).

Papillary thyroid carcinoma.

PTC is the most common type of TC, representing up to 84% of cases (Davies et al. 2015) with 5-year survival rate of 98% (Lubitz and Sosa, 2016). The etiology of PTC has been related to environmental, genetic and hormonal factors (Hemminiki and Li, 2003). From a clinical point of view, patients with PTC usually show cold nodule on radioactive iodine scan and, some of them, might also present lymphadenopathy. In the PTC diagnosis, the most common safe and cost-effective method for examining thyroid nodules is the fine needle aspiration biopsy (FNAB), which provides a definitive preoperative diagnosis of malignanc (Renshaw 2001). PTCs appear quite variable, from a solid and grey-white morphology to the cystic form, (Llyoid 2011) and heterogeneous. It can be classified in several histological variants: classic variant (CV-PTC), follicular variant (FV-PTC) and the tall cell variant (TCV-PTC) (**Figure 1**) (Giordano et al. 2018).

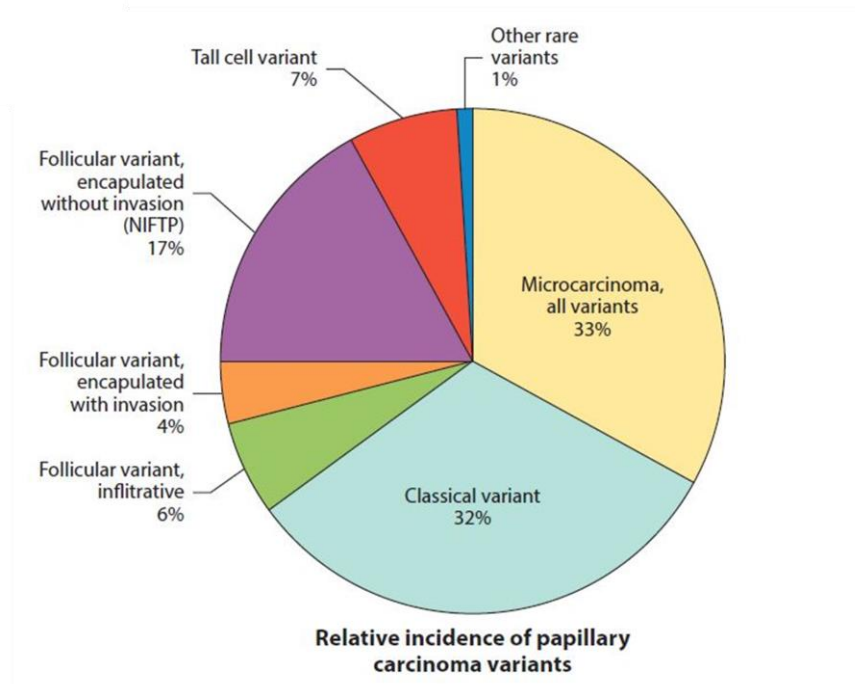


Figure 1. Relative frequency of the main variants of papillary carcinoma in the United States. (Giordano et al. 2018)

Furthermore, PTCs also show a distinctive set of molecular alterations (Khanafshar and Lloyd 2011), with several genetic features, which have been identified as fundamental in the tumorigenesis of various thyroid tumours (**Table 1**), and together with the FNAB, represent helpful diagnostic tools.

Table 1. Frequency of genetic alterations in commonly mutated genes across the spectrum of PTC

Tumor type	<i>BRAF</i> ^{V600E}	<i>RAS</i>	<i>RET/PTC</i>	<i>PAX8/PPARG</i>	<i>hTERT</i>	<i>TP53</i>
PTC, all	40-65%	10-30%	10-20%	<5%	8-27%	<1%
PTC, CV	50-75%	<10%	20-40%	<1%	<10%	<1%
PTC, FV	10-20%	30-50%	<5%	<10%	<10%	<1%
PTC, TCV	>95%	<1%	<1%	<1%	10-30%	<1%

(Giordano 2018)

These genetic alterations have been found in particular signaling pathways, such as the MAPK pathway (mitogen-activated protein kinase pathway) and the PI3K–AKT pathway (Xing 2013). Particularly, PTCs are characterized by recurrent mutations in genes involved in the MAPK pathway (i.e., RET rearrangement or BRAF and RAS activating point mutations) (Nikiforov and Nikiforova 2011), in an exclusive manner, suggesting that the activation of the MAPK pathway is essential for the neoplastic transformation (Kimura 2003). The relationship between environment and genetic factors, results in a remarkable heterogeneity and variability in the molecular background of all PTCs variants (Tallini et al. 2017). Tumor progression and aggressivity depend on additional changes implicated in cell adhesion, cell cycle, cell survival and other cellular functions. These complementary events, such as TP53 mutations and hTERT mutations, characterizes on hallmark of aggressive clinical features and poor outcome (Quiros et al. 2005; Costa et al. 2008). Common mutated genes in PTC are:

- **BRAF**

BRAF is a proto-oncogene encoding a serine-threonine protein kinase and it is the most potent activator of the MAPK kinase pathway. *BRAF* has been found mutated in several human cancer types, as colorectal, lung, melanoma, thyroid and others (Davies et al. 2002; Weir et al. 2004). In thyroid carcinoma BRAF mutation is characterized by a constitutively kinase activation of the protein due to the mutation on the serine/threonine kinase domain (V600E) (Xing 2010). *BRAF*^{V600E} mutation occurs in 40–65% of PTC (Xing 2005) constituting *BRAF*^{V600E}-like PTC with true papillary architecture. It has been previously elucidated the near-perfect mutual exclusivity between *BRAF*- and *RAS*-mutated tumors. This mutually exclusive relationship allows to define *BRAF*^{V600E}-*RAS* gene expression score, which provide a description between the biological properties of *RAS*-mutated tumors (*RAS*-

like) and *BRAF*^{V600E}-like tumors. Interestingly, *BRAF*^{V600E}-like PTCs show also *RAS*- gene expression patterns (Giordano 2018)

- **RAS**

The *RAS* genes family encodes proteins involved in the regulation of several cytoplasmic pathways (Papke and Der 2017): GTPase, which normally cycle between an active state (binding GTP) and an inactive state (binding GDP) (Bos et al. 2007). *RAS* is a common proto-oncogene, which is mutated in about one-third of all human cancers, especially pancreatic, lung and colorectal adenocarcinomas (Pylayeva-Gupta et al. 2011). Its mutation occurs in 10% to 30% of PTC, with follicular variant histology representing *RAS*-like nodules (Giordano 2016). *RAS* point mutations are highly presented in different types of TC, such as FTA, FTC and FVTPC (Giordano et al. 2005; Di Cristofaro et al. 2006) and usually favors the formation of persistently GTP-bound *RAS*, which is constitutively activated.

- **RET/PTC**

RET/PTC rearrangement is a chimeric oncogene encoding a protein containing a constitutively activated *RET* tyrosine kinase. *RET* is a transmembrane receptor that binds ligands in conjunction with coreceptors, to form a dimer (*RET* dimer-ligand-coreceptor) that regulates signaling pathways such as MAPK and PI3K-PTEN-AKT pathways (Acquaviva et al.2018). Among all the possible rearrangements of *RET/PTC*, the most common are *RET/PTC1*, *RET/PTC2*, and *RET/PTC3* and they occur in the 10-20% of cases (Catalano et al. 2010). The resultant chimeric form, characterized by the C-terminal and kinase domains of *RET* gene rearranged with N-terminal region from the partner gene, is a constitutively active kinase (Grieco et al. 1990).

- **PAX8/PPARG**

PPARG is a nuclear receptor protein and it binds with cofactors to activates the transcription of target genes. It has a central role in the regulation of adipogenesis, lipid metabolism and insulin sensitivity (Acquaviva et al.2018). In FTC, and in a small subset of PTCs, PPARG has been reported rearranged with inframe fusion of coding sequence of PAX8. The result is a PAX8 constitutively expressed which drives the expression of the chimeric oncogenic PAX8-PPARG protein (Giordano 2018).

- **TERT**

Recently, telomerase reverse transcriptase promoter mutations (hTERT) have been observed in 8–27 % of PTC with aggressive behavior, associated with worse outcome and disease-specific mortality (Vinagre et al. 2013; Landa et al. 2013; Liu et al. 2013). Telomerase reverse transcriptase (TERT) is a catalytic subunit of the enzyme involved in the maintenance of telomere length, and it plays a central role in cellular immortality and tumorigenesis. Cancer cells show a constitutive active TERT, which results in telomeres maintenance and unlimited cellular proliferation (Skvortzov et al. 2009). Indeed the promoter mutations is the most common noncoding mutation in cancer (Fredriksson et al. 2014), including melanoma, glioma, urothelial carcinoma and hepatocellular carcinoma (Vinagre et al. 2013). In PTC TERT mutations often co-occurs with both *BRAF*^{V600E} and *RAS* mutations, and with p53 mutations, leading to aggressive forms of the tumor (Asa 2017).

- **TP53**

TP53 is a tumor suppressor activated by DNA damaging agents and, in thyroid cancer cells, its activity is inhibited by three mechanisms: inhibition of transcriptional activity, protein stability and signaling (Manzella et al. 2017). p53 mutations occur in 50-80% of

undifferentiated thyroid cancers (Quiros et al. 2005), but several studies highlighted its fundamental role in the early stage of thyroid cancerogenesis. Indeed, p53 mutations were found in up to 40% of PTC (Cancer Genome Atlas Research Network 2014).

Cancer cells metabolism.

Cancer is a disease characterized by highly proliferating cells with common biological features, in which unrestrained proliferation is one of the most fundamental (Hanahan and Wieberg 2011). Several evidences indicate that cancer cells acquire genetic alterations that allow them to proliferate in extreme environments and they undergo a metabolic reprogramming to meet the increased demands of macromolecules and energy in order to sustain the proliferation (Locasale and Cantley 2010). Metabolism has a central role for the cellular homeostasis and survival and, for this reason; there are multiple regulating mechanisms, which converge to satisfy needs of high rate dividing cells, such as cancer cells. (Cairns et al. 2011). The first discovery about cancer's altered metabolism was conducted by Otto Warburg, over the first half of the twentieth century (Warburg 1956). Normal tissues metabolize glucose to pyruvate through glycolysis, in presence of oxygen, and then completely oxidize the generated pyruvate in the mitochondria through oxidative phosphorylation. Cancer cells redirect glycolytic pyruvate to fermentation, in order to produce lactate, away from mitochondria, which results in a shift from ATP generation through oxidative phosphorylation to ATP generation through glycolysis, even under normal oxygen concentrations (Vander Heiden et al. 2009). After the Warburg's discovery, altered metabolism remained a by-product and a consequence of the oncogene-induced reprogramming (Sciacovelli et al. 2014). The association between metabolism and cancer was then reported by the discovery that mutations of metabolic enzymes, such as succinate dehydrogenase (SDH) (Baysal et al. 2000) and fumarate hydratase (FH) (Tomlinson et al. 2002), were responsible for some hereditary forms of cancer, proving that altered metabolism could be the cause of the cancer transformation and development (Gottlieb and Tomlinson, 2005). Since that, accumulating evidence indicates that several oncogenes and tumor suppressors are implicated in the regulation of cancer metabolism (Locasale et al. 2009;

Sciacovelli et al. 2014). It is now clear that cancer-altered metabolism is considered to be a “hallmarks of cancer”, triggered by the activation of several oncogenic pathways (**Figure 2**) (Ward and Thompson 2012). Particularly, the tumorigenesis-associated metabolic alterations affect the metabolite flux across the cancer cells, conferring an advantage in the uptake of necessary nutrients, which can be preferentially conveyed into metabolic pathways that contribute to the cancer development (Pavlova and Thompson 2016). The main metabolic cancer features can be summarized into six points: deregulated uptake of both glucose and amino acids, aerobic glycolysis, increased nutrient acquisition, use of glycolysis/Krebs cycle intermediates for biosynthesis and NADPH production (Pavlova and Thompson 2016).

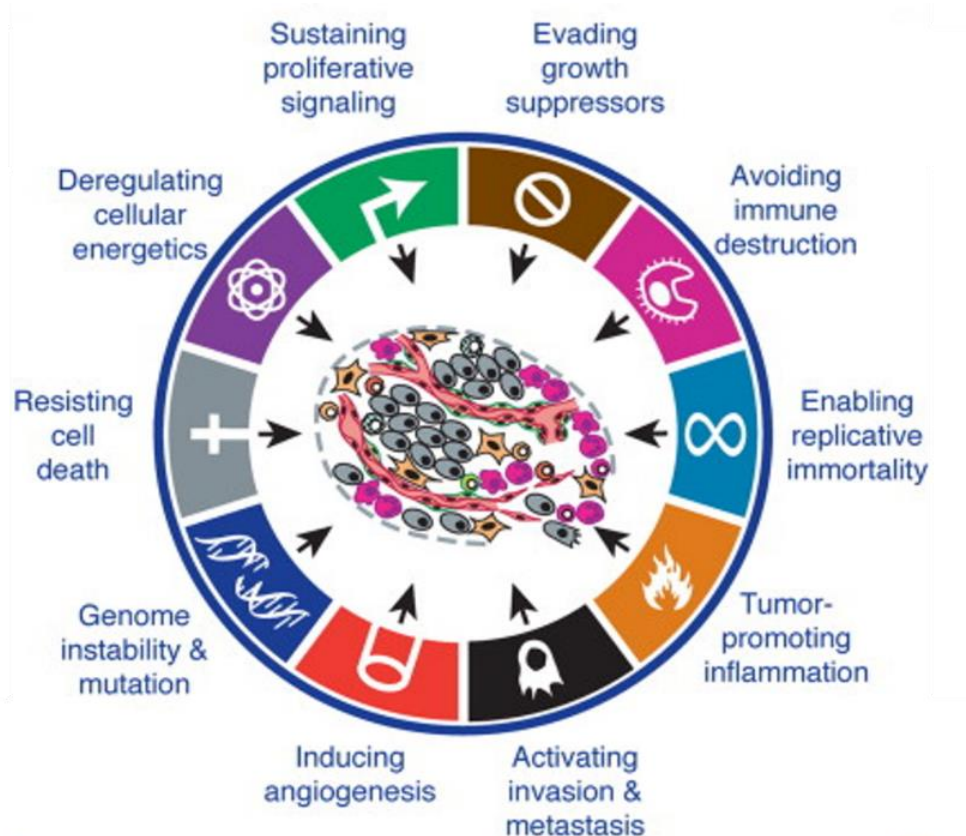


Figure 2. Hallmarks of cancer. Biological capabilities acquired during the multistep development of cancer. They include sustaining proliferative signaling, evading growth suppressors, avoiding immune destruction, enabling replicative immortality, tumor-promoting inflammation, activating invasion and metastasis, inducing angiogenesis, genome instability and mutation, resisting cell death, deregulating cellular energetics. (Hanahan and Weinberg 2011)

- **Aerobic Glycolysis**

Aerobic glycolysis, known also as “Warburg effect” is the metabolic process that converts glucose into lactate, even in the presence of abundant oxygen (Warburg et al. 1927). Warburg hypothesized that the aerobic glycolysis was triggered by non-functioning mitochondria, which were incapable of maintaining oxidative respiration (Warburg et al. 1927). However, it has now been elucidated that cancer cells do not necessarily exhibit compromised mitochondrial function (Salem et al. 2012). Glycolysis has the capacity to generate ATP at a higher rate than oxidative phosphorylation, indeed, ATP production by glycolysis is more rapid than by oxidative phosphorylation but less efficient in terms of ATP production. Consequently cancer cells regulate this metabolic process at various level, indeed, they have an increased uptake of glucose, overexpression of glucose transporters and glycolytic enzymes, in order to meet their increased energy, biosynthesis and redox demands (Cairns et al. 2011). The increased glucose uptake of cancer cells has provided useful for tumour detection and monitoring, through the [¹⁸F]fluorodeoxyglucose positron emission tomography (FDG–PeT) imaging. FDG–PeT uses a radioactive analogue of glucose to detect regions of high glucose uptake and consequently for identifying many tumours types (Gambhir 2002). One of the main regulatory mechanisms underlying aerobic glycolysis involves hypoxia-inducible factor (HIF-1). Hypoxia promotes the stabilization of HIF 1 and 2, which activate the expression of several components involved in angiogenesis, metastasis, and also glycolysis pathways (Rempel et al. 1996). HIF-1 switches from an inactive state, under normoxic conditions, to an active state, under oxygen-deprived hypoxic conditions. HIF-1 α becomes stable because hypoxic environment directly decreases prolyl hydroxylases (PHDs), an enzyme involved in the prolyl hydroxylation and subsequent ubiquitination (Hirota and Semenza 2005). Then, the formation of the heterodimer between HIF-1 α and HIF-1 β allows the DNA binding, which induces the expression of several genes (Erler et al.

2006). Therefore HIF-1 induces the upregulation of some glucose transporters, glycolytic enzymes (HKI, HKII, PFK-1, ALDO-A, ALDO-C, PGK1, ENO- α , PK-M2, PFKFB-3) and enzymes related to lactate production and lactate/proton extrusion (LDH-A, MCT4) (Marín-Hernández et al. 2009). Furthermore, under hypoxic conditions, HIF-1 regulates the expression of pyruvate dehydrogenase kinases (PDKs), which inactivate the mitochondrial pyruvate dehydrogenase complex and reduce the flow of glucose-derived pyruvate into the tricarboxylic acid (TCA) cycle (Semenza 2011). However, HIF1 can also be activated under normoxic conditions by oncogenic signalling pathways, including PI3K (Plas and Thompson 2005), by mutations in tumour suppressors such as VHL (Kaelig 2008), SDH (Selak et al. 2005) and FH (King et al. 2006). For these reasons, prevalence of HIF-1 overexpression in tumors is correlated with the severity of the cancer (Rankin and Giaccia 2008).

- **Tricarboxylic acid (TCA) cycle**

TCA cycle plays a central role for energy metabolism, macromolecule synthesis and redox balance (Anderson et al. 2018). Normal cells use glucose as a main source of pyruvate which enters in the TCA cycle, while cancer cells often shunt glucose away for catabolism by aerobic glycolysis, and for this reason they rely more on glutamine and fatty acids to fuel TCA cycle (Eagle 1955). Several evidences demonstrated that cancer cells uncouple glycolysis from TCA cycle, using different metabolites as source for the metabolic needs (Chen and Russo 2012). The replenishment of the TCA cycle from alternative metabolic sources is regulated by various oncogenes and tumor suppressors which regulate the expression of transporters and enzymes (Chen and Russo 2012). Amino acids, particularly glutamine, can enter the TCA cycle via conversion into acetyl-CoA or keto-intermediates (Anderson et al. 2018). Glutamine and its breakdown, glutaminolysis, is essential in replenishing cycle intermediates in cancer cells. For this reason, cancer cells upregulate glutamine transporters and enzymes, enabling cells to meet energetic and biosynthetic

demands through glutamine metabolism (DeBerardinis et al. 2007). Moreover, another fuel source in cancer cells is fatty acids, which fuel TCA cycle by generation of acetyl-CoA (Migita et al. 2008).

- **Glutaminolysis**

In order to maintain mitochondrial function, in spite of the limited pyruvate availability due to aerobic glycolysis, cancer cells fuel TCA cycle by anaplerotic processes (Yang et al. 2017). Many studies have highlighted the so called “glutamine addiction” for cancer cells, which are also dependent on glutamine for their replication and survival (DeBerardinis and Cheng 2010). Indeed glutamine serves as a critical nitrogen donor, enabling de novo synthesis of nucleotides, protein synthesis and energetic substrate in the TCA cycle anaplerosis (Yang et al. 2017). Glutaminolysis is the process by which cells convert glutamine into TCA cycle intermediates. Glutamine is converted into glutamate via glutaminase (GLS1/GLS2). Glutamate is then converted into α -ketoglutarate. Both α -ketoglutarate and glutamine-derived oxaloacetate can serve as anaplerotic substrates for the TCA cycle (Wise and Thompson 2010). Glutamine-derived glutamate can also be used for the glutathione biosynthesis by the enzyme glutathione cysteine ligase (GCL), making the role of the glutamine essential also for the regulation of the redox status (Kim and Kim 2013; Wise and Thompson 2010). Glutaminolysis is upregulated in many types of cancers due to the energy demands in tumor cells (Li et al. 2016). Among all the oncogenes regulating glutaminolysis, MYC is the main oncogene responsible for the mitochondrial reprogramming, resulting in increased expression of glutaminase enzymes and glutamine transporters (Gao et al 2009). MYC increases glutamine uptake inducing the expression of glutamine transporters (SLCA1 and SLC7A1) (Cairns et al. 2011). Furthermore, the tumor suppressor TP53 also contributes to the regulation of glutamine metabolism by affecting the activity of glutaminase enzymes (Curthoys and Watford 1995). Two are the phosphate-

activated GLS isoforms: GLS1 and GLS2 (Curthoys and Watford 1995). GLS2 is induced in response to intracellular ROS accumulation, through the p53 activation, which results in the activation of the glutathione biosynthesis, in order to counteract the oxidative stress (Suzuki et al. 2010). GLS1 is upregulated in cells with increased rates of proliferation, and accounts for the majority of glutaminase activity in some human tumor cells. Overexpression of GLS2 results in a reduction of tumor cell growth (Perez-Gomez et al. 2005). Different studies have shown that GLS1 is upregulated in different cancer phenotypes, such as gliomas, colorectal carcinomas, adenomas, and breast cancer cell lines, whereas, GLS2 expression is associated with resting or quiescent cell states (Szeliga et al. 2005; Szeliga et al. 2008; Turner and McGivan 2003). Particularly, KRAS downregulates expression of glutamate dehydrogenase, which converts glutamate into α -ketoglutarate and upregulates expression of glutamate-oxaloacetate transaminase, which convert the glutamate into oxaloacetate, to release aspartate for NADPH generation via malic enzyme 1 (Son et al. 2013).

- **Pentose phosphate pathways**

Pentose phosphate pathways (PPP) branches from glycolysis, at the first step of this process, and is required for the ribonucleotides biosynthesis and for NADPH production (Krushna et al. 2014). NADPH is fundamental for the fatty acids synthesis and for the redox balance (Nathan and Ding 2010). Therefore, PPP covers a fundamental role for cancer cells, particularly for highly glycolytic cancer cells, to meet their anabolic demands and counteract the oxidative stress (Cho et al. 2018). PPP activation has been demonstrated in different types of cancer and several oncogenic signaling pathways are involved in the regulation of this process (Jiang et al. 2014). Previous studies have highlighted the importance of PPP in rapidly growing cancer cells and consequently, an increased expression of PPP-related enzymes, particularly glucose 6 phosphate dehydrogenase (G6PD) enzyme, in human cancer

tissues (Lucarelli et al. 2015). Since PPP contributes directly to cell proliferation, survival and senescence, it is tightly regulated by many oncogenes, tumor suppressors, oncoproteins and intracellular metabolites (Jiang et al. 2014). *TP53* mutations, for instance, has been related to the regulation of PPP, increasing the metabolites flux in PPP and glycolysis (Jiang et al. 2014). Moreover, oncogene *KRAS* drives glycolytic intermediates into PPP in pancreatic ductal adenocarcinoma (Ying H et al. 2012). Recently it has been highlighted the regulatory role in PPP of PI3K/AKT signaling pathways, resulting in the regulation of G6PD (Wagle et al. 1998).

- **Lipid metabolism**

Rapid cell proliferation requires a constant supply of lipids to fuel membrane biosynthesis and protein modification, resulting in a strong lipid and cholesterol avidity (Omabe et al. 2015). Accumulation of cholesterol and lipids in cancer cells are stored in lipid droplets (LDs), which are now considered as a hallmark of aggressiveness (de Gonzalo-Calvo et al. 2015). Cancer cells regulate the activation of lipid catabolic and anabolic pathways in order to meet demands for membranes formation, energy production, production of signaling molecules and redox homeostasis (Luo et al. 2017). Particularly, fatty acid β -oxidation (FAO) pathway is the dominant energetic process in non-glycolytic tumors, making potentially useful for the design of therapeutic strategies (Liu et al. 2010). Several lipogenic enzymes are overexpressed in cancer cells, such as acetyl-CoA carboxylase (ACC), fatty acid synthase (FASN), and ATP citrate lyase (ACLY) that promote also cholesterol synthesis (Menendez and Lupu 2007; Zaidi et al. 2012). Therefore, genes involved in cholesterol-related pathways and FAO are finely regulated as well, proving to be crucial in supporting malignancy (Baenke et al. 2013).

- **Redox Balance**

Oxidative stress, implicated in cancer development and progression, results from an imbalance in the ROS production and cellular antioxidant molecules (Valko et al. 2006). Cancer stem cells have the advantage of the aberrant redox system, showing an increased level of ROS due to the rapid dividing activity (Liou and Storz 2012). ROS are chemical species that contain oxygen and include the superoxide anion (O_2^-), hydrogen peroxide (H_2O_2), and the hydroxyl radical (OH^\cdot) (Murphy 2009). Normal cells produce ROS as a physiological byproduct of metabolic processes, showing several downstream effects, depending on their intracellular concentrations. They are involved in various functions such as DNA synthesis, transcription factor activation, gene expression, and proliferation (Liou and Storz 2012). High concentration of ROS might cause damage to macromolecules, leading to senescence and apoptosis (Cairns et al. 2011). One of the most important source of ROS is the NADPH oxidases (NOXs), which catalyze the production of superoxide anion (O_2^-) from O_2 and NADPH (Brand 2010). Subsequently, the mitochondrial or cytosolic superoxide dismutase enzyme (SOD) converts superoxide anion into hydrogen peroxide (H_2O_2). The detoxification of H_2O_2 is mediated by the enzymatic activity of mitochondrial and cytosolic peroxiredoxins (PRXs), which converts H_2O_2 into water (Rhee et al. 2012). The resulting oxidized form of PRXs is then reduced by thioredoxin (TXN), thioredoxin reductase and reducing equivalent NADPH, in order to complete the catalytic cycle (Cox et al. 2009). Normal cells counteract ROS effects by regulating antioxidant molecules. An important antioxidant system is the Glutathione peroxidase (GPX), which is able to convert H_2O_2 in H_2O in the mitochondrial matrix and cytosol through H_2O_2 -mediated oxidation of reduced glutathione (GSH). Then glutathione reductase (GR) in the presence of NADPH, reduces oxidized glutathione (GSSG) back to GSH (Murphy 2012). Another abundant antioxidant, localized in peroxisomes, is the catalase, which detoxifies H_2O_2 into water.

However, H_2O_2 can become OH^\cdot and quickly causes the oxidation of lipids, proteins, and DNA, resulting in cellular damage (Halliwell 2000). As indicated above, the reduced form of NADP (NADPH) is essential and required to maintain antioxidant defenses, as a co-factor of most of the redox mechanisms (Ying 2008). The delicate balance between intracellular ROS production and antioxidant requests is closely dependent on various metabolic pathways. Indeed, several pathways, such as the oxidative PPP and glutaminolysis, or the activity of enzymes such as pyruvate kinase isoform M2 (PKM2), NADP-dependent isocitrate dehydrogenase (IDH) and malic enzyme 1 (ME1), are involved in antioxidant regeneration (Liu et al. 2014; Cairns et al. 2011). Among all the functions of ROS in cell physiology, they may act in the regulation of cell proliferation and cellular adaptation to metabolic stress (Finkel 2012). Moreover, because of these ROS cellular functions, evidences, over the past years, has indicated a consistent association between ROS and malignant transformation (Jackson and Loeb 2011). Cancer cells show an increased level of ROS, due to the increased dividing activity, compare to normal cells (Liou and Storz 2012). This increased ROS production causes the activation of signaling pathways necessary for tumorigenesis (*PIP3K*, *MAPK/ERK*, *HIF*, *NF- κ B*). In the tumor microenvironment, characterized by high proliferative cells, ROS regulation is crucial owing to the presence of oncogenic mutations that promote metabolic alterations, resulting in increased rates of ROS production. However, tumoral cells are able to counteract this accumulation of ROS by further upregulating antioxidant systems (Schafer et al. 2009). The main transcriptional target that enables the increased production of antioxidant proteins in cancer cells is through the activation of nuclear factor (erythroid-derived 2)-like 2 (NRF2) (Sporn and Liby 2012). Stabilization of the transcription factor NRF2 by inhibition of its negative regulator Kelch-like ECH-associated protein 1 (KEAP1) allows it to increase expression of antioxidants (Jaramillo and Zhang 2013). Once activated, NRF2 induces the transcription of many antioxidant proteins including GPXs and TXNs as well as enzymes involved in GSH

synthesis and cystine import. For this reason, NRF2 has also been shown to be essential for tumorigenesis, related to their ability to counteract oxidative stress (DeNicola et al. 2011). Several studies have elucidated the connection between redox balance and metabolism. Indeed, it has been suggested that, once the cancer develops, the metabolic activity is increased and this induces an increase of ROS with an activation of pathways involved in the cancer cell proliferation, survival and metabolic adaptation (Chandel and Tuveson 2014).

Thyroid cancer metabolism.

During thyroid tumorigenesis, as previous reported, several oncogenes and tumor suppressors are involved in different tumoral processes, such as abnormal proliferation, angiogenesis and resistance to apoptosis (Ciavardelli et al. 2017). Among all of these processes, toward thyroid malignancy, the metabolic alterations have gained increasing interest, since they are related to several thyroid biological functions. Indeed thyroid hormone biosynthesis is a highly energy requiring process, and mainly, the energy is provided by mitochondria through the oxidative phosphorylation (OXPHOS) (Kim et al. 2012). Previous studies have reported that highly proliferating cancer cells display a shift towards a high rate of glycolysis and, consequently, increased glucose uptake, consumptions and lactate production (Heiden et al. 2009). These metabolic alterations are usually regulated by transcription factors such as hypoxia inducible factor 1 alpha (HIF-1 α) (Denko 2008). HIF-1 α has been found to be overexpressed in aggressive types of TC (Burrows et al. 2010). Several glycolytic enzymes, upstream to HIF-1 α , such as the hexokinase II (HKII), phosphoglycerate kinase (PGK), glucose-6-phosphate dehydrogenase (G6PDH), and lactate dehydrogenase A (LDH-A), glucose transporter 1 (GLUT1) and the monocarboxylate transporter 4 (MCT4), have been found to be overexpressed in TC as well (Chen et al. 2015; Nahm et al. 2017; Grabellus et al. 2012). Thyroid cancer is characterized by different type of host cells, which represent the so-called tumor microenvironment. These cells are fibroblasts, immune cells and endothelial cells (Ciavardelli et al. 2017). Increased evidences showed that cancer associated fibroblasts (CAFs), which are stromal cells, support metabolic requirements and alterations of cancer cells. Cancer cells activate glycolysis and related enzymes and transporters, especially MCT4 in CAFs, which, consequently, provide metabolites, such as lactate, in order to satisfy energy requirements of cancer cells (Pavlidis et al. 2009). It has been demonstrated that lactate is exported via MCT4 by CAFs and is taken

up by cancer cells via MCT1, and then converted in pyruvate, defining the so-called “reverse Warburg” effect (Dhup et al. 2012). Recently it has been showed that the expression of MCT4 and MCT1, and the traslocase of outer mitochondrial membrane 20 (TOMM20), a marker of mithocindrial mass, is increased in both PTC and ATC (Curry et al. 2016; Gill et al. 2016; Nahm et al. 2017). Several studies have elucidated which oncogenes and other tumor-related molecules were related to the cancer metabolic reprogramming in TC. *BRAF*^{V600E} mutation has been associated to the Warburg phenotype in PTC, through the regulation of the expression of the isoform M2 of pyruvate kinase (PKM2), conferring an selective growth advantage (Feng et al. 2013). The overexpression of these proteins, involved in glycolytic processes, has been associated with the aggressive thyroid tumors, probably because of their increased need of energy to sustain the proliferation (Nahm et al. 2017). Glutaminolysis has been investigated in TC as well, considering its fundamental role for cancer development and progression (Smith et al. 2016). The expression of several glutamine metabolism-related proteins has been found altered in TC, particularly both ATC and PTC showed high expression of enzymes involved in glutaminolysis (Kim et al. 2016). Another important regulator of glucose metabolism is p53, which has been found frequently deleted or mutated in TC (Malaguarnera et al. 2007). p53 controls glucose uptake, modulating expression of glycolytic proteins such as GLUT1, inhibiting the glycolytic processes and promoting mitochondria oxidation. Consequently, because of deletion or mutation on p53, glucose uptake and glycolysis result increase in cancer cells (Morani et al. 2014). This strong glycolytic phenotype has been highlighted particularly in poorly differentiated TC (Grabellus et al. 2012; Frilling et al. 2001). Considering the essential contribution that metabolomics give to the elucidation of cancer metabolism, several metabolomics studies have been conducted in TC (Wojakowska et al. 2015). Although genomics, transcriptomics and proteomics have contributed to the knowledge of TC, they do not completely characterize the cancer phenotype most close to the cancer metabolome

(Liesenfeld et al. 2013). Metabolomics, instead, can provide information more closely connected to altered metabolism in cancer cells. Several studies on healthy tissues and malignant tissues have reported a principal role of alanine and lactic acid (Torregrossa et al. 2012; Deja et al. 2013). As reported above, lactic acid is a common features of Warburg phenotype associated to many types of tumors (Doherty and Cleveland 2013), and it has also been related to the angiogenesis processes (Goodwin et al. 2014; V'egran et al. 2011). Among all the amino acids, alanine and glutamine levels were found increased in malignant lesions compared with healthy tissues (Xu et al. 2015). In many cancer types glutamine fuel the protein and nucleotides biosynthesis, providing nitrogen, and the TCA cycle, providing intermediates (Wise and Thompson 2010). On the other hand high levels of serine and glycine were found in FNA specimens from malignant nodules and in cancer tissues (Ryoo et al. 2016). These amino acids can provide intermediates for lipid, nucleotides and proteins biosynthesis, showing an essential role for cancer progression (Locasale 2013; Amelio et al. 2014). Recently, in *BRAF^{V600E} like*-PTC serine/glycine-related proteins have been found higher than other TC types (Sun et al. 2016). In term of lipid metabolism, malignant TC showed high levels of fatty acids, such as palmitic, myristic, palmitoleic and oleic acids (Guo and Qiu et al. 2014; Guo and Wang et al 2014). Related to the lipid metabolism, choline (Gupta et al. 2011; King et al. 2005) and citrate (Ryoo et al. 2016) have been found respectively increased and decreased.

Cancer stem cells (CSCs)

Cancer is characterized by highly proliferative malignant cells, which are different in morphology and functions, resulting in a heterogeneous population of cells. These cells display different proliferative capacity, metabolic behavior, invasiveness and functions in the tumor microenvironment (Islam et al. 2015). Over the past decade, it has been demonstrated that cancers show a hierarchical organization, with a subset of cancer cells, called cancer stem cells (CSCs) or cancer initiating cells (TICs), which display self-renewal capacity. CSCs are known to be responsible for cancer initiation, metastasis, therapy resistance, and recurrence (Islam et al. 2015). The origin of CSCs is still debated and controversial, and several hypothesis have been proposed. The first hypothesis demonstrated that CSCs are the product of malignant transformation, including mutations affecting the control of cell proliferation in adult stem cells (Smalley and Ashworth 2003). The second hypothesis reported that the epithelial-mesenchymal transition (EMT) might be responsible for the de-differentiation of mature cancer cells that acquire the ability to self-renew (Mani et al. 2008). The third hypothesis is related to the induction of pluripotent stem cells, derived from a non-pluripotent cell, through the expression of specific genes involved in the reprogramming of somatic cells (Takahashi and Yamanaka 2006). Two models, hierarchical and stochastic, have been proposed for the explanation of cancer initiation and heterogeneity (**Figure 3**), although these two models are not exclusive. According to the hierarchical model, cancer initiation occurs when normal stem cells escape the regulation and they become cancer stem cells, with self-renewal and the ability to produce cancer progenitor cells. At the same time, also normal progenitor cells can escape the regulation and become cancer progenitor cells as well (Plaks et al. 2015). According to this model, from a clinical point of view, only the complete eradication of all CSCs will eliminate the possibility of relapse. On the other hand, the stochastic model supports the idea that every cell, within the

tumor mass, is equally responsible for the tumor initiation and progression. This ability is due to the sequential acquisition of oncogenic mutations, in genes involved in the regulation of the cell cycle, that contribute to the creation of cancer progenitor cells (Plaks et al. 2015).

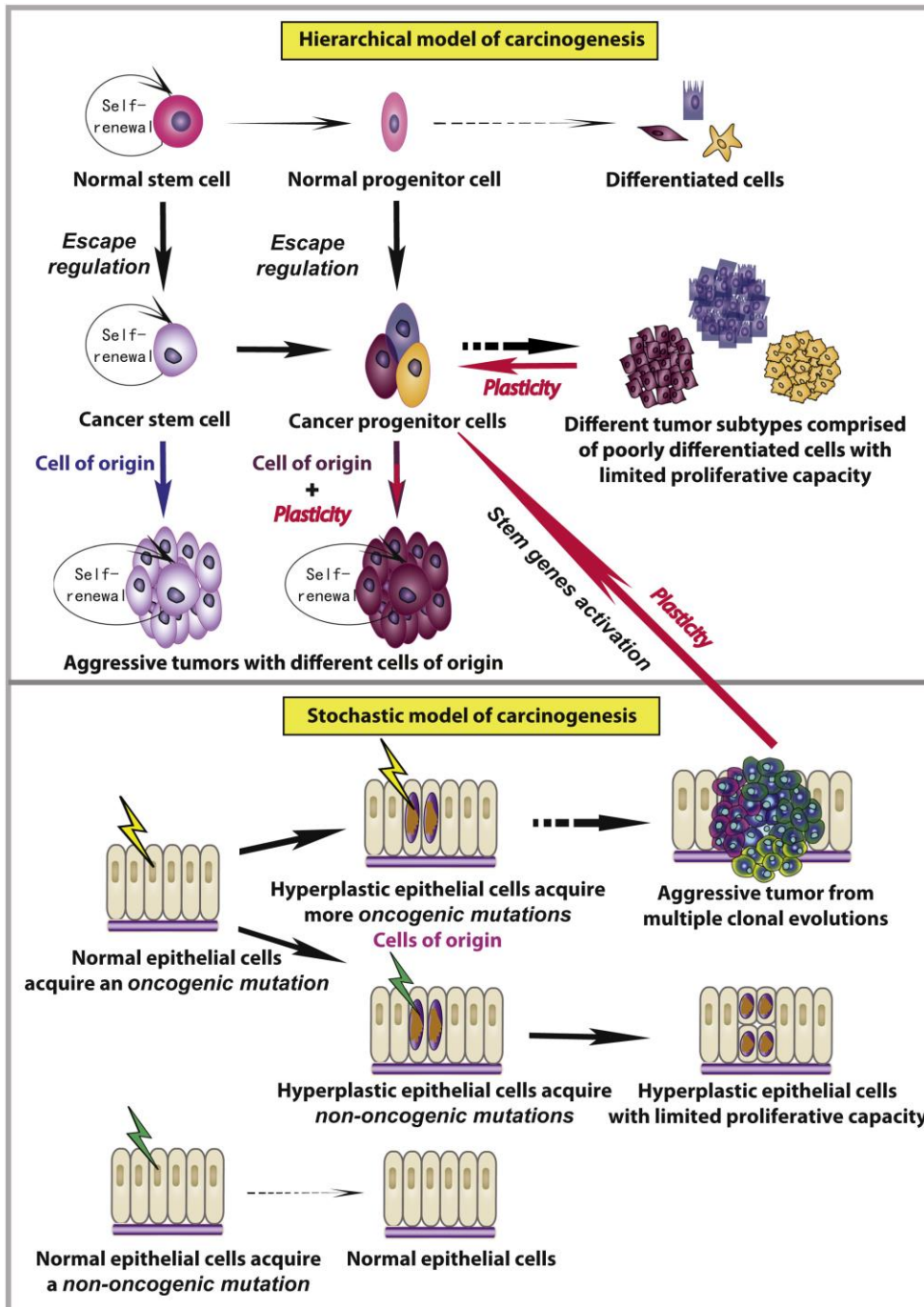


Figure 3. Models of Carcinogenesis: Hierarchical and stochastic model of carcinogenesis (Plaks et al. 2015)

The presence of CSCs has been demonstrated in several cancer types, leukemia (Lapidot et al. 1994), breast (Al-Hajj et al. 2013), glioblastoma (Singh et al. 2004), colorectal (Dalerba et al. 2007; O'Brien et al. 2007), pancreatic (Li et al. 2007), liver (Li et al. 2017), lung (Shukla et al. 2018), ovarian (Zhang et al. 2008) and thyroid cancer (Bhatia et al. 2014). CSCs are typically resistant to conventional cancer therapies and they are implicated in disease persistence or relapse. Indeed, the elimination of these cells is a great challenge and covers a fundamental role in the improvement of the survival of patients (Wang et al. 2017; Yiet al. 2017). As cancer cells adapt the metabolism to deal with the unfavorable microenvironments and the energetic needs, also CSCs show a metabolic rewriting (Yi et al. 2018). Studying metabolism in cancer has become a promising and emerging field of research; however, the cellular heterogeneity within tumors creates bias in most studies. Highlighting the different phenotypes of normal cancer cells and CSCs may results in a better understanding of the metabolic addiction and consequently of different responses to metabolic therapies (Peiris-Pagès et al. 2016). Although the metabolism of CSCs has been intensely investigated in recent years; it remains controversial whether CSCs mainly rely on glycolysis or OXPHOS. Stem cells rely more on glycolysis compared to their differentiated cells, which rely more on oxidative phosphorylation. Previous studies underlined that induced pluripotent stem (iPC) cells acquire stemness proprieties through the metabolic reprogramming, shifting from mitochondrial respiration to a metabolism that is mainly glycolytic (Zhou et al. 2012). Stem cells are also able to reprogram their metabolism to generate large amounts of energy needed for the differentiation process (Jang et al. 2015). Nevertheless, metabolic features associated to CSCs and the metabolic effects on CSCs physiology remain poorly explored, and it is deeply dependent of the tumor type. A new paradigm about the acquisition of stemness features linked to the metabolic reprogramming has been recently proposed. Indeed combined biological, biochemical and genetic studies has revealed that CSCs may be generated from metabolic adaptations, which affect chromatin organization and activate

epigenetic program. These metabolic-driven reprogramming of CSCs is called metastemness hypothesis, and together with the traditional clonal evolution model they explained the origin of CSCs in cancer (**Figure 4**) (De Francesco et al. 2018).

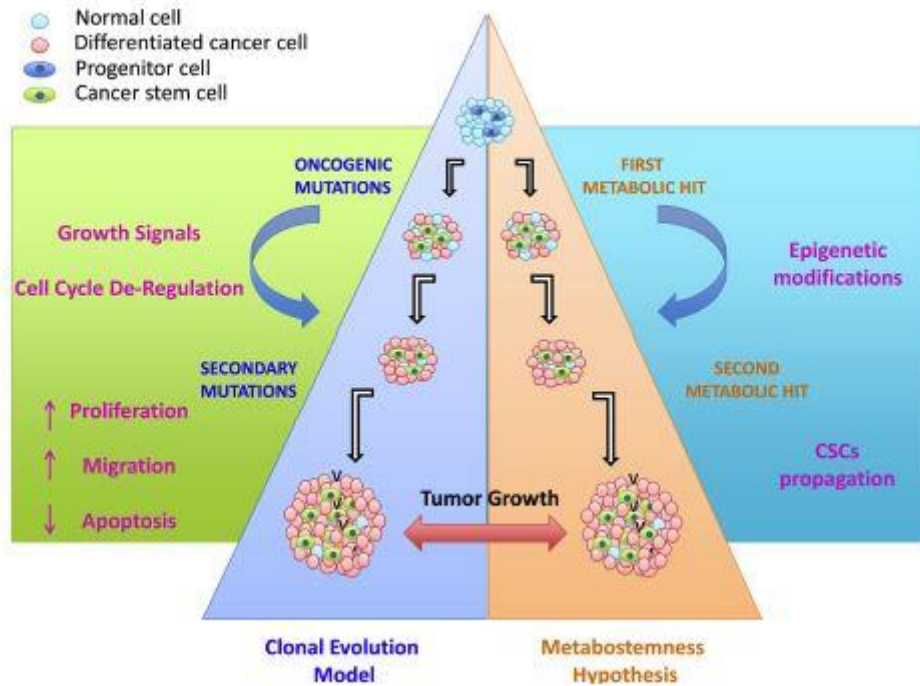


Figure 4. Metabostemness hypothesis for the tumor heterogeneity and the origin of CSCs. To explain tumor heterogeneity, two models have been proposed: the clonal evolution model and the metabostemness hypothesis (De Francesco et al. 2018).

Several studies suggest that CSCs are more glycolytic compared with other differentiated cancer cells in vitro and in vivo (Ciavardelli et al. 2014; Emmink et al. 2013; Liao et al. 2014; Palorini et al. 2014). According with these findings, glucose uptake, expression of enzymes involved in the glycolysis, lactate and ATP content were found to be significant increased in CSCs and linked to a decrease of oxidative phosphorylation (Guha et al. 2013; Petros et al. 2005). Moreover, experiments in breast cancer cell lines suggested that CSCs functions are deeply linked and dependent on the switch from OXPHOS to aerobic glycolysis (Dong et al. 2013). Mitochondria revert to an immature state in some glycolytic CSCs,

characterized by low levels of ROS compared with differentiated cells (Prigione et al. 2010). Consequently, reduced levels of ROS are essential for maintaining quiescence and self-renewal ability (Jang and Sharkis 2007). On the other hand, CSCs in other cancer types have demonstrated OXPHOS dependence for the energy production. Previous studies have reported that CSCs may also rely on mitochondrial FAO for ATP and NADPH production (Sancho et al. 2016). Although the OXPHOS phenotype of some CSCs have not yet been fully understood, this metabolic feature renders CSCs resistant to inhibition of glycolysis, providing higher independency from microenvironmental nutrients (Sancho et al. 2016). For this reason, OXPHOS-dependent CSCs acquire an advantage as they make a better use of nutrients to meet energetic demands. Furthermore, it has been demonstrated that lactate excretion from differentiated cells may fuel the mitochondrial metabolism in OXPHOS-dependent CSCs (Nakajima and Van Houten 2013). Understanding the metabolic dependence of CSCs in various tumors could be an effective pharmacological strategy for the elimination of CSCs. Particularly, OXPHOS-dependent CSCs that are not able to meet their energetic demands by glycolysis, might be eradicated by targeting mitochondrial OXPHOS (Sancho et al. 2016). However, targeting either glycolysis or OXPHOS pathways may result inconclusive and unsatisfactory, mainly due to the metabolic heterogeneity and plasticity of CSCs (Valent et al. 2013).

Targeting cancer cells metabolism: Vitamin C anti-tumoral effects

Tumor initiation and progression are deeply associated to the metabolic reprogramming, whose metabolic features can be exploited to treat cancer. Understanding the differential metabolic dependencies of tumors has the potential to provide new therapeutic strategies (Luengo et al. 2017). Indeed the inhibition of metabolic processes and enzymes involved in the metabolic programming may have a promising effect on tumors by depleting bioenergetic sources and anabolic reactions. These effects result in growth stop, apoptosis induction and, eventually, inhibition of invasion (Kroemer and Pouyssegur 2008). Several inhibitors of metabolic enzymes have been described, such as glucose transports, glycolytic enzymes, fatty acid synthesis and oxidative phosphorylation inhibitors (Simons et al. 2007, Kim et al. 2007; Pedersen 2007; Bonnet et al. 2007, Kim et al. 2007; Pedersen 2007; Bonnet et al. 2007, Hatzivassiliou et al. 2005; Beckers et al. 2007; Wang et al. 2005, Pouyssegur et al. 2006; Chi et al. 2007). Tumors characterized by glycolytic phenotypes could be more sensitive than other tumors to agents targeting the glycolytic enzymes (Hamanaka and Chandel 2012). On the other hand, tumors characterized by alteration in the TCA cycle and/or glutamine-dependence could be sensitive to agents targeting glutamine metabolism such as glutaminase (Teicher et al. 2012). Nevertheless, it has been well verified that tumor mass is characterized by a heterogeneous cell population, and within this population, cancer stem cells have been as responsible for metastasis, therapy resistance and tumor relapse (Clevers 2011). As such, targeting CSCs may be a useful strategy to improve the cancer therapies. Considering that CSCs show several oncogenic alterations which trigger metabolic changes and that metabolism has been shown to deeply influence the maintenance of CSCs, targeting their metabolism plays a fundamental role for identification and eradication on CSCs (De Francesco et al. 2018).

Since the discovery of vitamin C, the evaluation of its biological functions is continually rising. Particularly, the use of pharmacological concentrations (high dose) of vitamin C in cancer started with the discoveries of Linus Pauling and Ewan Cameron, who reported the positive effect of vitamin C in cancer treatment (Cameron and Pauling 1976). Furthermore, vitamin C has long been used in the prevention of several diseases, where it primarily acts as antioxidant (Fang et al. 2002; Ames et al. 1993) while evidences that vitamin C is selectively toxic to some types of tumor cells, functioning as a pro-oxidant, are now increasing (Bram and Froussard 1980; Fujinaga and Sakagami 1994). Vitamin C uptake is mediated by two membrane transporters: the sodium-ascorbate co-transporters (SVCTs) and hexose transporters (GLUTs). Particularly SVCTs import vitamin C in its reduced form (ascorbate), while GLUTs (mainly GLUT1) import dehydroascorbate (DHA), the oxidized form, followed by intracellular reduction at the expense of GSH, thioredoxin, and NADPH (Savini et al. 2008; Vera et al. 1995; Welch et al. 1995). Previous studies have been demonstrated that the cytotoxicity of high-dose of vitamin C is mediated by delivering hydrogen peroxide (H_2O_2) and, consequently, it acts as pro-oxidant inside the cells (Du et al. 2012). The production of H_2O_2 results in depletion of intracellular antioxidant, such as intracellular GSH, causing oxidative stress and cancer cell death (Du et al. 2012). Several studies reported the different sensitivity to vitamin C-induced cytotoxicity in cancer cells (**Table 2**) (Takemura et al. 2010; Du et al. 2010; Roomi et al. 1998).

Table 2. Cytotoxicity of vitamin C in cancer cells.

Cell Line	IC50 (mM)
HL-60	0.33 ± 0.18
NB4	0.76 ± 0.14
NB4-R1	0.45 ± 0.24
NB4-R2	0.75 ± 0.3
KG1	0.79 ± 0.22
K562	0.5 ± 0.11
U937	0.3 ± 0.16
OVCAR	>10
SK-OV3	>10
JLP119	<1
MCF7	2
MB231	7
Hs587T	20
KNL205	<1
RAG	<2
CT26	4
B16	7
LL/2	11
Hs587/bST	>20
CCD34SK	>20

HL-60, human myeloid leukemia; NB4, NB4-R1, NB4-R2, human acute promyelocytic leukemia (APL); KG1, human myeloblast; K562, human chronic myelogenous leukemia; U937, human histiocytic lymphoma; OVCAR, SK-OV3, ovarian cancer; JLP119, human lymphoma; MCF7, MB231, Hs587t, human breast cancer; KLN205, mouse lung cancer; RAG, mouse kidney cancer; CT26, mouse colon cancer; B16, mouse melanoma; LL/2, mouse lung cancer; Hs587Bst, human normal breast cells; CCD34SK, human normal fibroblast cells (Chen et al. 2005; Park et al. 2014).

However, the anti-proliferative effects seem to affect the cancer cells metabolism, but the mechanism underlying this effect is not fully understood. Recently Yun J et al., have reported that high-dose of vitamin C is able to selectively inhibit glycolysis in KRAS and BRAF driven colorectal cancer cells by increasing oxidative stress (Yun et al. 2015). Furthermore, high-dose of vitamin C was found to be able to affect the viability of breast adenocarcinoma

and colon cancer cells by inhibiting energetic processes such as glycolysis and TCA cycle, and consequently the ATP production (Uetaki et al. 2015). Taken together these findings support the hypothesis that vitamin C-induced cytotoxicity can be mediated also by alterations in metabolic pathways, affecting energetic processes and survival of cancer cell.

Metabolomics

- **The metabolomic approach**

Metabolomics is a comprehensive analysis of small molecule metabolites (< 1kDa) of biological samples. This analytical approach involves the study of intermediates and products of metabolism, such as carbohydrates, fatty acids, amino acids, nucleotides, organic acids, vitamins, antioxidants and many other classes of compounds (Klupczyńska et al. 2015). Metabolome, the complete set of metabolites of a sample, can be characterized from all levels of biological complexity: organisms, tissues, cells or cell compartments (Fiehn 2002). Metabolomics allows studying the metabolic fingerprint and it provides a 'top-down', an integrated view of the organism (Nicholson and Lindon 2008). The metabolic information is deeply dependent on physiological or pathological state of organism, tissue or cells. The described metabolic phenotype might provide an insight into the biological status and it might be used as information about the organism (Holmes et al. 2008). Considering that metabolites are the final product of the genic expression and the protein activity, among the other “omics” technologies, metabolomics is the research platform most closely related to the phenotype (Nicholson et al. 1999). Several metabolomic studies have been conducted with the aim to discriminate samples, based on the different metabolomes, between different physiological and/or pathological conditions, making the metabolomics approach useful to discover biomarkers and to identify the biochemical pathways involved in biological processes (Spratlin et al. 2009). The metabolomics analytical workflow can be divided into different crucial steps, from the sample collection to the sample acquisition and data analysis **(Figure 4)**.

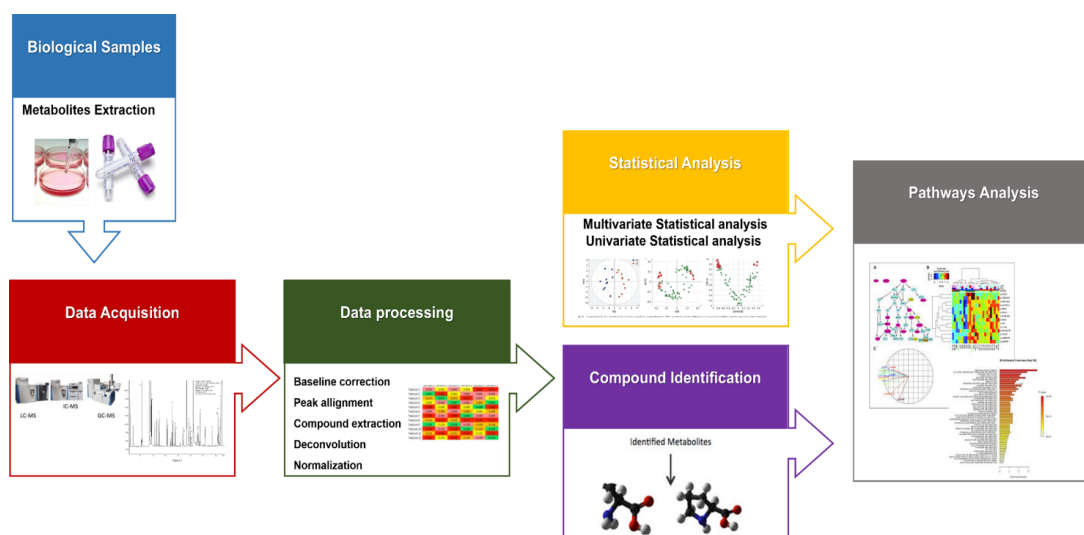


Figure 5. General metabolomics workflow. Flowchart of metabolomics analytical approach, from the sample pre-treatment to the data interpretation.

Sample collection is a critical step, which may determine the success of metabolomic experiment. There is a wide variety of biological samples that can be used for metabolomics studies, and the sample state (in term of typology, collection technique, sex, ages, diet) may affect the analysis, introducing variation or bias into the experiments (Snyder et al. 2015). Furthermore, the sample preparation might remove the complexity or problems from the collection step. Indeed, the extraction processes may “clean” the sample and increase the specificity and sensitivity of the method. The instrumental approach, to detect the metabolites within samples, can be divided as well as either targeted or untargeted. The first studies a define number and type of metabolites, maximizing the sensitivity; the second approach scans the greatest number of metabolites inside the biological sample (Fiehn 2002). For the instrumental analysis different analytical techniques can be used, and the choice depends both on the type of the sample and on the type of required information (Beger 2013). The analytical platforms typically employs either nuclear magnetic resonance spectroscopy (NMR) or mass spectrometry (MS), which usually is coupled with separation technologie, such as gas-chromatography (GC-MS), liquid chromatography (LC-MS) and capillary

electrophoresis (CE-MS) (Armitage and Barbas 2014). Mass spectrometry employs a range of different mass analyzers depending on the type of experiment, such as single quadrupole, triple quadrupole, time-of-flight mass spectrometer, ion traps. Among all the separation techniques, GC-MS and LC-MS are the most widely used in metabolomics approach, while recently CE-MS is getting more attention in this field. (Ramautar et al. 2013). GC-MS allows the analysis of metabolites in the mass range of 650-1000m/z and its applications are dependent on chemical reactions which enhance the volatility of the metabolites and ensure the chemical separation (Halket, et al. 2005; Garcia and Barbas 2011). GC-MS presents different advantages, such as high separation efficiency and high reproducibility. An universal electron ionization (EI) is applied and it provides a standardized mass spectral fingerprints (Fiehn et al. 2000). One of the disadvantages is that metabolites, after the required derivatization, are not very stable and they can be degraded during injection and separation (Kanani et al. 2008; Koek et al. 2006). In terms of type of MS detectors for GC-MS analysis single quadrupole or a time-of-flight (TOF) are the most used. On the other hand, LC-MS has the advantage of requiring minimal sample preparation, without derivatization before the analysis. It is highly applicable to the analysis of a wide range of semi-polar compounds and highly sensitive. The traditional reverse-phase chromatography is used in the separation of non polar and slightly polar molecules (Roberts et al. 2012) whereas HILIC (hydrophilic interaction liquid chromatography) mode is becoming the most common technique for strongly and polar metabolites (Bajad et al. 2006). Several MS detectors can be used in LC-MS analysis, ranging from ultra-high resolution MS, such as Fourier transform ion cyclotron resonance (FT-ICR) or Orbitrap FT, and high resolution MS (TOF) to low resolution MS (ion traps, triple quads (Dwivedi et al. 2008)). One of the disadvantages of LC-MS is the ion suppression, indeed the ionization processes may depend on the presence of matrix compounds, and this effect is closely dependent on the type of ionization (ESI or APCI). Metabolite detection employs several options including single (MS) or tandem

(MS/MS) mass analysers, which show different sensitivity and resolution performances (Gowda and Djukovic 2014). The MS/MS mode, which is characterized by an additional MS/MS fragmentation, offers more information about the identification and the structure of the metabolites. Despite the most common approach to study cancer has been the molecular biology for decades, metabolomics is becoming one of the fastest analytical technologies in cancer research, considering the metabolic cancer phenotypes as a possible therapeutic target. Taking into account the increased interest on targeting metabolism of cancer cells, metabolomics approach is rising year by year, in the investigation of metabolic changes associated with the tumor phenotypes (Armitage and Barbas 2014).

- **Metabolomics in thyroid cancer research**

Several studies in cancer research have been focused on the investigation of metabolic features linked to the neoplastic transformation and development. The most studied pathways are glycolysis, TCA cycle and oxidative phosphorylation, with all their related regulation mechanism. Numerous works have proved successful application of genomics, transcriptomics, and proteomics in the field of thyroid cancer research (Xing et al. 2013; Krause et al. 2009). Determining the type of thyroid cancer and, consequently, the prognosis and the treatment is a crucial step in the clinical practice. Unfortunately, classical histopathological approaches can be inconclusive and for this reason, molecular and metabolic biomarkers are increasingly needed in thyroid cancer research (Wojakowska et al. 2015). The metabolomics approach implemented in identification of biomarkers for diagnosis and classification of thyroid tumors has been dynamically expanding in recent years and, significant differences were observed between the metabolomes of normal thyroid tissues and neoplastic lesions, as well as between benign and malignant nodules (Miccoli et al. 2012; Guo et al. 2014). Furthermore, several studies have shown the link between TC oncogene mutations and metabolic alterations, particularly involved in glucose uptake,

glycolysis, and glutamine metabolism (Ciavardelli et al. 2017). Interestingly, *BRAF*^{V600E} has been associated with a glycolytic phenotype in PTC, through the regulation of the expression of the isoform M2 of pyruvate kinase (PKM2), constituting an aggressive tumor features of PTC (Feng et al. 2013). Therefore, aggressive tumors, harboring *BRAF*^{V600E} mutation, according with their need for glucose to fuel proliferation, express the highest levels of metabolic carriers, such as GLUT1 and MCT4 (Ciavardelli et al. 2017). On the other hand, also alterations in glutamine metabolism have been related to *BRAF*^{V600E} positive PTC, particularly high expression rate of proteins involved in glutaminolysis (Kim et al. 2016). Furthermore, RAS, PTEN and TP53 mutations, frequently mutated in TC (Ciavardelli et al. 2017; Carracedo and Pandolfi 2008), have been studied in association with metabolic features involved in glucose metabolism (Ciavardelli et al. 2017). From this point of view, metabolomics can help to provide fundamental mechanistic insight into thyroid cancer development and progression. Numerous studies clearly highlighted the investigative power and utility of metabolomics in discriminating healthy tissues or benign thyroid nodules and malignant lesions (Ciavardelli et al. 2017). In particular, increased levels of lactic acid, often paralleled by alanine, have been found relevant in TC subtypes (Ryoo et al. 2016). High levels of lactic acid are a common feature of tumors characterized by a Warburg phenotype, and particularly, the shuttle of lactate between cancer and stromal cells is an underlined feature of the microenvironment of TC (Gill 2016). Indeed, in a previous study, high levels of amino acids and lactate, combined with a decrease of choline and scyllo-inositol were identified in malignant lesions such as PTC, FVPTC and FTC, compared control samples, through a HR-MAS ¹H-NMR approach (Miccoli et al. 2012). Furthermore, potential biomarkers, including alanine, methionine, glutamate, glycine, tyrosine, phenylalanine, hypoxanthine, acetone and lactate, were commonly found in thyroid lesions (Deja et al. 2013), confirming the promising role of metabolomics in thyroid cancer research. Meanwhile, decrease of glucose, fructose, and galactose and increase of malonic acid and

inosine, detected with GC-MS based metabolomics analysis, were reported as discriminant features for PTC tissue (Chen et al. 2015). Also glutaminolysis, frequently altered in tumor cells due to its role in the providing of nitrogen or protein and nucleotide synthesis and intermediates for TCA cycle (Wise and Thompson 2010), has been found increased in TC malignant lesions compared with healthy tissue (Xu et al. 2015). Significant alteration of lipid profiles, such as higher levels of saturated fatty acids, such as myristic and palmitic acids, have been reported in TC compared with adjacent non-tumor tissues or benign lesions (Tian et al. 2015). Interestingly, PTC and ATC tissues also showed increased expression levels of key enzymes involved in FA biosynthesis (Tian et al. 2015).

II. Aim of the Project

The general aim of this work is the evaluation of changes in metabolic processes occurring in cancer development and progression, such as energetic metabolism and redox balance, in association with cancer genetic background. Based on previous studies on cancer metabolism and cancer metabolic plasticity, and considering the cross talk among oncogenic, metabolic and redox events during tumorigenesis, this thesis aimed to highlighted the need for a holistic and translational approach of studying cancer. Particularly, we focused our studies on PTC, by using *in vitro* model of PTC-derived cell lines with different genotypes. The possibility to detect changes in metabolism and understand metabolic sensitivity and dependence of cancer cells represents an intriguing prospective for the study of cancer and, particularly, for the management of aggressive tumors. Since the initiation, metastasis, therapy resistance, and recurrence of tumor are now believed to be caused and triggered by a subset of cancer cells, such as CSC, the characterization and elimination of these cells is a great challenge and covers a fundamental role in the improvement of the survival of patients. Therefore profiling the metabolism of CSCs is important to identify the metabolic dependencies, as potential “Achilles heel” of PTC. The identification of metabolic features and consequently therapeutic targets covers a fundamental role also for the improvement of cancer therapy, targeting pathways needed for the proliferation and survival of cancer cells through enzymatic inhibitors or compound with anti-tumoral effects.

For these reasons, we focused our project on three main parts:

- 1) Characterize metabolic changes and alterations of redox balance, associated with oncogene pathways, in PTC-derived cell lines. Particularly, we analyzed three PTC-derived cell lines harboring the PTC recurrent somatic genetic alterations (e.g. *BRAF*^{V600E}, *TP53*, *hTERT* mutations and *RET/PTC* rearrangement), using an immortalized normal thyrocytes cell line Nthy-ori3-1, negative for the PTC genetic mutations, for comparisons.

- 2) Identify metabolic phenotype and dependency of CSCs, generated by PTC-derived cell lines through the spheroid-formation assay by means of a metabolomic approach, considering the key role of these CSCs in cancer development and progression.
- 3) Explore the anti-tumoral effects of vitamin C in terms of anti-proliferative and modulation of metabolic processes, in PTC-derived cell lines, understanding how vitamin C affect selectively energetic pathways and redox balance and how different genetic backgrounds affect the cell sensitivity to vitamin C treatment.

III. Materials and methods

Cell culture and treatment

The cell lines used and their respective tissue origin and genetic background are listed in **Table 3**. The human PTC-derived B-CPAP, K-1, TPC-1 cell lines and the SV40-immortalized human thyroid cell line Nthy-ori3-1 cell line were grown as a monolayers in culture in Dulbecco's Modified Eagle's Medium/Ham's F-12 (DMEM/F12) supplemented with 10% fetal bovine serum (FBS, Life Technologies, Milan, Italy), 100 UI/ml penicillin and 100 µg/ml streptomycin (Sigma-Aldrich, Milan, Italy), at 37°C in a humidified 5% CO₂ atmosphere. For subculture, cells were detached from the flasks by trypsinization. Cells were subcultured 2 times per week at a dilution of 1:10. All cell culture work was performed under sterile conditions. Vitamin C was obtained from Sigma-Aldrich (Milan, Italy) and stored at 4°C. Cells were seeded for at least 24h prior the treatment with the vitamin C, at different cell density and in different supports, based on the assay. Vitamin C was solubilized either DMEM or sterile PBS (60 mg/ml) and then diluted for the treatments. Dose-dependent and time-dependent effects of Vitamin C in cell viability were determined. Vitamin C experiment was also coupled with 2.5mM of *tert*-butyl hydroperoxide (TBH), as pro-oxidant, and 10mM of N-acetyl cysteine (NAD), as anti-oxidant).

Table 3. Thyroid cell lines, tissue origins and genetic background.

<i>Cell lines</i>	<i>Tissue origin</i>	<i>hTERT</i>	<i>BRAF^{V600E}</i>	<i>RET/PTC</i>	<i>TP53</i>	<i>References</i>
B-CPAP	PTC	C228T	GTG-> GAG*	wt	GAC->TAC	Meireles et al, 2007; Liu et al., 2013; Caria et al., 2017
K1	PTC	C228T	GTG-> GAG**	wt	wt	Meireles et al., 2007; Liu et al., 2013; Caria et al., 2017
TPC-1	PTC	C228T	wt	<i>RET/PTC1</i>	wt	Meireles et al., 2007; Maric et al., 2011, Liu et al., 2013; Caria et al., 2017
Nthy-ori 3-1	NTT	wt	wt	wt	wt	Maric et al., 2011; Caria et al., 2017

* homozygous; ** heterozygous; PTC: papillary thyroid carcinoma; NTT: normal thyroid tissue; wt: wild type.

Sphere formation assay

A sphere-forming assay was used to assess self-renewal and sphere-forming efficiency (**Figure 5**). B-CPAP, TPC-1 and Nthy-ori3-1 monolayer cells were grown for one week with reduced FBS (5%). Adherent cells were then gently dissociated with StemPro Accutase (Life Technologies), and single cells were cultured in permissive condition, at a density of 2×10^4 cells/ml in low-attachment flasks (Corning, Corning, NY, USA). Cells were cultured in serum-free medium (SFM) as follows: DMEM/F12 with 2% B27 supplement (Life Technologies) and epidermal growth factor (EGF), and basic fibroblastic growth factor (bFGF) (Miltenyi Biotec, Calderara di Reno, BO, Italy) (20 ng/ml each). Every 15 days, spheres that had formed were counted, dissociated, and replated to generate new spheres. The numbers of spheres counted were expressed as a percentage of total plated cells. To induce differentiation of thyrospheres into adherent cells, thyrospheres were cultured in medium supplemented with 10% FBS for at least 4 weeks, and then harvested for molecular analysis. To confirm self-renewal, primary thyrospheres of approximately 200 μm in size were enzymatically dissociated and seeded in SFM every seven days (2×10^4 cells/ml) in order to obtain next generation spheres.

Functional parameters and stemness markers of thyrospheres were compared to thyrospheres generated by the control line Nthy-ori 3-1 (SV-40 immortalized normal human thyroid follicular cells) and showed in **Table 4**, as previously published (Caria et al. 2018).

Table 4. Functional parameters and stemness markers of thyrospheres.

Assays	Nthy-ori3-1	B-CPAP	TPC-1
Formation Assay capability	YES	YES	YES
Selpf-renewal	5 generations	21 generations	5 generations
mRNA expression	Nthy-ori3-1 thyrospheres	B-CPAP thyrospheres	TPC-1 thyrospheres
<i>OCT4</i>	YES	YES	YES
<i>Nanog</i>	YES	YES	YES
<i>ABCG2</i>	YES	YES	YES
<i>ALDH1A1</i>	NO	YES	NO
<i>TTF1</i>	NO	YES (low)	NO
<i>PAX8</i>	YES	YES	YES
Protein expression			
OCT4	YES	YES	YES
Nanog	YES	YES	YES
ABCG2	YES	YES	YES
ALDH1A1	NO	YES	NO
CD44	YES	YES	YES
TTF1	NO	NO	NO
CK19	NO	YES	NO
SSAE-1	YES	YES	YES
Genetic Alterarions	NO	YES (<i>hTERT</i> , <i>BRAF^{V600E}</i> , <i>TP53</i>)	YES (<i>hTERT</i> , <i>RET/PTC1</i>)

(Caria et al. 2017; Caria et al. 2018)

Evaluation of Cytotoxicity

The MTT ((3-(4,5-dimethylthiazol-2-yl)-2,5-diphenyltetrazolium bromide) tetrazolium) cytotoxicity assay was chosen as method for evaluating the cytotoxicity of Vitamin C. MTT is a yellow tetrazolium dye that is reduced by living and metabolically active cells, turning it into an insoluble, purple formazan dye. MTT reduction is specifically carried out by enzymes in the mitochondria. As the quantity of reduction of yellow dye is related to living cells, it enables the estimation of cell viability by measuring the optical density (OD) of the purple formazan produced by the cells (Mosmann 1983).

Briefly, the cells were seeded at the density of 7.5×10^3 cells, in a 96-well plate and left to grow for 24 h. Then, in order to evaluate the sub-lethal concentration for the metabolic and molecular assays, vitamin C was added at six different concentrations (0,1 mM-10 mM) and incubated for 48 h. MTT reagent was prepared by dissolving in PBS and further diluted to 1mg/ml in DMEM. 50 μ L of the MTT reagent 1 mg/ml were added to each well, and the plates were incubated for additional 2h. The resulting formazan crystals were dissolved in 100 μ L of dimethyl sulfoxide (DMSO). The viability was measured at 540 nm using a micro plate reader (Infinite 200, Tecan, Salzburg, Austria) prior 5 minutes shaking. Cell viability was expressed as average \pm SD of percentage of control (untreated cells).

Reactive Oxygen Species (ROS) Assay

For the investigation of intracellular ROS generation, a 2',7'-dichlorofluorescein diacetate (H₂DCFDA) assay was performed (Eruslanov and Kusmartsev 2010). The cell-permeant H₂DCFDA is a chemically reduced form of fluorescein used as an indicator probe for ROS. Upon cleavage of the acetate groups by oxidation, the nonfluorescent H₂DCFDA is converted to the highly fluorescent 2',7'-dichlorofluorescein (DCF). ROS levels and fluorescence intensity are proportional. ROS were measured in BCPAP, K1, TPC-1 and immortalized non tumoral Nthy-ori 3-1 cell lines, seeded in 96-well plates (7.5x10⁴/ml) and grown for 48 hours. Cells were washed with PBS solution and incubated for 30 min with 10 μM of H₂DCFDA (Sigma-Aldrich, Milan, Italy). H₂DCFDA was then removed and cell were washed with PBS. ROS production was measured by reading the fluorescence emitted after 2 hours, using a micro plate reader (Infinite 200, Tecan, Salzburg, Austria) at a controlled temperature of 37 °C. The measurement was performed using an excitation of 490 nm and an emission of 520 nm. For the determination of the ROS production vitamin C-induced cell were seeded in 96-well plates (7.5x10⁴/ml) and grown for 48h. Cells were washed with PBS solution and incubated for 30 min with 10 μM of H₂DCFDA as described above. Cells were then treated with vitamin C, using the different sub-lethal concentrations (15mM, 10mM, 5mM, 5mM respectly for Nthy-ori3-1, TPC-1, K-1 and B-CPAP). *tert*-Butyl hydroperoxide (TBH) was used as positive control, since it is a strong oxidant compound, and N-acetyl-cysteine (NAC), a natural ROS scavenger, was used as a control to ensure effectiveness of the assay. Vitamin C was aslo used in combination with respectively TBH and NAC. ROS production was measured by reading the fluorescence emitted after 2 hours, as described above.

Determination of intracellular aminothiol levels.

High-performance liquid chromatography linked with electrochemical detector (HPLC–ECD) method has been used for the simultaneous determination of intracellular aminothiols (GSH, GSSG, cysteine and cystine), using the method described by Khan et al (Khan et al. 2011) Cells were seeded in 6-well plates (1×10^5 cells/ml) and incubated for 48h. After incubation, cells were scraped and extracted with 150 μ l of 10% meta-phosphoric acid and 150 μ l of 0.05% trifluoroacetic acid (TFA) (Sigma-Aldrich, Milan, Italy) solution. After centrifugation the clear supernatant was injected into the HPLC system. GSH, GSSG, Cysteine and Cystine amount were measured by electrochemical detection, using an HPLC (Agilent 1260 infinity, Agilent Technologies, Palo Alto, USA) equipped with an electrochemical detector (DECADE II Antec, Leyden, The Netherlands) and an Agilent interface 35900E. A C-18 Phenomenex Luna column, 5 μ m particle size, 150 \times 4.5 mm, was used with a mobile phase of 99% water with 0.05% TFA (v/v) and 1% MeOH at a flow rate of 1 ml/min. Electrochemical detector was set at an oxidizing potential of 0.74 V. A calibration curve was created using standards of GSH, GSSG, Cysteine and Cystine (Sigma-Aldrich, Milan, Italy) injected at different concentrations. Data were collected and expressed as ng of GSH, GSSG, Cysteine and Cystine to μ g of measured proteins, analyzed by Bradford assay (Bradford 1976).

Protein extraction and quantification

Total proteins were extracted with the Bradford assay (Bradford 1976), with some modifications. PTC-derived cell lines, B-CPAP, K1, TPC-1, and the immortalized non tumoral Nthy-ori 3-1 cell line were seeded in 6-well plates (1×10^5 cells/ml). Treatment with vitamin C was performed the day after the seeding, using the sub-lethal concentration. Cells were incubated with vitamin C for 24h and then, vitamin C was replaced with culture medium, and treated and no treated cells were incubated for further 24h. After 48 hours from the seeding, growth medium was removed and cells were washed with ice-cold PBS prior to the addition of 180 μ l CelLytic M lysis buffer (Sigma-Aldrich, Milan, Italy) for protein extraction, added with mammalian protease and phosphatase inhibitor cocktail (1:100 v/v). Cells were scraped on ice and lysates were incubated for 15 min on ice before centrifugation at 12500 g at 4 °C for 7 minutes and then stored at -20°C prior quantification. The calibration curve was generated using bovine serum albumin (BSA) in CelLytic M reagent, at different standard concentrations (0.1mg/ml-10mg/ml). Bradford Reagent solution totaling 500 μ l was incubated with either 10 μ l of standard or protein sample at room temperature for 5 minutes. The absorbance was measured at 595 nm using a micro plate reader (Infinite 200, Tecan, Salzburg, Austria) at a controlled temperature of 37 °C. The equation of the line of the standard curve was used to calculate the protein concentration of the cell samples.

Immunoblotting.

For immunoblotting experiments, the antibodies listed in **Table 5.** were used.

Equal amounts (20µg/lane) of proteins were electrophoresed on SDS-10% polyacrylamide gels (Bio-Rad, Hercules, CA, USA). The same protein sample preparation was used for all gels. After gel electrotransfer onto nitrocellulose membrane (Osmonics, Westborough, MA, USA), the membranes were stained with 0,5% (wt/vol.) Ponceau S red (ICN Biomedicals, Aurora, Ohio, USA). After blocking in TBS containing 0.05% Tween 20 (Sigma-Aldrich, Saint Louis, MO, USA) and 5% BSA (Sigma Aldrich), membranes were incubated with the specific primary antibodies diluted in blocking buffer. Filters were incubated with anti-mouse or anti-rabbit horseradish peroxidase conjugated IgGs (Santa Cruz Biotechnology, CA, USA). Immunoreactive bands were identified with a chemiluminescence detection system, as described by the manufacturer (Supersignal Substrate, Pierce, Rockford, IL, USA). The molecular weights of the bands were calculated from comparison with pre-stained molecular weight markers that were run in parallel with the samples. Densitometric analysis of immunoreactive bands was performed using the program ImageJ (JAVA, Wayne Rasband, National Institute of Health, USA).

Table 5. Antibody List

Antigen	Host	Class	Company
β-Actin	Mouse	Monoclonal	Sigma-Aldrich
Glutaminase 1	Rabbit	Polyclonal	Abcam
Glutamate-cysteine ligase	Rabbit	Polyclonal	Sigma-Aldrich
ALDH1-A1	Rabbit	Polyclonal	Millipore
CD44	Mouse	Monoclonal	ThermoScientific
CD19	Mouse	Monoclonal	Millipore
TTF-1	Rabbit	Monoclonal	Abcam

Immunofluorescence.

For immunostaining, cells were enzymatically dissociated and cultured directly on previously sterilized slides and placed in square tissue culture dishes (quadriPERM[®], Sarstedt AG & Co, Nümbrecht, Germany). The cells were maintained for 16 h at 37°C in a humidified 5% CO₂ atmosphere. Cells were fixed with 4% paraformaldehyde for 10 minutes at room temperature. Immunostaining was performed as previously described (24) using rabbit polyclonal anti-GLUT1 (1:200; Abcam, CA, USA) and rabbit polyclonal anti MCT4 (1:100; Abcam, CA, USA) antibodies. Alexa-conjugated (Alexa Fluor 488 or 594, Life Technologies) goat anti-rabbit IgG were used as secondary antibodies. Nuclei were counterstained with 4',6-diamidino-2-phenylindole (DAPI).

Glucose uptake assay.

The measurement of glucose uptake was quantified using the fluorescent D-Glucose analogue 2-deoxy-2-[(7-nitro-2,1,3-benzoxadiazol-4-yl)amino]-D-glucose (2-NBDG), which can be taken up by cells through glucose transporters (Zou et al. 2005). Fluorescence generated by this fluorescent glucose analog is proportional to glucose uptake by the cells and can be used to measure glucose uptake using fluorescent microscopy and flow cytometry. For the assay optimization, cells were plated in 96-well plates at a cell density of 1×10^5 cells/ml and incubated for 24h. The day after the seeding, cells were washed with PBS to ensure the removal of growth medium and consequently glucose. The assay optimization was performed with two different concentrations of 2-NBDG, according to the manufacturing information, (50 and 100 μ M) and with different incubation times of the fluorescent. Finally, the concentration of 50 μ M and the incubation time of 30 minutes were chosen for performing the experiments. Briefly, cells were seeded in 96-well plates at the density of 1×10^5 cells/ml and incubated for 24h. The day after the seeding, cells were washed with PBS to ensure the removal of growth medium and consequently glucose, followed by the addition of 50 μ M of 2-[N-(7-nitrobenz-2-oxa-1,3-diazol-4-yl)amino]-2-deoxy-Dglucose (2-NBDG, fluorescently-tagged glucose derivative, N13195; Invitrogen), which was incubated for 30 minutes. For the vitamin C treatment, different concentrations of vitamin C (15mM for Nthy-ori3-1, 10mM for TPC-1 and 5 mM for K1 and B-CPAP) were prepared in PBS and added with 2-NBDG. After the incubation, external 2-NBDG, with and without vitamin C, was washed off and replaced with PBS. Relative glucose uptake was measured by reading the fluorescence emitted using a micro plate reader (Infinite 200, Tecan, Salzburg, Austria) at a controlled temperature of 37 °C. The measurement was performed using an excitation of 485 nm and an emission of 530 nm.

Glucose Addiction Assay.

To perform the glucose addiction assay, cells were exposed to three metabolic conditions. Control cells were grown in DMEM/F12 with 3.1g/L glucose supplemented with 10% fetal bovine serum (FBS, Life Technologies, Milan, Italy), 100 UI/ml penicillin and 100 µg/ml streptomycin (Sigma-Aldrich, Milan, Italy). The first experimental condition was DMEM with 4.5g/L glucose, (High glucose) supplemented with 10 % heat-inactivated FBS (56 °C,30 min), 100 U/ml penicillin G, 100 µg/ml streptomycin. The second experimental conditions was DMEM with 1 g/L glucose, supplemented with 10 % heat-inactivated FBS (56 °C,30 min), 100 U/ml penicillin G, 100 µg/ml streptomycin. The third experimental condition was DMEM with 0 g/L glucose, supplemented with 10 % heat-inactivated FBS (56 °C,30 min), 100 U/ml penicillin G, 100 µg/ml streptomycin. Cells were seeded at 1×10^5 /ml in 12well plates. After 24h from the seeding, cells were exposed to the experimental conditions for 6 h, 24 h and 48 h. Subsequently, cells were washed with PBS and then gently dissociated with StemPro Accutase (Life Technologies) and counted with Scepter™ 2.0 Cell Counter (Merck Millipore), according to the manufacturer's instructions.

Apoptosis Analysis: Flow Cytometric Analysis with Annexin V/Propidium Iodide staining

In order to investigate cell death induced by vitamin C treatment, a flow cytometric analysis, using the cell apoptosis kit Annexin V/Propidium Iodide (PI) double staining uptake (Invitrogen, Life Technologies, Italia).

The percentage of apoptotic and necrotic cells, induced by vitamin C, was determined by flow cytometric analysis with Annexin V and propidium iodide staining. Annexin V binds with phosphatidylserine externalized from inner plasma membrane after cells undergo apoptosis, serving as a signal for macrophages to eliminate the apoptotic cells at a later stage (Cohen et al. 1992). In healthy cells, phosphatidylserine molecules are embedded in the inner layer of the cell membrane. (Cohen et al. 1992). Propidium iodide (PI) is a viability dye, and it is widely used in conjunction with Annexin V to determine if cells are viable.

In brief, 5×10^5 cells/ml were seed in 6-well plates (Corning, USA) with complete DMEM/F12. Cells were then treated with vitamin C for 48 hours. The cells were washed once with PBS 1X, re-suspended in 100 μ L of annexin binding buffer plus 1 μ l of Annexin V fluorescein isothiocyanate and 1 μ l of PI. Then, the reaction was performed in the dark for 15 min at room temperature. Stained cells were then analyzed by flow cytometry, measuring the fluorescence emission at 530 and 620 nm using 488 nm excitation laser (MoFlo Astrios EQ, Beckman Coulter). Cell apoptosis was analyzed using Software Summit Version 6.3.1.1, Beckman Coulter.

Sample preparation for metabolomics analysis

In order to perform metabolomics analysis, PTC-derived cell lines and the immortalized non tumoral cell line, were seeded in Petri dishes (100mm) at the density of 1.8×10^6 cells. For thyrospheres extraction, adherent cells were cultured in permissive condition, at a density of 2×10^4 cells/mL, in low attachment flasks and in a serum-free medium (SFM) supplemented with epidermal growth factor and basic fibroblastic growth factor. After 48h of growing, the growth medium was removed from the Petri-dishes and aliquoted (500 μ l) in EppendorfTM tubes in order to be extracted as the cells. Both thyrospheres and adherent cells were collected at a density of 4×10^6 cells/mL and washed with a physiological solution to ensure the removal of medium. Adherent cells were then scraped with a mixture of 1 mL of ice-cold methanol and water (80–20) and transferred in EppendorfTM tubes. Thyrosphere cells were centrifuged at 1300 rpm for 10 min and the cell pellet was reconstituted with 1 mL of cold methanol and water (80–20) for metabolite extraction. The extraction was combined with 10 min of ultrasonic treatment at 4°C, to ensure the complete lysis of the cells. The lysate suspensions were then centrifuged at 4500 rpm for 30 min. The upper aqueous phase was separated, aliquoted in Eppendorf tubes and dried in an EppendorfTM Concentrator Plus overnight.

Ultra high performance liquid chromatography-tandem mass spectrometry analysis.

Metabolites in the polar dried fraction of the samples were quantified using an ultra performance liquid chromatography coupled with a TSQ Quantiva™ Triple Quadrupole Mass Spectrometer (UHPLC-MS/MS) using two targeted analysis, based on positive and negative ion mode. For the first analysis samples were reconstituted with 200 µL of acetonitrile:water (7:3v/v) with ammonium carbonate 0,1 M. A BEH amide HILIC column (100 × 2.1 mm, 1.7 µm; Waters Ltd) was used and the mobile phase consisted of: (A) a 0.1% of ammonium carbonate water solution and (B) an acetonitrile solution (600 µL/min of flow rate). For the second analysis sample were reconstituted in water with 0,1% of formic acid and injected using a reverse phase column ACE Excel C18-pfp (150 × 2,1 mm, 2 µm; ACE). The mobile phase consisted of: (A) a 0.1% of formic acid water solution and (B) a 0.1% of formic acid acetonitrile solution. Aqueous metabolites were acquired through selected reaction monitoring (SRM) mass spectrometry analysis following prior infusion of standard compounds. Both mass spectrometry analyses were performed using an mix containing isotope-labelled standards: [¹³C, ¹⁵N] L-proline, L-leucine-d10, L-Valine-d8, L-phenylalanine d5, Succinate-¹³C and Serotonine-d4 (Sigma Aldrich, Gillingham, Dorset, UK) and [¹³C, ¹⁵N] L-glutamate (10 um each) (Cambridge Isotope Laboratories, Andover, MA, USA). The Xcalibur software (Thermos fisher scientific, Waltham, Massachusetts, United States) was used for data acquisition. Putative recognition of all detected metabolites was performed using a targeted MS/MS analysis. Metabolites with different isoforms (2/3-phosphoglycerate and glucose-6-phosphate/fructose-6-phosphate) were not chromatographically resolved, thus peaks of these metabolites were considered as the sum of both isoforms. Calculated masses and mass fragments of the calculated compounds were

reported in **Table 6**. Peak areas, for each detected metabolites, were then normalized by total area and reported as ranks in the bar graph.

Table 6. UHPLC/MS-MS detected compound with calculated masses, mass fragments, polarity and column.

Compound	RT	Precursor (m/z)	Product (m/z)	Polarity	Column
2/3 Phosphoglycerate	4.02	185.000	97.065	Negative	BEH amide
Acetyl-CoA	3.65	810.225	303.049	Positive	BEH amide
ADP	3.92	428	136.174	Positive	BEH amide
Alanine	0.73	90.1	44.275	Negative	C18-pfp
α-ketoglutarate	3.35	145	101.123	Negative	BEH amide
Arginine	0.68	175.15	70.2	Positive	C18-pfp
Asparagine	0.62	133.1	116.049	Positive	C18-pfp
Aspartic Acid	0.7	134.175	74.175	Positive	C18-pfp
ATP	4.05	508	136.189	Positive	BEH amide
cAMP	1.84	330.1	136.21	Positive	BEH amide
CDP	3.98	404	112.132	Positive	BEH amide
Citrate	1.32	191	111	Negative	C18-pfp
CMP	3.96	324.1	112.194	Positive	BEH amide
Coenzyme A	3.74	768.374	261.111	Positive	BEH amide
CTP	4.19	484	112.234	Positive	BEH amide
Dihydroxyacetone phosphate	3.88	169	97.143	Negative	BEH amide
Glucose 6 phosphate/ Fructose 6 phosphate	4.05	259	97.077	Negative	BEH amide
Fructose bisphosphate	4.24	339	97.084	Negative	BEH amide
Fumaric Acid	3.48	115	71.172	Negative	BEH amide
GDP	4.1	444	152.08	Positive	BEH amide
Glucose	2	179	89	Positive	BEH amide
Glutamic Acid	0.74	148	84.15	Positive	C18-pfp
Glutamine	0.72	153.1	89.169	Positive	C18-pfp
Glyceraldehyde-3-phosphate	3.83	169.009	97	Negative	BEH amide
Glycine	0.68	76.1	48.2	Positive	C18-pfp
GMP	3.99	364.1	152.197	Positive	BEH amide
GTP	4.23	524	152.106	Positive	BEH amide
Histidine	0.68	156.1	110.15	Negative	C18-pfp
Isocitrate	1.71	191	111	Negative	C18-pfp
Lactic Acid	2.5	89	43	Negative	BEH amide
Malic Acid	3.67	133	115.081	Negative	BEH amide
Methionine	3.4	150.05	61.16	Positive	C18-pfp
NAD+	3.82	664.1	136.237	Positive	BEH amide
NADH	3.72	666.183	301.929	Positive	BEH amide
NADP+	4.15	744.1	136.2	Positive	BEH amide
NADPH	4.09	744.057	396.942	Negative	BEH amide

Nicotinamide	1.23	123.152	80.165	Positive	C18-pfp
Nicotinic Acid	1.23	124.07	80.111	Positive	C18-pfp
Oxaloacetate	3.34	131	87.084	Negative	BEH amide
Phenylalanine	3.61	166.1	120.15	Positive	C18-pfp
Phosphoenolpyruvate	3.94	167	79.081	Negative	BEH amide
Pyruvic acid	2.75	87	43	Negative	BEH amide
Serine	0.69	106.075	60.2	Positive	C18-pfp
Succinic acid	3.51	117	73	Negative	BEH amide
Succinyl-CoA	3.92	868.1	361.214	Positive	BEH amide
Tryptophan	4.23	205.2	188.093	Positive	C18-pfp
Tyrosine	2.25	182.075	136.125	Positive	C18-pfp
UDP	4	405	97.062	Positive	BEH amide
UMP	3.85	325	97.179	Positive	BEH amide
UTP	4.19	485	378.973	Positive	BEH amide

Compound name, retention time, calculated masses, mass fragments, polarity and column for all detected metabolites.

Gas chromatography-mass spectrometry analysis.

Dried extracts from thyrospheres and adherent cells were derivatised with 50 μL of a solution of methoxyamine in pyridine (10 mg/mL) (Sigma-Aldrich, St. Louis, MO, USA). After 1h at 70°C, 50 μL of N-Methyl-N-(trimethylsilyl)-trifluoroacetamide, MSTFA, (Sigma-Aldrich, St. Louis, MO, USA) was added and left at room temperature for one hour. Successively, cellular extracts were re-suspended with 50 μL of hexane and transferred into vials for the GC-MS analysis. Samples were injected splitless into a 7890A gas chromatograph coupled with a 5975C Network mass spectrometer (Agilent Technologies, Santa Clara, CA, USA) equipped with a 30 m \times 0.25 mm ID, fused silica capillary column, which was chemically bonded with 0.25 μM TG-5MS stationary phase (Thermo Fisher Scientific, Waltham, MA, USA). The injector temperature was 250°C. The gas flow rate through the column was 1 ml/min. Transfer line temperature was 280 °C. The column initial temperature was kept at 60 °C for 3 min, then increased from 60°C to 140°C at 7°C/min, held at 140°C for 4 minutes, increased from 140°C to 300°C at 5°C/min and kept in isocratic mode at 300°C for 1 minute. Peak detection and deconvolution, filtering and normalization were performed using a pipeline on Knime (Liggi et al. 2018). A total of 24 metabolites was detected (**Table 7**) and the identification was performed using the standard NIST 08 (<http://www.nist.gov/srd/mslist.cfm>), Fiehn 2013 (<http://fiehnlab.ucdavis.edu/Metabolite-Library-2007>) and GMD (<http://gmd.mpimp-golm.mpg.de>) mass spectra libraries and, when available, by comparison with authentic standards.

Table 7. GC/MS identified metabolites with masses (m/z) and retention time (RT).

Compound	m/z	RT (minutes)
Alanine	116	9.92
Aminomalonic Acid	147	18.32
Aspartic Acid	160	16.97
Citric acid	273	19.41
Cholesterol	368/485	49.67
Fructose	217/307	29.08
Galactitol	319	30.46
Glucose	317	29.62
Glutamate	84/156/264	20.59
Glycero-1-phosphate	299	26.77
Glycine	147	14.1
Isoleucine	86	11.55
Lactic Acid	117	8.89
Malic Acid	147	18.99
Myo Inositol	605	33.42
Oxalic Acid	133	10.75
Palmitic Acid	313	32.97
Phenylalanine	120	21.04
Proline	70	11.54
Pyruvic Acid	174	8.75
Ribitol	217	25.64
Sorbitol	205	30.36
Stearic Acid	132	36.59
Succinic Acid	147	14.37
Valine	144	12.24

Nuclear magnetic resonance spectroscopy: ^1H -NMR.

Dried polar extracts from adherent cells were suspended in 690 μL potassium phosphate buffer in D_2O (0.1 M, pH 7.4) and 10 μL of TSP (sodium 3-trimethylsilyl-propionate-2,2,3,3,- d_4) as internal standard (98 atom% D, Sigma-Aldrich, Milan). An aliquot of 650 μL was transferred to 5-mm NMR glass tubes. NMR experiments were carried out using a Varian UNITY INOVA 500 spectrometer operating at 499.839 MHz for proton and equipped with a 5 mm double resonance probe (Agilent Technologies, CA, USA). ^1H -NMR spectra were acquired at 300K with a spectral width of 6000 Hz, a 90° pulse, an acquisition time of 2s, a relaxation delay of 2s, and 256 scans. The residual water signal was suppressed by applying a presaturation technique with low power radiofrequency irradiation for 2s. ^1H -NMR spectra were imported in ACD Lab Processor Academic Edition (Advanced Chemistry Development, 12.01, 2010) and pre-processed with line broadening of 0.5 Hz, zero-filled to 64K, and Fourier transformed. Spectra were manually phased and baseline corrected and chemical shifts referenced internally to TSP at $\Delta = 0.0$ ppm. The ACD Labs intelligent bucketing method was used for spectral integration between 0.50–8.50 ppm. A 0.01 ppm bucket width was defined with an allowed 50% looseness resulting in buckets that ranged between 0.005 and 0.015 ppm in width.

Statistical Analysis

- **Multivariate statistical analysis**

Multivariate statistical data analysis was performed using SIMCA (version 14.0, Umetrics, Umea, Sweden). Raw data from untargeted analysis, both from ¹H-NMR (for adherent cells) and GC/MS (for thyrosphere and adherent cells) techniques were processed and organized in matrix for the multivariate statistical analysis to investigate separation across the cell samples. To account for variable dilution factors of metabolite concentrations, datasets were normalized to the total area. All imported data were scaled for the multivariate statistical analysis, using Pareto scaling for ¹H-NMR data and UV-scaling for GC/MS data. A Principal component analysis (PCA), a unsupervised analysis, coupled with Hotelling t-squared was used to identify the presence of outliers. PCA is characterized by a linear transformation which preserves as much of the variance in the original data (Jolliffe 2012). Subsequently a supervised analysis, such as Partial Least Squares Discriminant Analysis (PLS-DA) was performed to investigate all the metabolic differences between the PTC-derived cell lines. Indeed, PLS-DA relies in the class membership of each observation and allows the investigation of clusters within the datasets (Barker and Rayens 2003). Variable importance projection list (VIP), showing the most important variables over the models as a whole, was used to detect the metabolites responsible for the separation. Only metabolites with VIP values >1.0 were further considered for the univariate stastical analysis.

- **Univariate statistical analysis**

GraphPad Prism software (version 7.01, GraphPad Software, Inc., CA, USA) was used to perform the univariate statistical analysis of the data. Statistical significance was calculated comparing average of results from each PTC-derived cells with control cells. Since the

comparisons were performed in two-group case (each tumoral cells vs. control cells) a Student t-Test was chosen to verify the statistical significance.

IV. Results

Part one: Metabolic and redox reprogramming in PTC-derived cell lines

Bioenergetic metabolic changes in PTC-derived cell lines.

To investigate metabolic changes in PTC-derived cell lines, the metabolomic profile was characterized by untargeted ¹H-NMR and targeted UHPLC-MS/MS analysis of the cellular extracts. Principal components analysis (PCA) coupled with Hotelling's t-squared was performed using the ¹H-NMR untargeted profile, to examine the distribution of samples and ensure the absence of outliers (**Figure 6A**). Data were then subjected to a supervised Partial Least Square-Discriminant Analysis (PLS-DA) to evaluate differences between the cell lines. PLS-DA showed a clear separation between PTC-derived and control cells (**Figure 6B**). Then changes in energetic pathways, such as glycolysis, TCA cycle and part of glutaminolysis, were investigated by using UHPLC/MS-MS with a targeted analysis. Our results revealed that the majority of metabolites associated with glycolysis were increased in B-CPAP compared to K1 and TPC-1, such as glucose-6-phosphate/fructose-6-phosphate (G6P/F6P), dihydroxyacetone phosphate (DAHP), glyceraldehyde-3-phosphate (GAP), and 2/3-phosphoglycerate (2PG/3PG), phosphoenolpyruvate (PEP). Glucose levels were significantly decreased in TPC-1 and K1, compared to the control line. Considering the three PTC-derived cell line, glucose showed an increasing trend from K1 to Nthy-ori3-1 cells (K1<TPC-1<B-CPAP<Nthy-ori3-1). On the contrary, lactate was found significantly increased only in K1, compared to the control line, while B-CPAP cells showed a significant decrease of this metabolite (**Figure 7**). Moreover, G6P/F6P, 2PG/3PG, PEP and pyruvic acid levels were significantly decreased in K1 and TPC-1 cells compared to the control line. Conversely, F1,6P was found to be significantly decreased only in TPC-1 and B-CPAP compared to the control line. Considering metabolites involved in the TCA cycle, levels of acetyl-CoA were found to be significantly decreased in all PTC-derived cells compared to Nthy-ori3-1 cells. On the contrary, citrate was significantly increased in B-CPAP and K1, while isocitric acid was significantly decreased in B-CPAP and K1 as well. α -ketoglutarate

levels were significantly increased in all PTC-derived cells. Succinyl-CoA was found to be significantly decreased in TPC-1 and K1, as well as succinic and fumaric acids which were significantly decreased in K1 and B-CPAP cell lines. While fumarate was increased only in B-CPAP. Conversely, acetyl CoA, isocitrate, succinyl CoA, succinate and oxaloacetate were significantly decreased for all cancer cells (**Figure 7**). We further investigate the glutaminolysis pathway, measuring glutamine and glutamate and α -ketoglutarate levels (described above). Glutamine was significantly increased in all PTC-derived cells, while glutamate was significantly increased only in B-CPAP cells and significantly decreased in K1 cells compared to control cells. Instead, aspartate levels were found to be significantly increased only in TPC-1 (**Figure 7**).

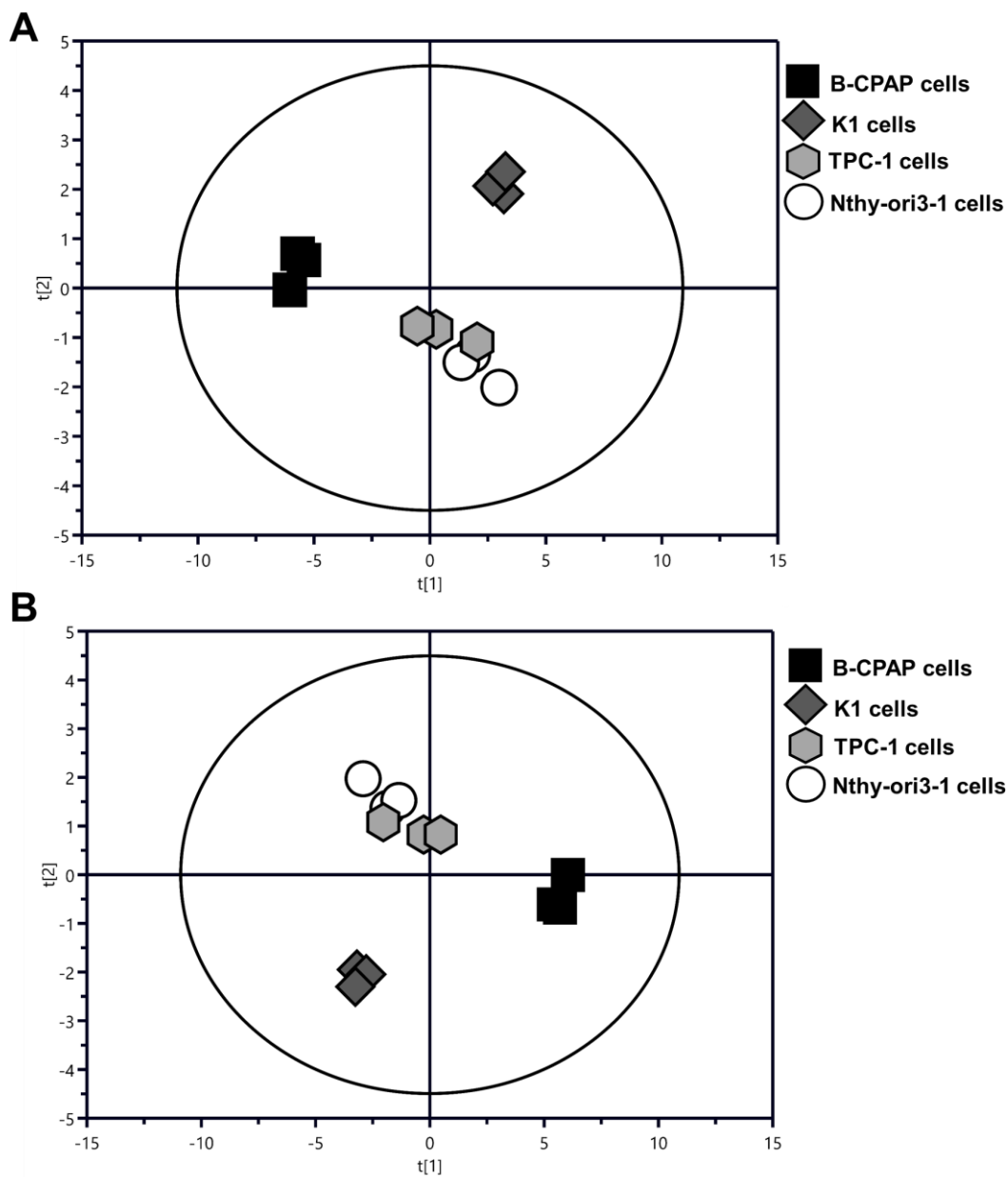


Figure 6. Multivariate statistical analysis of PTC-derived and control cells untargeted $^1\text{H-NMR}$ profile. A) PCA of PTC-derived and control cells. B) PLS-DA of PTC-derived and control cells ($R^2\text{X}$: 0.877, $R^2\text{Y}$: 0.647, Q^2 : 0.484, $p=0.00090$).

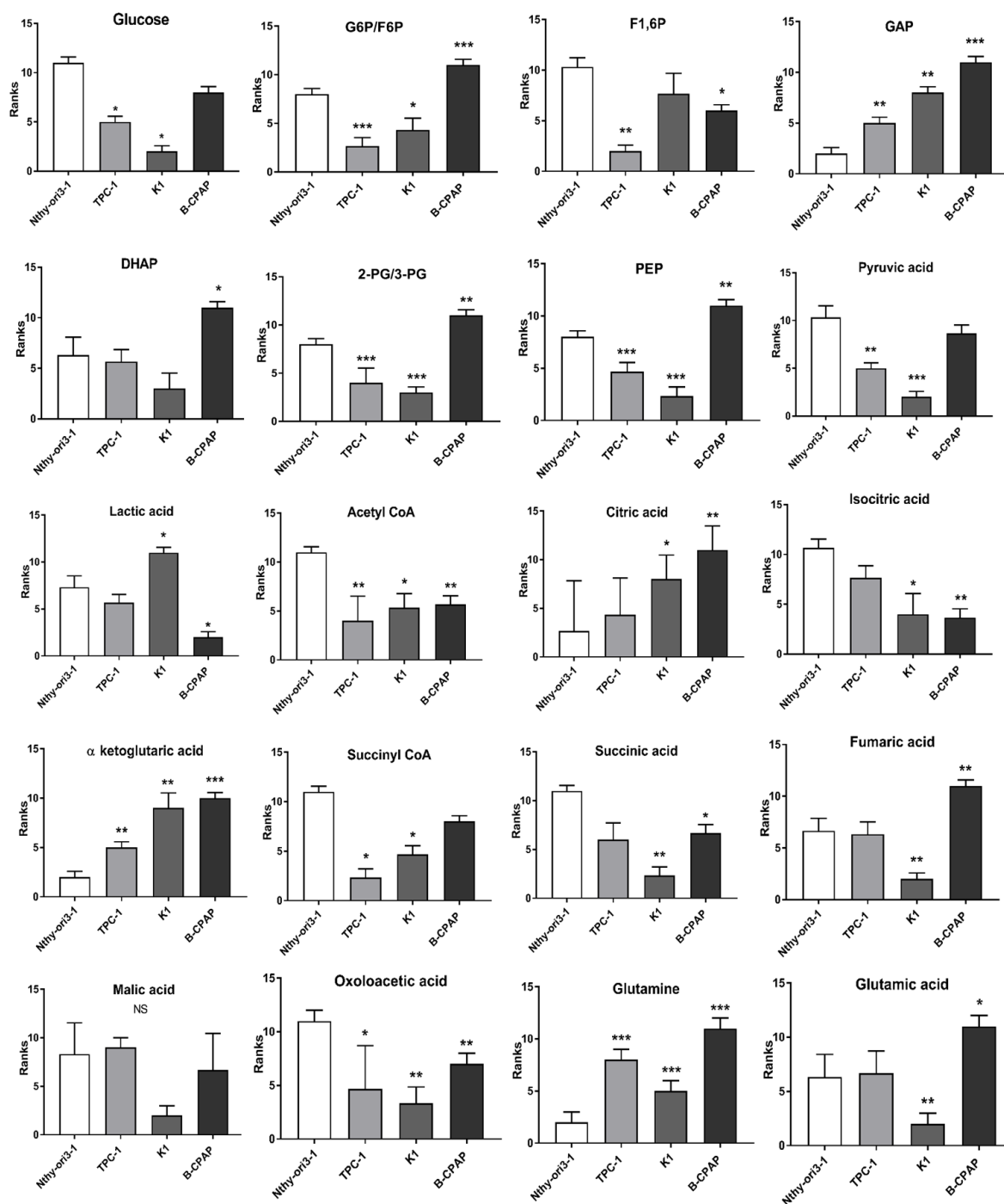


Figure 7. Energetic metabolites in PTC-derived cell lines. Metabolites levels were measured using UHPLC-MS/MS. Bar graphs indicate the peak areas of the metabolites (n=3) normalized for total area and expressed in the graphs as ranks (data transformation in which numerical or ordinal values are replaced by their rank when the data are sorted). Statistical analyses were performed by Student T-test. Data are presented as means \pm standard deviation. All experiments were performed three times independently, each time in triplicate to confirm the results. Results were considered significant when * $P < 0.05$, ** $P < 0.01$, *** $P < 0.001$.

Glucose and lactate exchange across the membrane of PTC-derived cells

In order to better define the role of lactate in glucose homeostasis as well as in the function of glycolysis in thyroid cancer cells we examined the glucose uptake, which is the rate-limiting step in aerobic glycolysis, extracellular levels of lactate and their respective carriers. Particularly, among all the members of mammalian GLUTs family, we focused on GLUT1, which is reportedly expressed abundantly in cancer cells (Furuta et al. 2010) while for the lactate excretion we investigated the expression of MCT4.

Relative glucose uptake was assessed through the fluorescent glucose analog 2-NBDG. Our data revealed that only B-CPAP cells showed a significant increased uptake of glucose (B-CPAP > K1 > TPC-1 > Nthy-ori3-1) (**Figure 8A**). Aliquots of growth medium were collected for the measurement of extracellular lactate, excreted by the cells due to its accumulation. Peak area of lactate was reported as percentage of the control line. Only B-CPAP cells displayed a significant increase of extracellular lactate compared the other cell lines (**Figure 8B**).

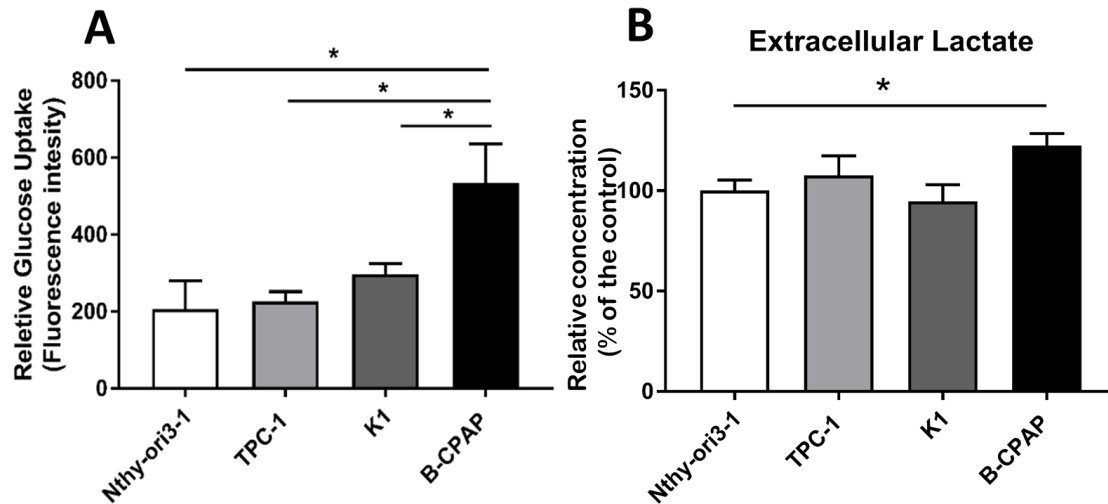


Figure 8. Relative glucose uptake and extracellular lactate level. **A)** Quantification of the relative glucose uptake was measured through the fluorescent glucose analog 2-NBDG in cancer cells and control cell lines. **B)** Extracellular lactate levels, quantified in the growth medium, expressed as percentage of the relative concentration of the Nthy-ori3-1 cells. Data are presented as means \pm standard deviation. All experiments were performed three times independently, each time in triplicate to confirm the results. Statistical analysis was performed by Student t-Test. Results were considered significant when * $P < 0.05$, ** $P < 0.01$, *** $P < 0.001$.

To further confirm the cellular exchange of glucose and lactate across the cellular membrane, metabolites carriers, glucose transporter GLUT1 and lactate transporter MCT4, were analyzed by immunofluorescence analysis. Our data reported that Nthy-ori3-1 and TPC-1 cells were barely positive for both carriers expression (**Figure 9A and 9B**) while K1 and, mostly, B-CPAP cells were positive for GLUT1 and MCT4 (**Figure 9E, F, G and H**).

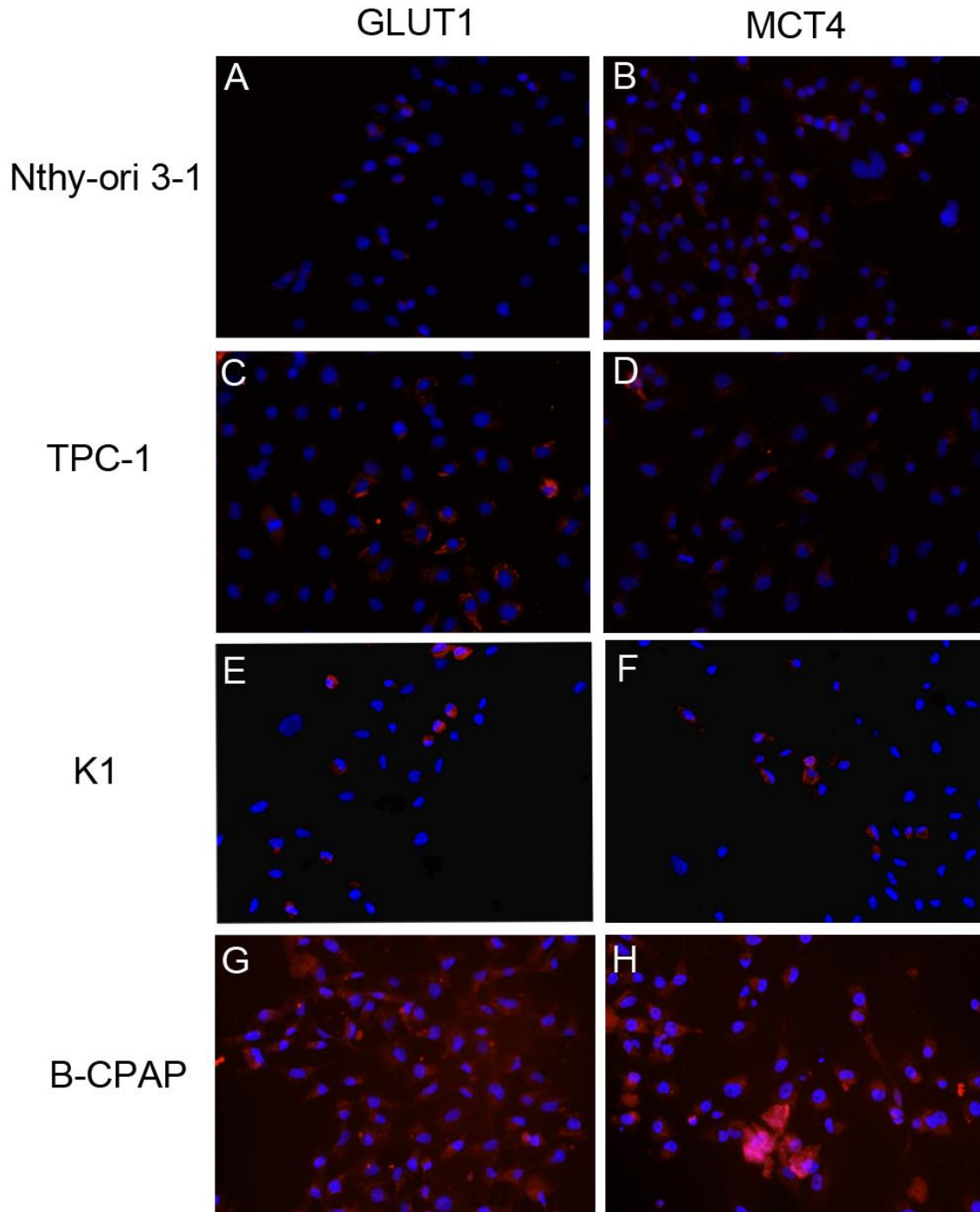


Figure 9. Expression of GLUT-1, MCT-4 in thyroid cells. Immunofluorescence pattern in Nthy-ori3-1 for both GLUT1 (A) and MCT4 (B), in TPC-1 for GLUT1 (C) and MCT4 (D), in K1 for GLUT1 (E) and MCT4 (F) and in B-CPAP for both GLUT1 (G) and MCT4 (H). Nuclei were stained with DAPI (blue), GLUT1 and MCT4 were stained in red.

Cell viability was measured after the exposure for 6h, 24h and 48h of glucose at different concentrations. After only 6 h of exposure of high, low and no glucose concentration, the cell viability was not affected for all PTC-derived cell lines and the control line (**Figure 10A**). After 24h of incubation, the low glucose condition induced a significant decreased of viability only in K1 cell, while, at the same incubation time, the no glucose condition induced a significant decreased of viability in all PTC-derived cells and control cells (**Figure 10B**). Interestingly, after 48h of exposure the high glucose condition resulted in increased cell density for K1 and B-CPAP cells. Moreover, no glucose concentration, at 48 hours of exposure, resulted in a significant decreased in cell viability for all PTC-derived cells and the control cells (**Figure 10C**). All the statistical results are listed in **Table 7**.

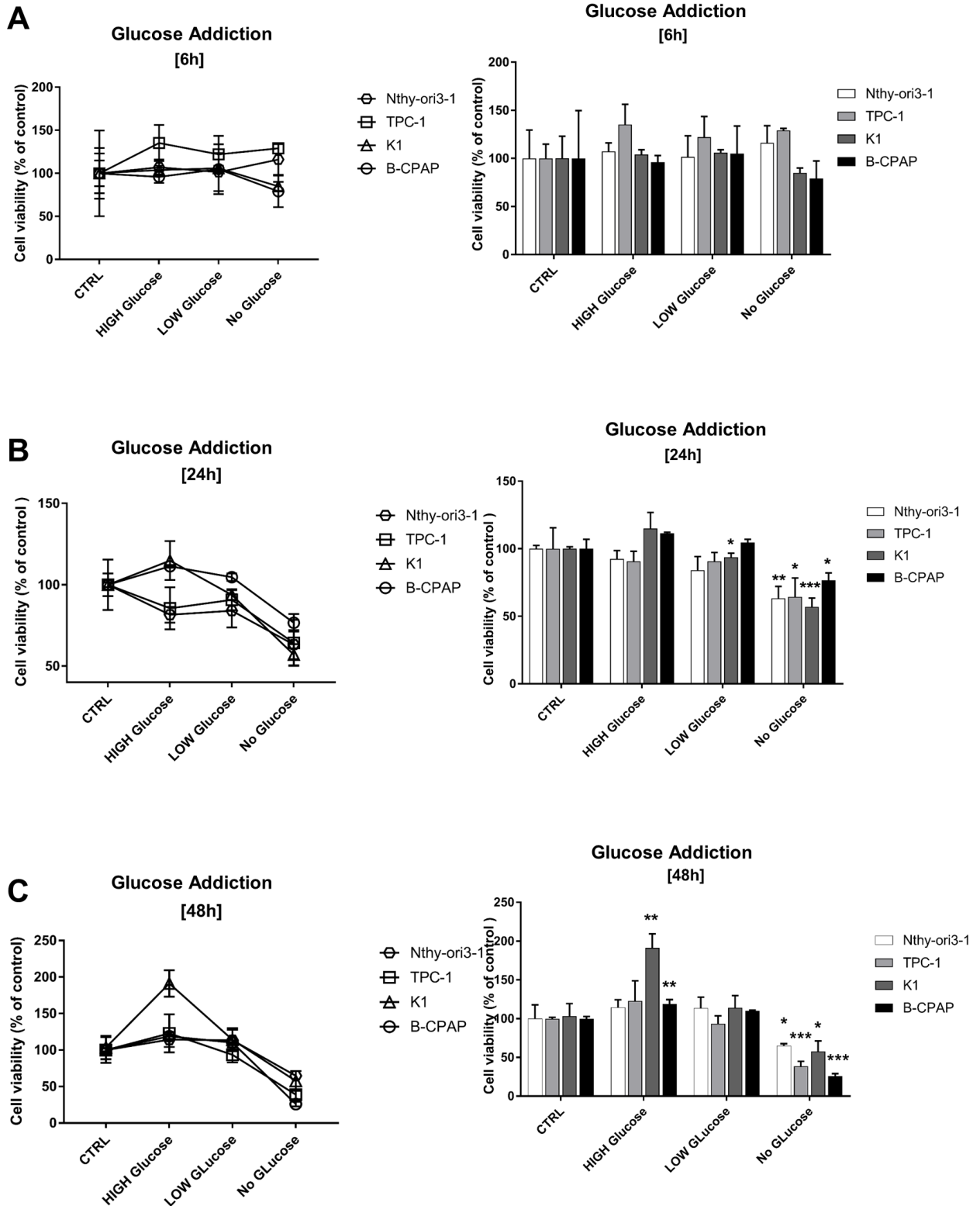


Figure 9. Glucose addiction assay. Cell viability after the exposure 6h (A), 24h (B) and 48h (C) glucose starvation. Data, expressed as % of control for each cell line (cells seeded in DMEM/F12), are presented as means \pm standard deviation. All experiments were performed three times independently, each time in triplicate to confirm the results. Statistical analyses were performed by Student T-test. Results were considered significant when * $P < 0.05$, ** $P < 0.01$, *** $P < 0.001$, against control.

Incubation	Metabolic conditions	Nthy-ori3-1	TPC-1	K1	B-CPAP
6h	High Glucose	NS	NS	NS	NS
	Low Glucose	NS	NS	NS	NS
	No Glucose	NS	NS	NS	NS
24h	High Glucose	NS	NS	NS	NS
	Low Glucose	NS	NS	*	NS
	No Glucose	**	*	***	*
48h	High Glucose	NS	NS	**	**
	Low Glucose	NS	NS	NS	NS
	No Glucose	*	***	*	***

Table 8. Statistical analysis results of glucose starvation assay. NS= not statistical significance. Statistical analysis was performed by Student t-Test. Results were considered significant when *=p<0.05; **=p<0.001; ***=p<0.0001.

Redox status in PTC-derived cell lines

We further investigated the redox state of the three PTC-derived cell lines in comparison with the non tumoral control line, Nthy-ori3-1. We assessed intracellular aminothiols, as intracellular antioxidant species (reduced and oxidized glutathione, cysteine and cystine) through high pressure liquid chromatography (HPLC) coupled with an electrochemical detector (ECD), intracellular reactive oxygen species through a colorimetric assay and intracellular electron carriers (NAD^+ and NADP^+) involved in oxidation-reduction reactions through UHPLC-MS/MS analysis.

Peak areas of intracellular aminothiols were normalized using protein contents (ng of aminothiols per μg of proteins) and expressed as ratio of reduced and oxidized forms. GSH/GSSG ratio, considered a marker for oxidative stress, was significantly decreased in B-CPAP, K1 and TPC-1 cancer cells compared to control cells, (**Figure 11A**). Similarly, the cysteine/cystine ratio, another important biomarker of redox status of cells, was significantly decreased in B-CPAP, K1 and TPC-1 cells compared to control cells (**Figure 11B**). To further elucidate alteration in the redox state of thyroid cancer cells in comparison with non tumoral cells, we investigated the intracellular ROS levels, exposing cells to 2', 7'-dichlorodihydrofluorescein diacetate $\text{H}_2\text{-DCF-DA}$ (10 μM) for 30 minutes. Intracellular ROS levels, expressed in percentage of control (non tumoral cell line, Nthy-ori3-1) were significantly increased in cancer cells compared to non tumoral cells (**Figure 11C**). Electron carriers, such as NAD^+ , NADH , NADP^+ , NADPH and respectively ratio were detected by targeted UHPLC-MS/MS analysis and reported as ranks of peak areas normalized by total area. Levels of NAD^+ were significantly increased in K1 and B-CPAP cells while NADH levels were decreased in all PTC-derived cells, compared to the control cells (**Figure 11D**). Consequently, we found a significant increase of NAD^+/NADH ratio in K1 and B-CPAP cells (**Figure 11D**). Similarly, NADP^+ levels were significantly increased in B-CPAP and

K1 cells compared to the control cells, while $\text{NADP}^+/\text{NADPH}$ ratio was increased only in B-CPAP cells (**Figure 11E**).

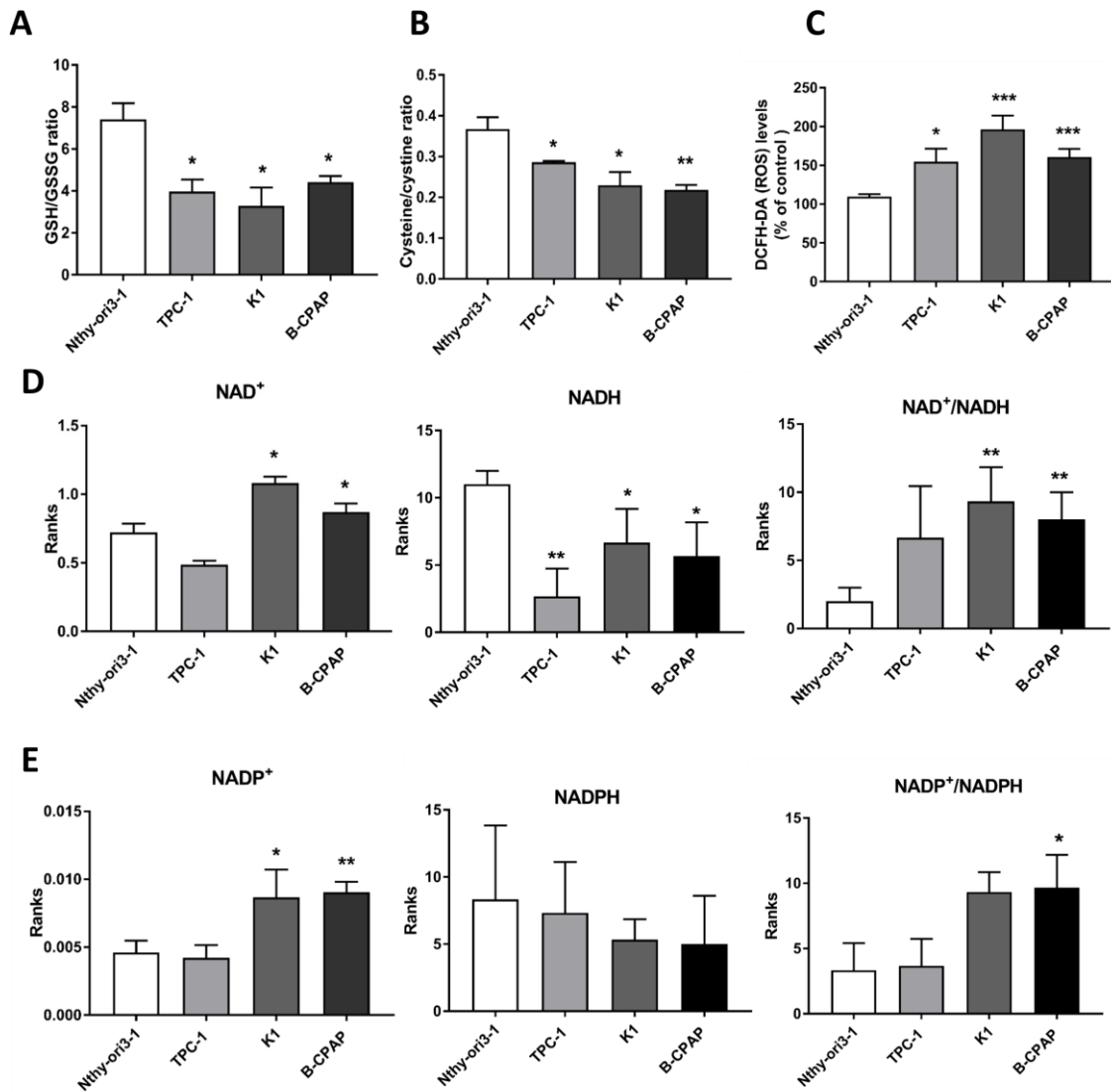


Figure 11. Redox control in human thyroid cell lines. (A) Levels of GSH/GSSG ratio in human thyroid cell lines. (B) Levels of Cysteine/Cystine ratio in human thyroid cell lines. (C) ROS level in human thyroid cancer cell lines, expressed as % of control (human thyroid cell line, Nthy-ori3-1), were probed with DCFH-DA (10uM) for 30 minutes. (D) Intracellular NAD⁺, NADH and NAD⁺/NADH ration levels. (E) Intracellular NADP⁺, NADPH and NADP⁺/NADPH ratio levels detected by ultra high performance liquid chromatography–mass spectrometry (UHPLC-MS/MS) targeted analysis as described in Material and Methods. Data are presented as means ± standard deviation. All experiments were performed three times independently, each time in triplicate to confirm the results. Statistical analysis were performed by Student t-Test. Results were considered significant when * P<0.05, ** P<0.01, *** P<0.00

Glutamate cysteine ligase and glutaminase 1 expression.

According to the alteration in the redox state of thyroid cancer cells, we investigated changes in GSH synthesis, studying the expression of the catalytic subunit of GSH synthetic enzymes glutamate-cysteine ligase (GCL). Expression of GCL was measured by immunoblotting and reported as fold change of the control non tumoral line. GCL levels were found significantly increased in B-CPAP and K1 compared to non tumoral cells (**Figure 12A**)

On the other hand, we decided to further investigated the role of the glutaminolysis pathways in thyroid cancer cells by assessing the expression of Glutaminase-1 (GLS1), an enzyme involved in the utilization of glutamine in the first step of glutaminolysis. GLS1 expression levels, reported as fold change as describe above, were found to be significantly overexpressed in all PTC-derived cells compared to non tumoral cells (**Figure 12B**).

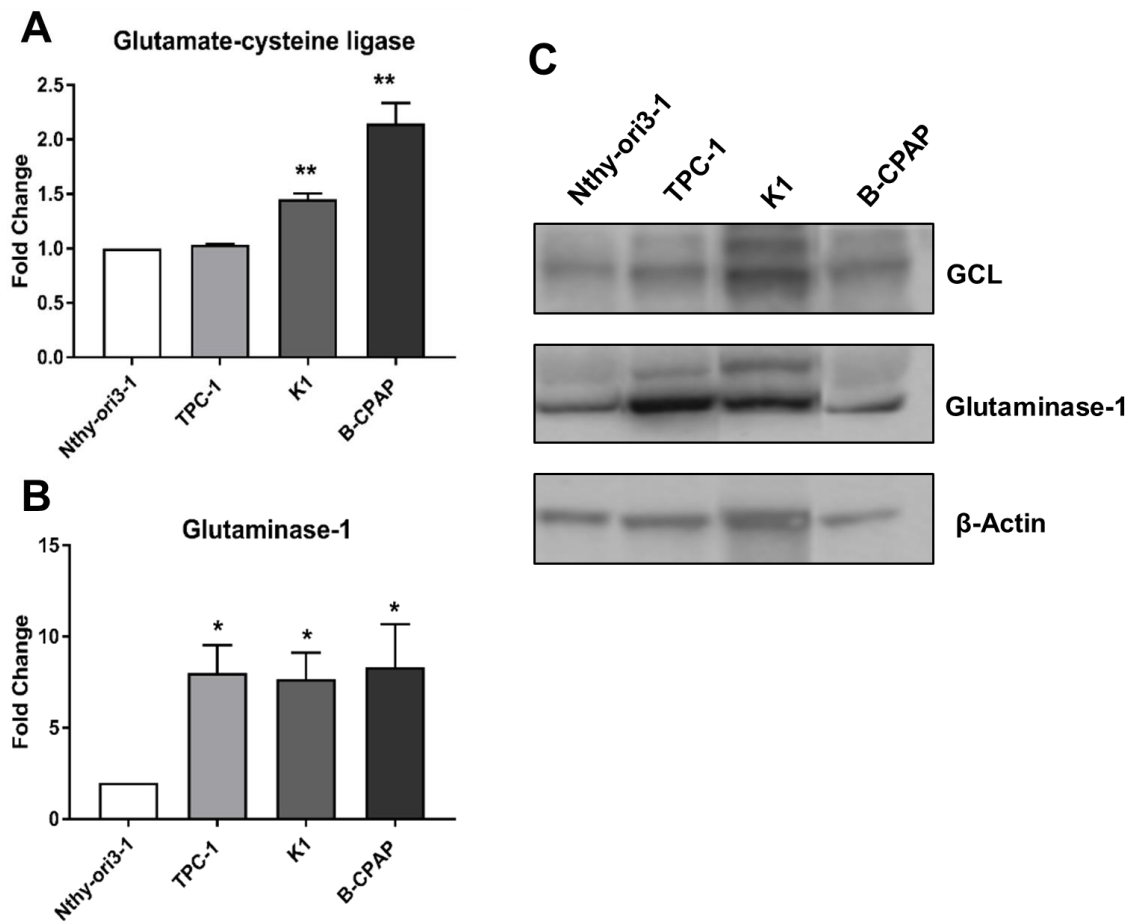


Figure 12. Expression of glutamate-cysteine ligase and glutaminase 1. **A)** Expression of glutamate-cysteine ligase in PTC-derived control cells. **B)** Expression of glutaminase 1 in PTC-derived and control cells. **C)** Captures of gels for both proteins and the reference gene. Data are expressed as fold change of expression in the control cells, and were normalized to actin as reference gene. All experiments were performed three times independently, each time in triplicate to confirm the results. Statistical analysis were performed by Student's t-Test. Results were considered significant when * $P < 0.05$, ** $P < 0.01$, *** $P < 0.001$.

IV. Results

Part two: Metabolomic alterations in CSCs-like in thyrospheres derived from PTC-cell lines.

Thyrospheres Forming Assay and stemness profile

Adherent cells were seeded at a density of 2×10^4 cells/ml in serum-free medium (SFM) supplemented with epidermal growth factor (EGF) and basic fibroblastic growth factor (bFGF). In these conditions, B-CPAP, TPC-1 and Nthy-ori3-1 cells were able to form thyrosphere in SFM. Cells began to form spheres on day 3 reaching their maximum after seven days of suspension culture (**Figure 13 A-B-C-D**). Stemness markers were expressed in PTC-derived thyrospheres. Particularly CD44 was expressed in thyrospheres from both B-CPAP, TPC-1 and Nthy-ori3-1 cell lines, (**Figure 13E**) while aldehyde dehydrogenase 1 (ALDH1) was expressed only in B-CPAP thyrospheres (**Figure 13F**). The TTF-1 transcription factor and the differentiation marker CK19 were detected only in B-CPAP adherent cells as well as in Nthy-ori3-1 cell but were negative in TPC-1 (**Figure 13 G**). To evaluate the presence of self-renewing cells within thyrospheres, primary thyrospheres were enzymatically dissociated and re-seeded at the initial cell density. B-CPAP cells had an extensive capacity for self-renewal, reaching at least 21 generations (**Figure 13 H**), whereas TPC-1 and Nthy-ori 3-1 self-renewal capacity was instead limited to five and four generation, respectively (**Figure 13 I**)

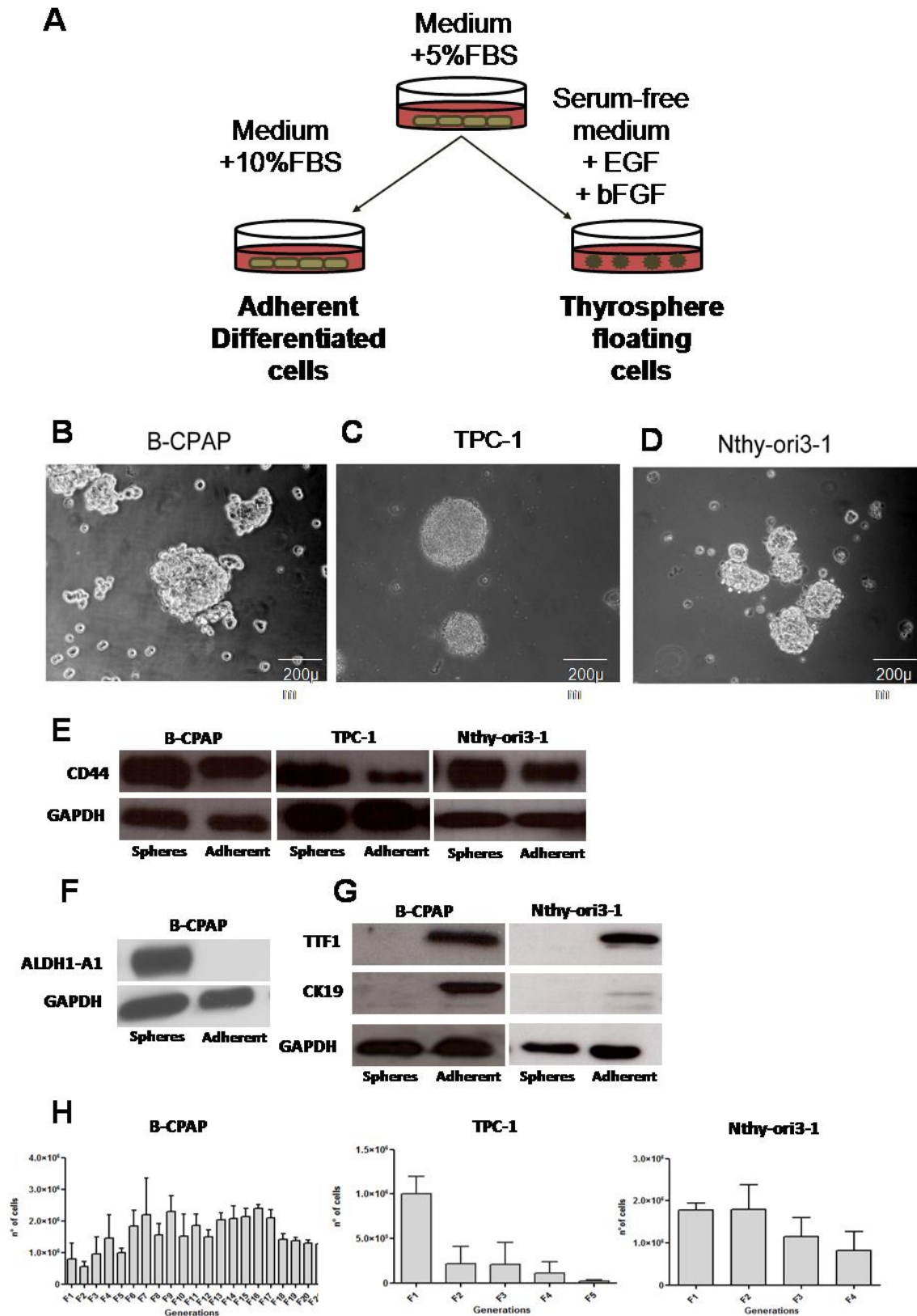


Figure 13. Thyrospheres forming assay. (A) The sphere-forming assay workflow. (B) A representative image of thyrospheres formed by B-CPAP cells at 7 days, 20x. (C) A representative image of thyrospheres formed by TPC-1 at seven days, 20x (D) A representative image of thyrospheres formed by Nthy-ori3-1 at seven days, 20x (E-G)

Western blot analysis of stemness (ALDH1-A1, CD44) and differentiation markers (TTF1 and CK19) in adherent and thyrosphere cells.(H) Self-renewal assay of cell lines: graphs show the total number of cells (Y axis) for each generations after 7 day of culture in serum-free medium.

Multivariate statistical analysis of GC-MS metabolomics profile of thyrosphere and adherent cells.

The aqueous metabolites contents of thyrospheres and adherent cells from B-CPAP, TPC-1 and Nthy-ori3-1 cells were characterized by GC-MS analysis. Metabolites, including amino acids, sugars, organic and fatty acids were detected. A PCA coupled with Hotelling t-squared was used to ensure the absence of outliers (data not shown). Three PLS-DA were performed to elucidate the discriminant metabolic features between thyrosphere and parental cells from the three cell lines. PLS-DA showed a clear separation between thyrosphere and adherent cells for all the comparisons (**Figure 14A-C**) and the models were validated by permutation test (n=200). All the statistical parameters (R^2X , R^2Y , Q^2 and P value) are showed in **Table 5**. Separation between thyrospheres and adherent cells for all the three models is accomplished by the presence of metabolic variables that contribute to the discrimination between the sample groups. Variable importance in projection list (VIP) was used to detect the metabolites responsible for the separations (VIP values < 1.0 and these metabolites underwent to Student t-Test.

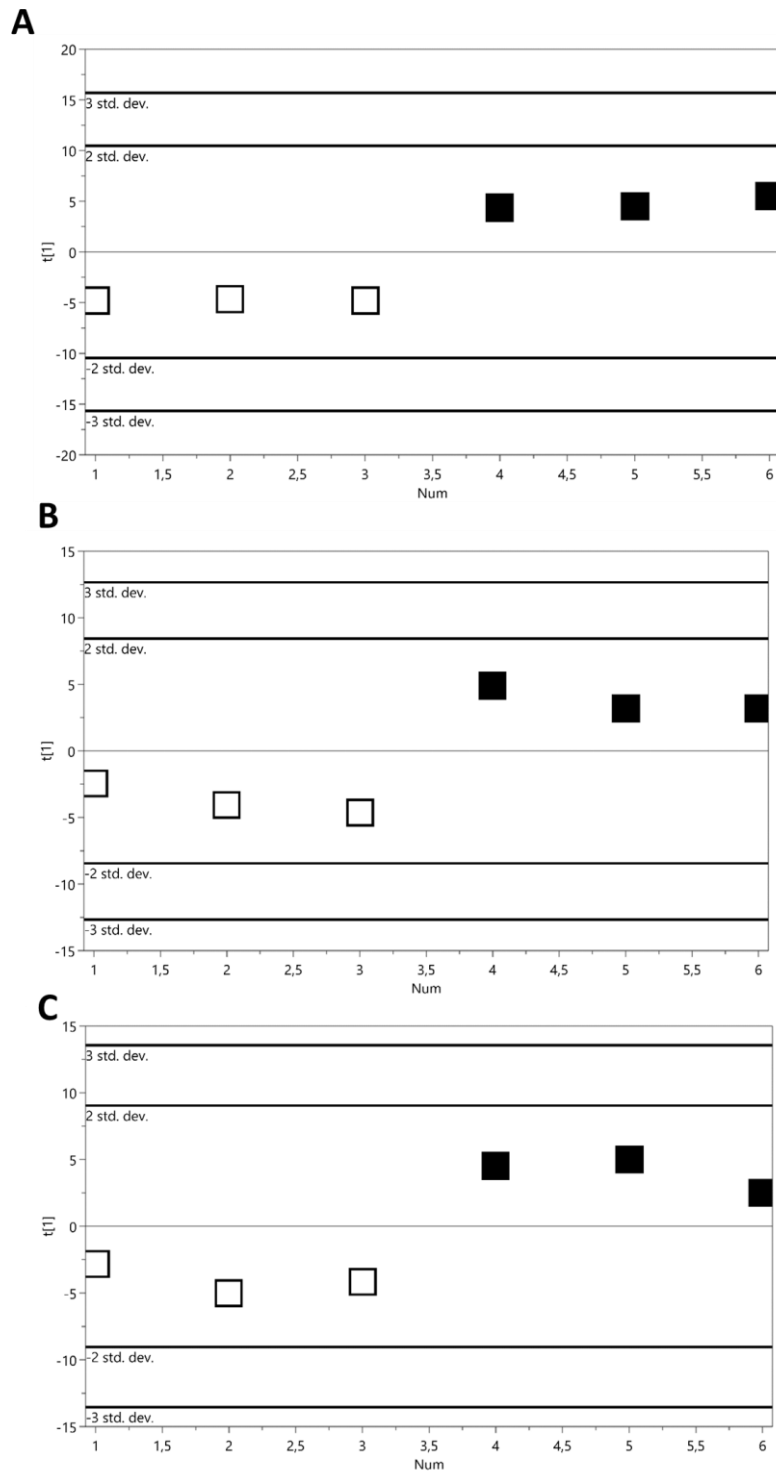


Figure 14. Multivariate statistical analysis of thyrospheres and adherent thyroid cell lines. A) PLS-DA scores plot of metabolic profile of B-CPAP thyrosphere and adherent cells, B) PLS-DA scores plot of metabolic profile of TPC-1 thyrosphere and adherent cells, C) PLS-DA scores plot of metabolic profile of Nthy-ori3-1 thyrosphere and adherent cells. Legend: ■ : thyrospheres, □ : adherent cells.

Table 9. Multivariate statistical analysis parameters

PLS-DA Models	R²X	R²Y	Q²	P value
A. B-CPAP thyrosphere vs. adherent cells	0.651	0.995	0.97	0.0051
B. TPC-1 thyrosphere vs. adherent cells	0.618	0.947	0.903	0.0302
C. Nthy-ori3-1 thyrosphere vs. adherent cells	0.495	0.942	0.854	0.0560

Metabolic comparison between B-CPAP adherent cells and thyrospheres

In term of metabolites involved in energetic pathways, such as glycolysis, B-CPAP thyrospheres showed a significant decrease of glucose, pyruvate and fructose (**Figure 15**). Among the discriminant metabolites that are directly or indirectly components of the Krebs' cycle, succinic acid, malate, aspartate and glutamate were found significantly increased in thyrospheres (**Figure 15**). Some amino acids, such as glycine, isoleucine, proline, phenylalanine, valine and threonine were significantly increased in thyrospheres, while alanine was significantly decreased (**Figure 15**). Myo-inositol and polyols, such as ribitol and sorbitol, were significantly increased as well. Regarding lipid features, palmitic acid, stearic acid and cholesterol were also significantly increased (**Figure 15**).

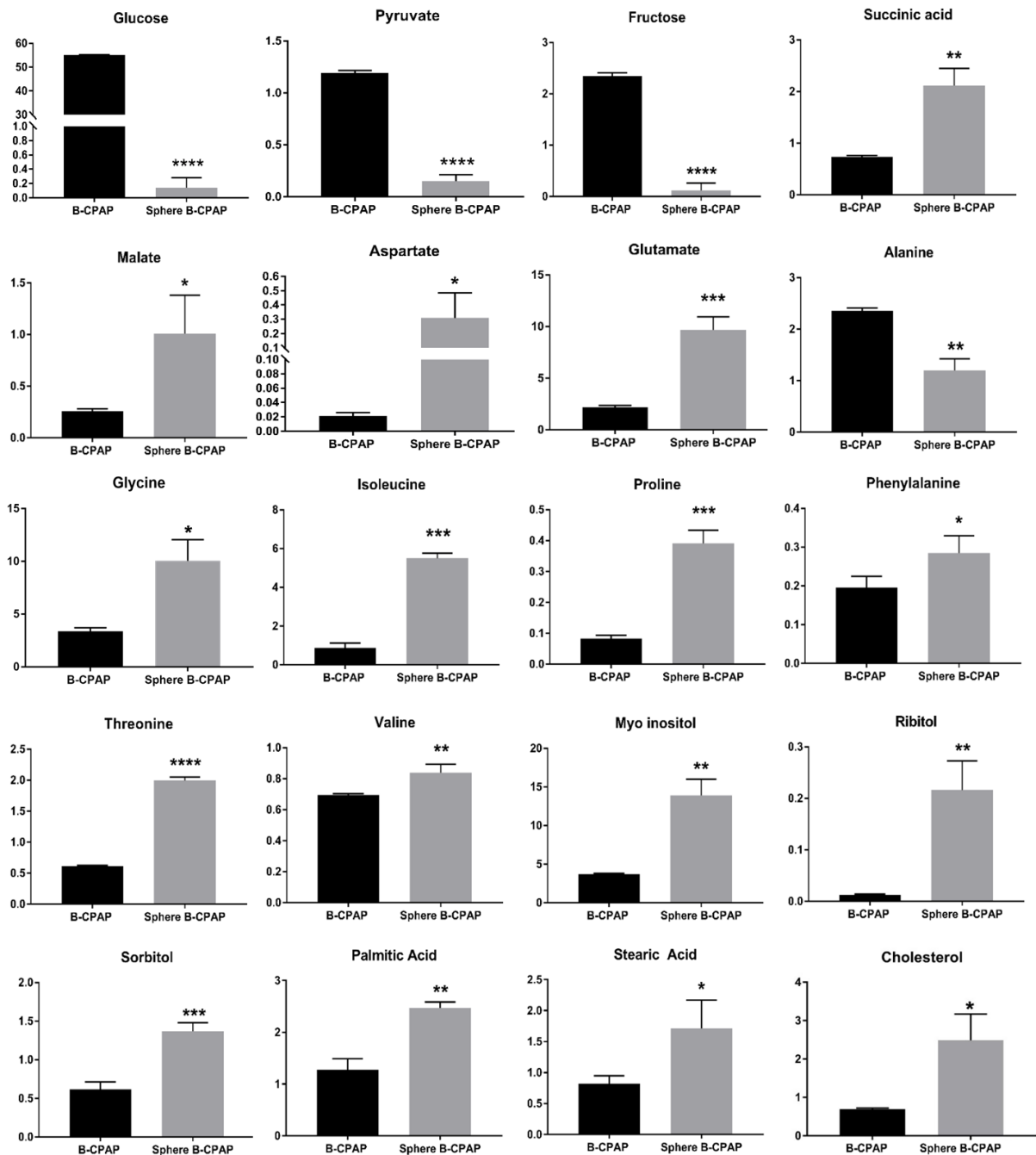


Figure 15. Metabolomic changes in B-CPAP derived thyrosphere and adherent cells. Bar graphs of discriminant metabolites, indicating the relative concentration of the metabolites. Statistical analyses were performed by unpaired Student t-Test. Data are presented as means \pm Standard Deviation. All experiments were performed three times independently, each time in triplicate to confirm the results. * $P < 0.05$, ** $P < 0.01$, *** $P < 0.001$, **** $P < 0.0001$.

Metabolic comparison between TPC-1 adherent and thyrospheres.

In the comparison between TPC-1 adherent and thyrospheres, levels of glucose and fructose were significantly decreased in thyrospheres, while citric acid and succinic acid and were significantly increased. Amino acids, such as glutamate, alanine, phenylalanine and valine were found significantly increased in thyrospheres compared to adherent cells. Levels of galactitol were found significantly decreased, instead of palmitic acid and cholesterol, which were found significantly increased in thyrospheres (Figure 16).

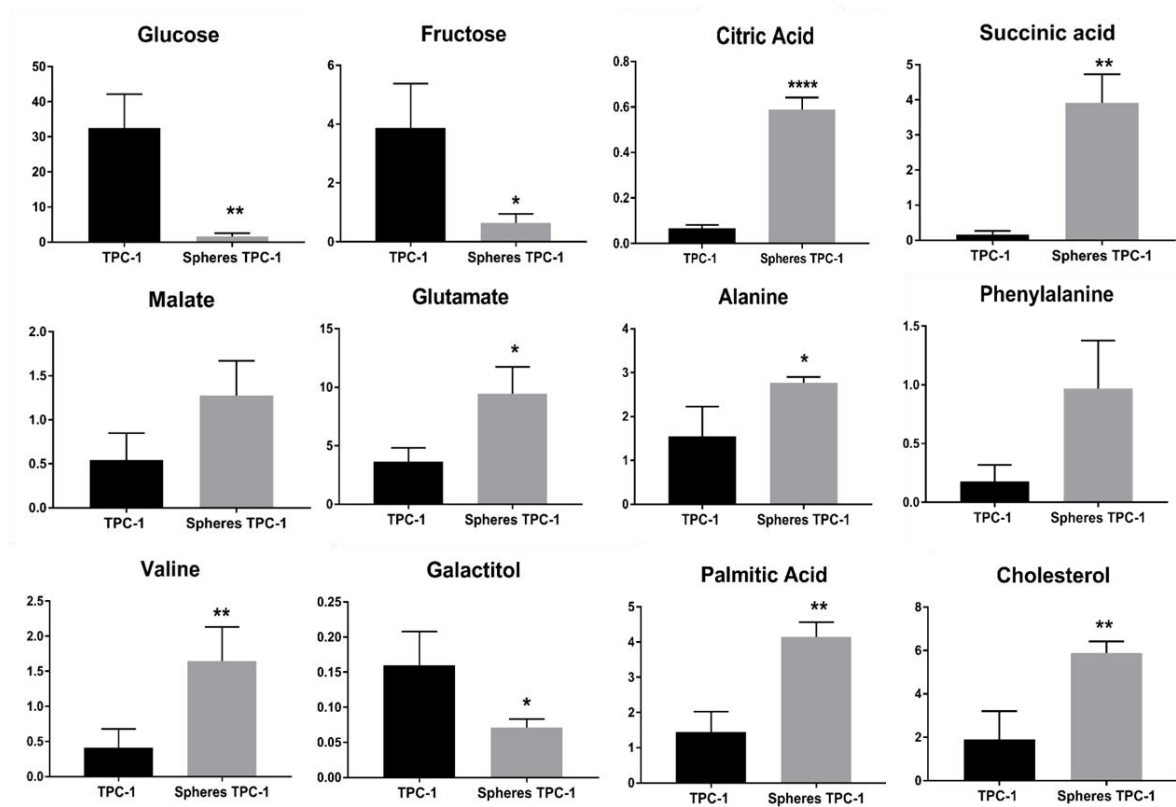


Figure 16. Metabolomic changes of TPC1 derived thyrosphere and adherent cells. Bar graphs of discriminant metabolites, indicating the relative concentration of the metabolites. Statistical analyses were performed by unpaired Student t-Test. Data are presented as means \pm Standard Deviation. All experiments were performed three times independently, each time in triplicate to confirm the results. * $P < 0.05$, ** $P < 0.01$.

Metabolic comparison between Nthy-ori3-1 adherent cells and thyrosphere

Glucose and pyruvate were significantly decreased in thyrospheres. No significant difference was found for Kreb's cycle metabolites, but valine, myo inositol, cholesterol, ribitol and galactitol were found to be significantly increased, while palmitic acid and sorbitol were found significantly decreased (Figure 17).

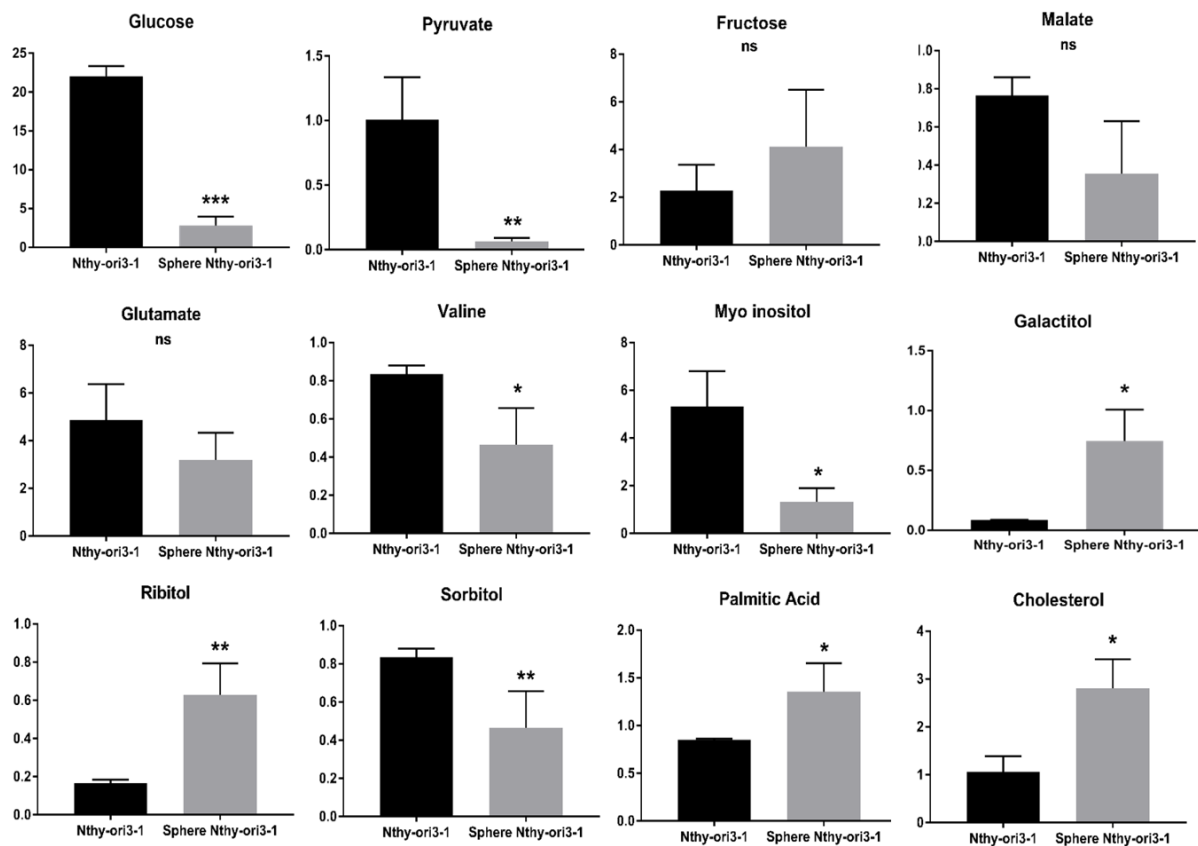


Figure 17. Metabolomic changes in Nthy-ori3-1 derived thyrosphere and adherent cells. Bar graphs of discriminant metabolites, indicating the relative concentration of the metabolites. Statistical analyses were performed by unpaired Student t-Test. Data are presented as means \pm Standard Deviation. All experiments were performed three times independently, each time in triplicate to confirm the results.* $P < 0.05$, ** $P < 0.01$, *** $P < 0.001$.

Metabolomic comparison between B-CPAP, TPC-1 and Nthy-ori3-1 thyrospheres

A further multivariate statistical model was performed between B-CPAP, TPC-1 and Nthy-ori3-1 derived thyrosphere cells. PLS-DA showed a separation between the three groups of thyrospheres (**Figure 18A**; $R^2X= 0.738$ $R^2Y= 0.949$ $Q^2=0.998$). Metabolites involved in energetic and biosynthetic pathways were studied and Student t-Test performed. Glucose, pyruvate and fructose were significantly decreased in both B-CPAP and TPC1 thyrospheres, while pyruvate was significantly increased in B-CPAP and TPC-1 compared to Nthy-ori3-1, but it was significantly decreased in B-CPAP compared to TPC-1 thyrospheres. Citric acid was significantly increased in TPC-1 compared both B-CPAP and Nthy-ori3-1 thyrospheres, while it was significantly decreased in B-CPAP compared to Nthy-ori3-1 thyrospheres (**Figure 18B**). Malic acid levels were significantly increased in both tumoral thyrospheres from B-CPAP and TPC-1 compared to Nthy-ori3., as well as aspartate and glutamate. Among all the amino acids, TPC-1 showed significantly higher levels of alanine, isoleucine, proline and valine compared both B-CPAP and Nthy-ori3-1 thyrospheres, although also B-CPAP showed significantly increased levels of alanine, isoleucine, proline and valine compared to Nthy-ori3-1 thyrospheres. Moreover, our data showed a significant increase in myo-inositol only in B-CPAP thyrospheres compared to TPC-1 and Nthy-ori3-1, as well as ribitol, while sorbitol, was significantly increased only in Nthy-ori3-1 thyrospheres. With reference to lipids, palmitic acid was significantly increased in both B-CPAP and TPC-1 compared to Nthy-ori3-1, where TPC-1 showed the higher level. Stearic acid was significantly increased in TPC-1 thyrospheres, while cholesterol was significantly increased in B-CPAP. The metabolic variations, resulting from the comparison between B-CPAP, TPC-1 and Nthy-ori3-1 thyrosphere cells described above, and the involved pathways are summarized pathways analysis (**Figure 19**).

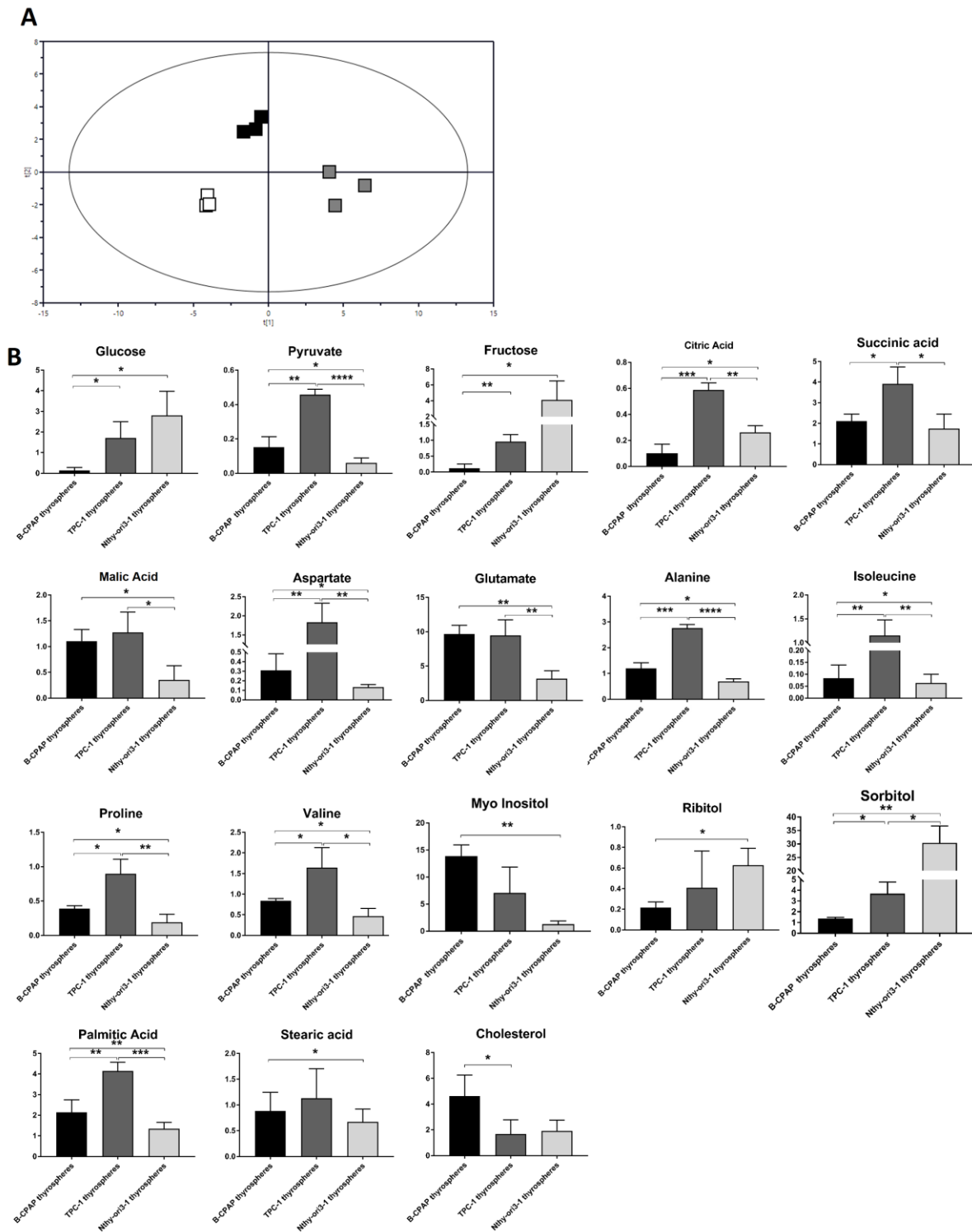


Figure 18. Metabolomic changes between B-CPAP, TPC-1 and Nthy-ori3-1 derived thyrosphere cells. **A)** PLS-DA scores plot of metabolic profile of B-CPAP, TPC-1 and Nthy-ori3-1 thyrosphere (Black box: B-CPAP thyrospheres, Grey box: TPC-1 thyrospheres, White box: Nthy-ori3-1 thyrospheres) . **B)** Bar graphs of discriminant metabolites, indicating the relative concentration of the metabolites obtained by the chromatogram area and then normalized by total area. Statistical analyses were performed by Unpaired Student t-Test. Data are presented as means \pm Standard Deviation. All experiments were performed three

times independently, each time in triplicate to confirm the results. * P<0.05, ** P<0.01, *** P<0.001.

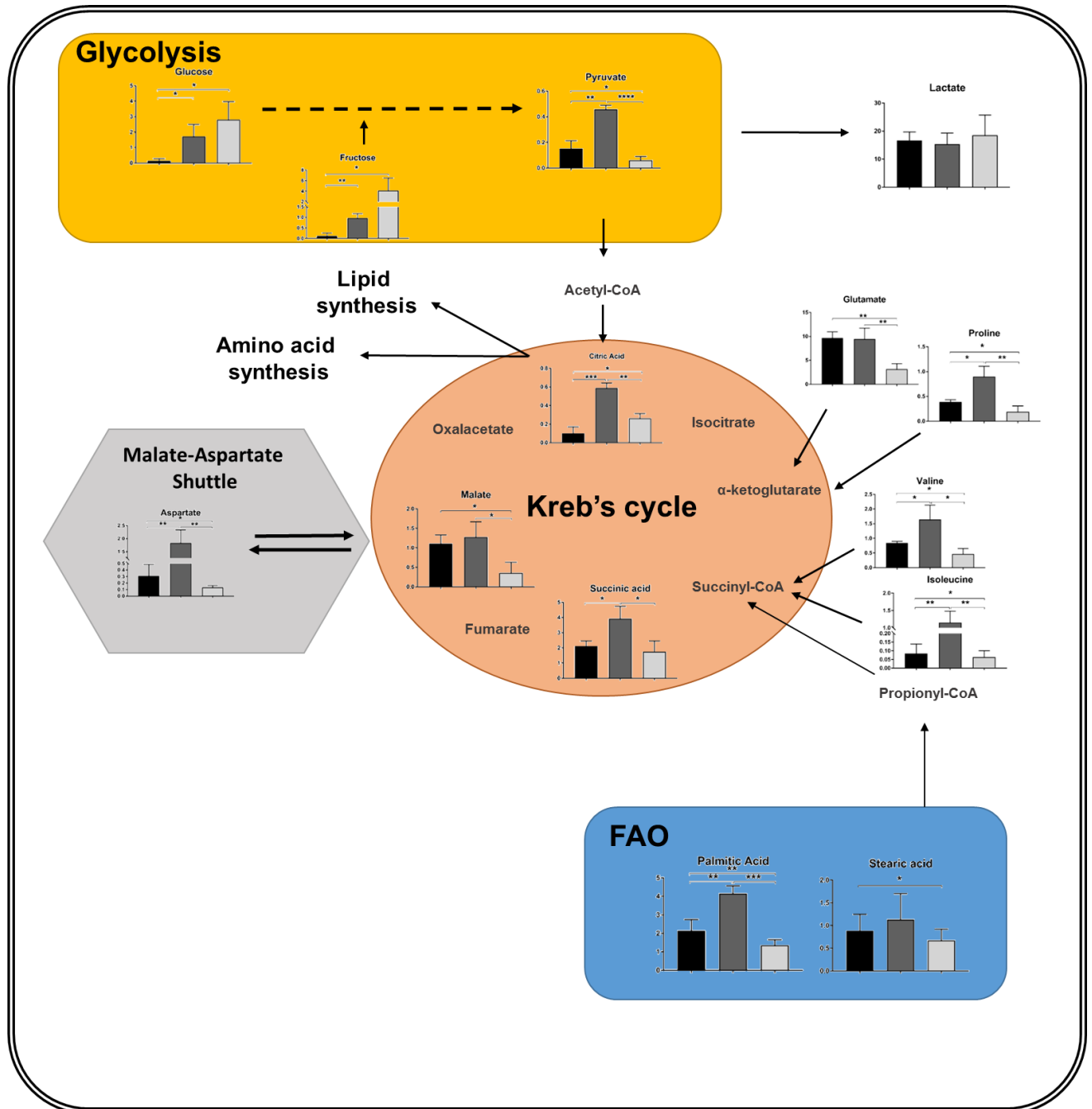


Figure 19. Summary of the metabolic variations and pathways resulting from the comparison between B-CPAP, TPC-1 and Nthy-ori3-1 thyrosphere cells.

IV. Results

Part three: Anti-tumoral effects and metabolic reprogramming Vitamin C-induced.

Citotoxicity Vitamin C-induced in PTC-derived cell lines.

In order to evaluate the cellular cytotoxic effects of Vitamin C in PTC-derived cell lines and non tumoral cell line, a MTT assay was performed. PTC-derived cell lines were treated with different concentrations of Vitamin C (0.5mM-15mM), incubated for 24 and 48 hours.

After 24h of incubation, cell viability was not affected by the exposure to vitamin C (**Figure 20 A**). On the contrary, 48h of vitamin C incubation induced a significantly decreased in cell viability. Nthy-ori3-1 cells were the least sensitive to vitamin C, with a half-maximal inhibitory concentration (IC₅₀) of 15mM, followed by TPC-1 with IC₅₀ of 10mM. Instead B-CPAP and K1 cells were the least sensitive, with an IC₅₀ of 5mM (Nthyori3-1>TPC-1>K1 and B-CPAP) (**Figure 20B and C**).

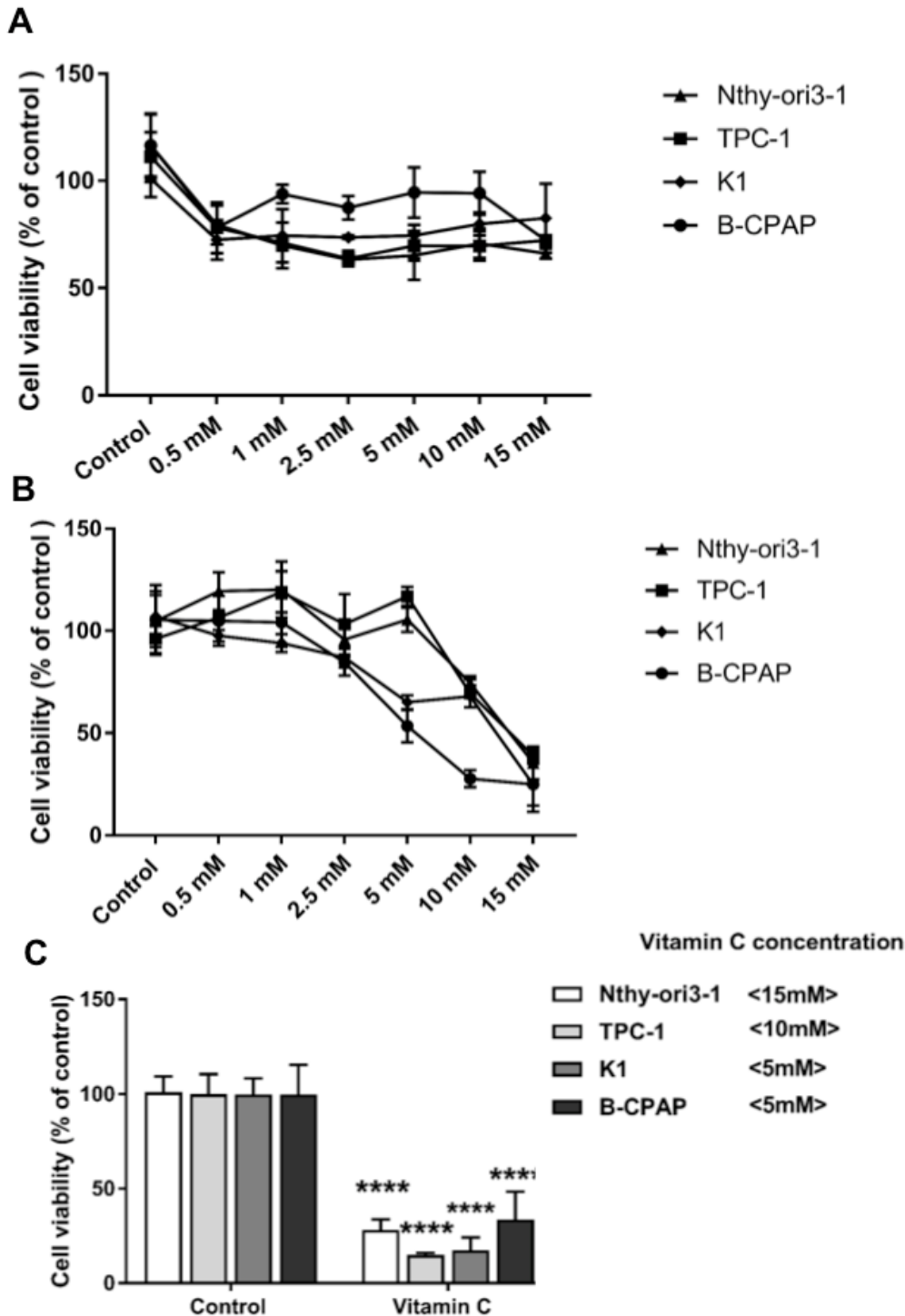


Figure 20. Effects of vitamin C in cell viability. **A)** Vitamin C effects in the cell viability after 24h of incubation. **B)** Vitamin C effect in the cell viability after 48h of incubation. **C)** Decreased cell viability after EC_{50} of Vitamin C treatment (48h) (15mM for Nthy-ori3-1, 10mM for TPC-1 and 5mM for K1 and B-CPAP). Data, expressed as % of control, are presented as means \pm Standard Deviation. All experiments were performed three times independently, each time in triplicate to confirm the results. Statistical analysis were performed by Student t-Test. Results were considered significant when $****P < 0.0001$.

Oxidative stress and aminothiols modulation by vitamin C

We investigated changes in the redox balance after vitamin C treatment, by measuring the ROS production in cells exposed to 1',7'-dichlorodihydrofluorescein diacetate H₂-DCF-DA (10 μ M). Oxidant TBH was used as positive control, while NAC was used as antioxidant, in order to confirm the presence of oxidative stress induced by vitamin C. In Nthy-ori3-1 cells TBH as well as vitamin C treatment induced significant increase of ROS compared to the no treated cells (**Figure 21**). Treatment with the anti-oxidant NAC seems to be not effective in the counteracting the vitamin C effect, as demonstrated by the significant increase of ROS, due to the treatment of vitamin C. In TPC-1 and K1 cells, intracellular ROS levels were found significantly increased following by the exposure of TBH but not vitamin C, compared to the control. Although Vitamin C did not significantly increase ROS levels in TPC-1, compared to the control, NAC treatment, coupled with Vitamin C treatment, significantly reduced ROS levels compared to cells treated with Vitamin C in both cell lines, while in TPC-1 cells NAC significantly reduced ROS levels also compared to untreated cells. In B-CPAP cells both TBH and vitamin C treatments significantly induced the production of ROS and this effect was suppressed by treatment with the antioxidant NAC.

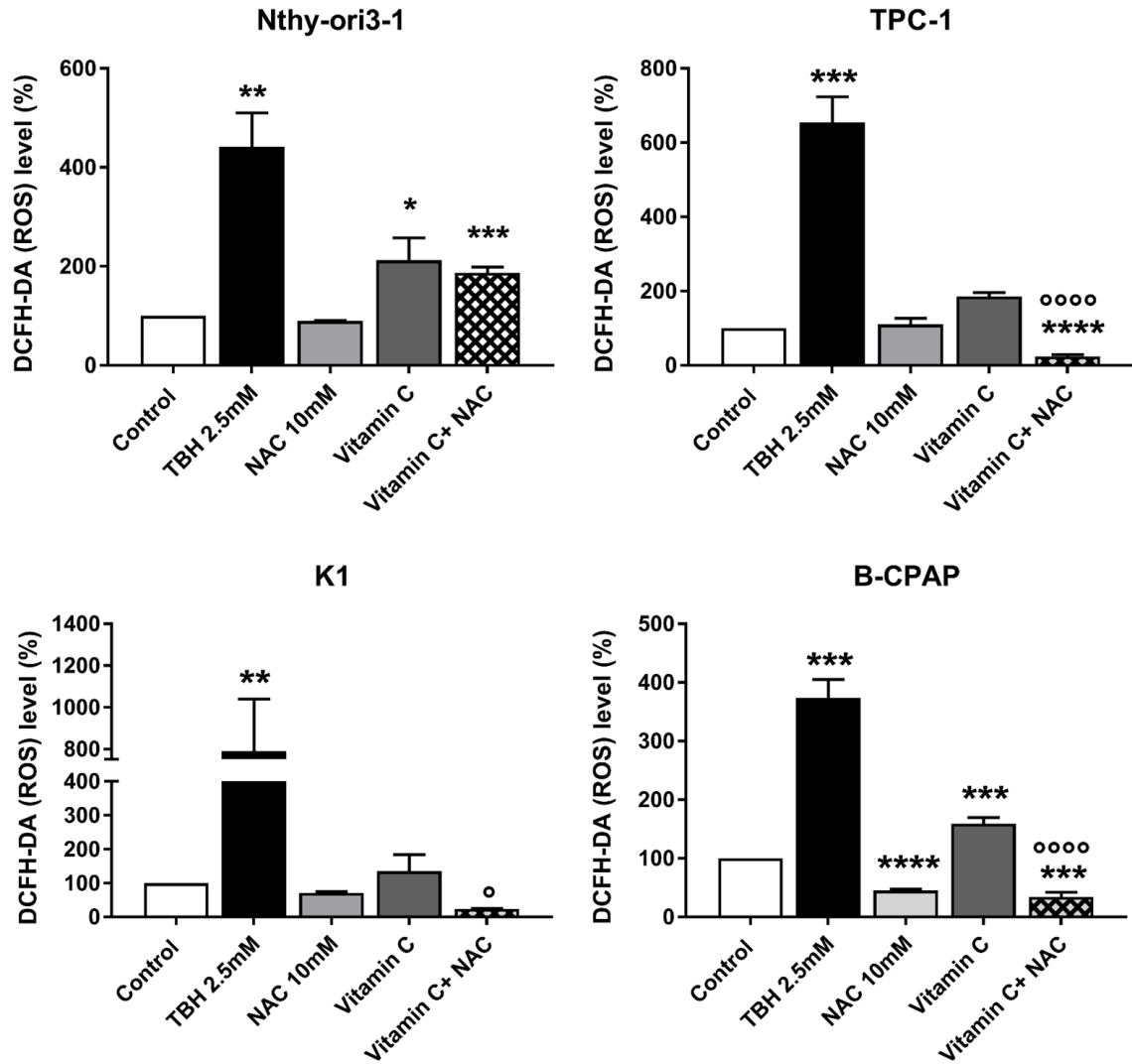


Figure 21. ROS production vitamin C-induced in thyroid cell lines. ROS level in PTC-derived cell lines and non tumoral thyroid cell line, expressed as % of control (untreated cells for each cell line) after vitamin C (15mM for Nthy-ori3-1, 10mM for TPC-1 and 5mM for K1 and B-CPAP), TBH (2.5mM) and NAC (10mM) treatments. Data are presented as means \pm Standard Deviation (n=3). All experiments were performed three times independently, each time in triplicate to confirm the results. Statistical analysis was performed by Student t-Test. Results were considered significant when * / $^{\circ}$ P<0.05, **/ $^{\circ}$ P<0.01, ***/ $^{\circ}$ P<0.001, ****/ $^{\circ}$ P<0.0001 (* statistical significance refers to negative control not treated cells, $^{\circ}$ statistical significance refers to positive control TBH treated cells).

We further investigated the redox perturbation in thyroid cancer cells by measuring intracellular antioxidant species. The GSH/GSSG ratio was significantly decreased due to the vitamin C treatment only in B-CPAP cells (**Figure 22 A**). Similar trend was found for the cysteine/cystine ratio, which was found significantly decreased in B-CPAP, K1 and the control cells, although a not significant decrease of cysteine/cystine ration was found in TPC-1 as well (**Figure 22 B**).

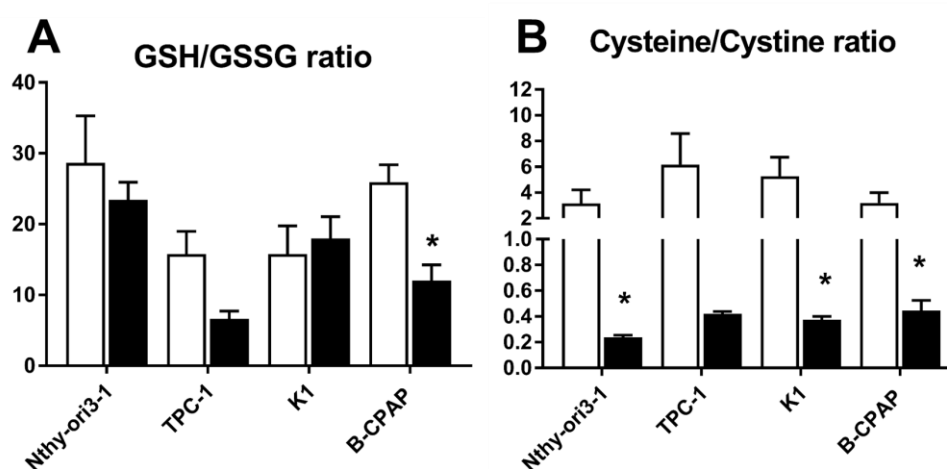


Figure 22. Antioxidants ratio modulation vitamin C-induced. (A) Levels of GSH/GSSG ratio in PTC-derived cell lines and control cell line, (B) levels of Cysteine/Cystine ratio after 24h of incubation with vitamin C (15mM for Nthy-ori3-1, 10mM for TPC-1 and 5 mM for K1 and B-CPAP). Peak areas of intracellular aminothiols were normalized using protein contents (ng of aminothiols per μg of proteins) and expressed as ratio of reduced and oxidized forms. Data are presented as means \pm standard deviation. All experiments were performed three times independently, each time in triplicate to confirm the results. Statistical analysis were performed by Student t-Test. Results were considered significant when * $P < 0.05$, ** $P < 0.01$, *** $P < 0.001$. (Legend: white bar= untreated cells, black bar= treated cells).

Metabolic effect induced by Vitamin C treatment in PTC-derived cell lines.

The effect of vitamin C on the metabolism of PTC-derived cells has been studied, focusing on energetic pathways, such as glycolysis, TCA cycle and electron carriers, changes in nucleotide levels and glucose uptake rate. Energetic metabolites and nucleotides were measured by using UHPLC-MS/MS with a targeted analysis. Our results revealed that metabolites upstream of glycolysis (glucose, glucose-6-phosphate/fructose-6-phosphate, fructose-1,6-biphosphate, glyceraldehyde-3-phosphate and dihydroxyacetone phosphate) were significantly increased in PTC-derived cell lines B-CPAP, K1 and TPC-1, and in the control line Nthy-ori3-1 (**Figure 23A**). On the contrary, those metabolites downstream of glycolysis (2/3-phosphoglycerate, phosphoenolpyruvate, pyruvate) were decreased after vitamin C treatment. Similarly, TCA cycle seems to be affected by vitamin C treatment. Indeed metabolites involved in the first step of the cycle, such as coenzyme A and acetyl-CoA, were significantly increased in all thyroid cell lines, with the exception of B-CPAP cells, where acetyl-CoA was found significantly reduced. Moreover, metabolites upstream of TCA cycle (citrate, isocitrate, α ketoglutarate, succinyl-CoA) were significantly decreased due to the treatment, while metabolites such as succinate, fumarate, malate, oxaloacetate were found to be significantly increased (**Figure 23 B**).

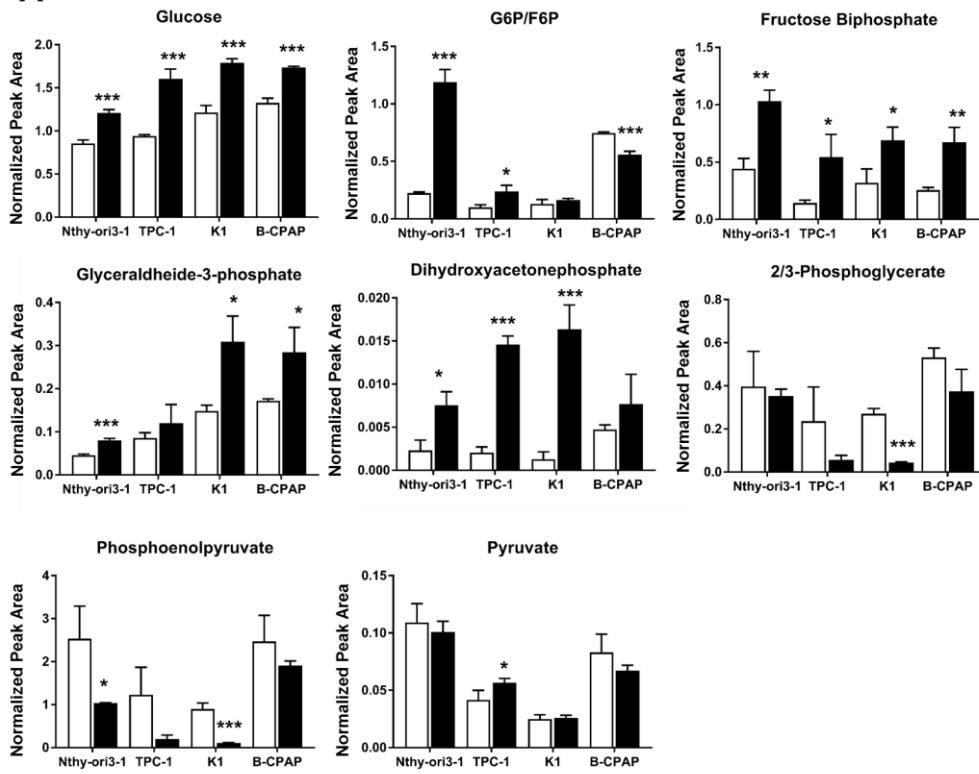
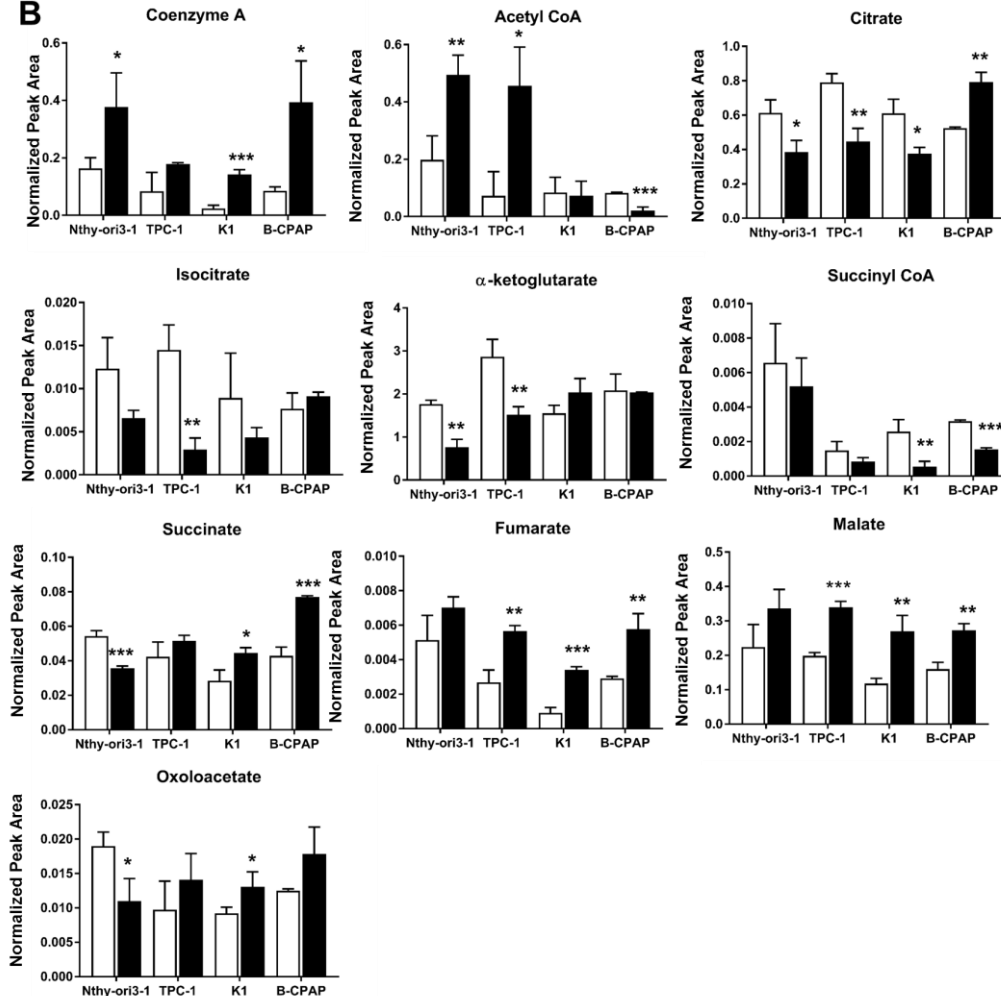
A**B**

Figure 23. Metabolic alterations in glycolysis and TCA cycle vitamin C-induced. Intracellular levels of glycolytic metabolites (A), TCA cycle metabolites (B) measured after 24h of incubation with vitamin C (15mM for Nthy-ori3-1, 10mM for TPC-1 and 5 mM for K1 and B-CPAP). Data are presented as means \pm standard deviation of peak areas of the metabolites, normalized for total area. All experiments were performed three times independently, each time in triplicate to confirm the results. Statistical analysis were performed by Student T-test. Results were considered significant when * $P < 0.05$, ** $P < 0.01$, *** $P < 0.001$. (Legend: white bar= control not treated cells, black bar= vitamin C treated cells).

To better investigate the effect of the vitamin C treatment on the glucose homeostasis, we examined the glucose uptake by using the fluorescent glucose analog 2-NBDG. Our data revealed that for all PTC-derived cells and the control cells the treatment with vitamin C significantly reduced the glucose uptake (**Figure 24**).

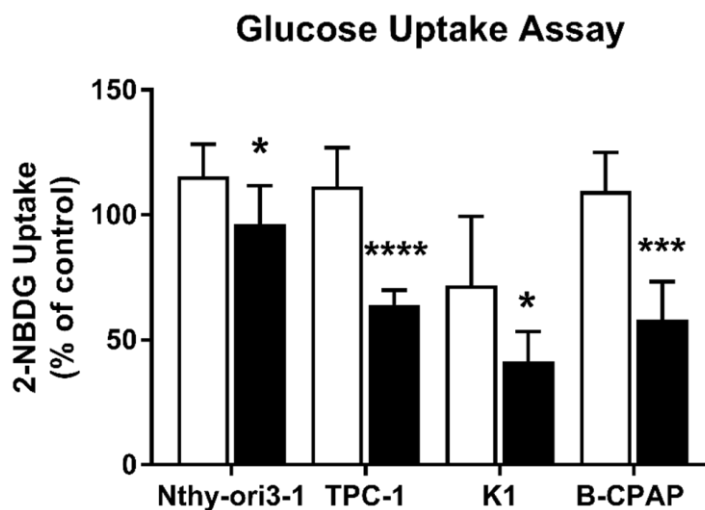


Figure 24. Relative glucose uptake after vitamin C treatment. Quantification of the relative glucose uptake was done through the fluorescent glucose analog 2-NBDG in cancer cells and control cell lines treated with vitamin C (15mM for Nthy-ori3-1, 10mM for TPC-1 and 5 mM for K1 and B-CPAP). Data are expressed in percentage of control (not treated cells). Data are presented as means \pm standard deviation. All experiments were performed three times independently, each time in triplicate to confirm the results. Statistical analysis were performed by Student T-test. Results were considered significant when * $P < 0.05$, ** $P < 0.01$, *** $P < 0.001$. (Legend: white bar= control not treated cells, black bar= vitamin C treated cells).

Furthermore, metabolites involved in the NAD⁺ salvage pathway (nicotinic acid, Nicotinamide and NAD⁺) were detected by UHPLC-MS/MS. Levels of Nicotinic Acid were found significantly decreased only in the control cells, while Nicotinamide was significantly decreased in TPC-1, K1 and B-CPAP. Similarly, NAD⁺ levels were significantly reduced by vitamin C in K1 and B-CPAP cells (**Figure 25**).

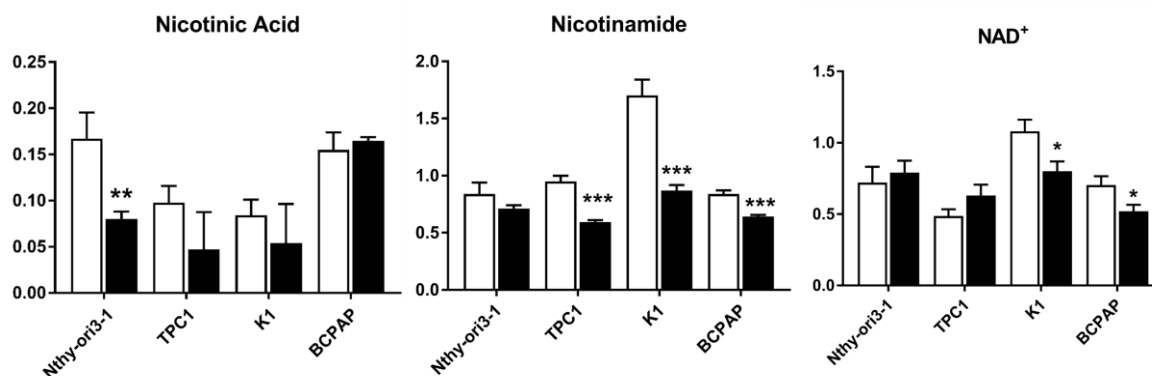


Figure 25. Changes in Nicotinamide and NAD⁺ levels vitamin C-induced. Intracellular Nicotinic Acid, Nicotinamide and NAD⁺ levels measured after 24h of incubation with vitamin C (15mM for Nthy-ori3-1, 10mM for TPC-1 and 5 mM for K1 and B-CPAP). Data are presented as means \pm standard deviation of peak areas of the metabolites, normalized for total area and expressed in the graphs as ranks. All experiments were performed three times independently, each time in triplicate to confirm the results. Statistical analysis were performed by Student T-test. Results were considered significant when * $P < 0.05$, ** $P < 0.01$, *** $P < 0.001$. (Legend: white bar= control not treated cells, black bar= vitamin C treated cells).

Preliminary results: detection of apoptosis or necrosis induced by Vitamin C treatment.

To better understand the mechanism of cell death of Vitamin C, we examined if the treatment resulted in cells death through apoptosis or necrosis, by using Annexin V/Propidium Iodide Assay. Scatterplots (**Figure 26**) represent the percentage of live cells and cells undergo apoptosis and necrosis for both untreated and treated PTC-derived and control cells. After 48h exposure to Vitamin C (15mM for Nthy-ori3-1, 10mM for TPC1, 5mM for K1 and B-CPAP cells) the percentage of apoptotic cells (early apoptotic plus late apoptotic cells) in treated control cells was 44.13%, while the percentage of necrotic cells was 4.88% (Figure 26 A). Therefore, in PTC-derived cells vitamin C treatment induced cell death by necrosis. In particular, the percentage of necrotic cells in TPC-1 cells was 72.34% (**Figure 26B**), in K1 was 76.71% (**Figure 26 C**) and in B-CPAP was 78.35% (**Figure 26 D**).

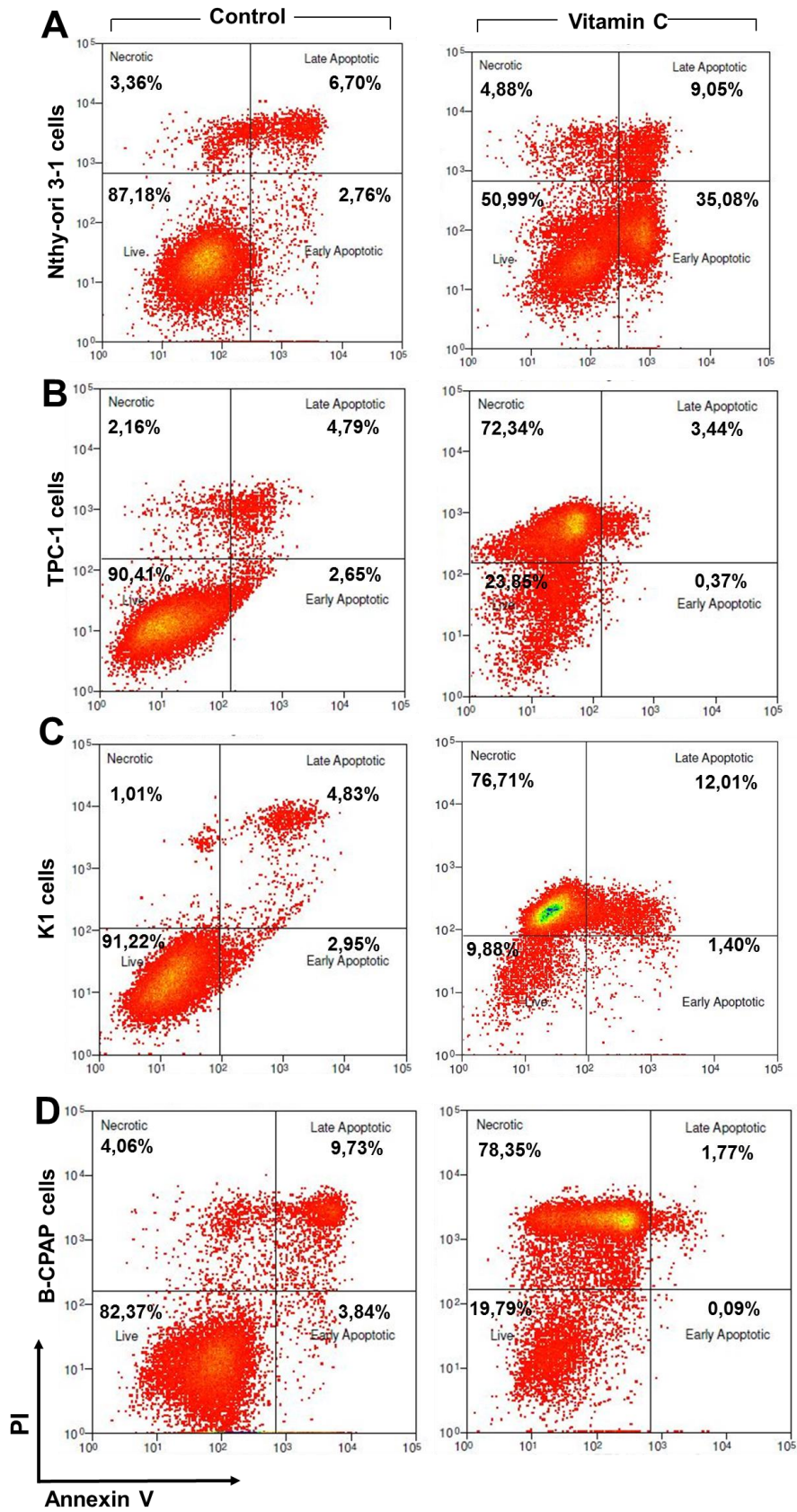


Figure 26. Representative scatter-plots of flow cytometric analysis of apoptotic/necrotic cell. Scatterplots of control cells (left) and cells treated with vitamin C (48h of incubation) (right) for (A) Nthy-ori3-1, (B), TPC-1, (C) K1 and (D) B-CPAP cells

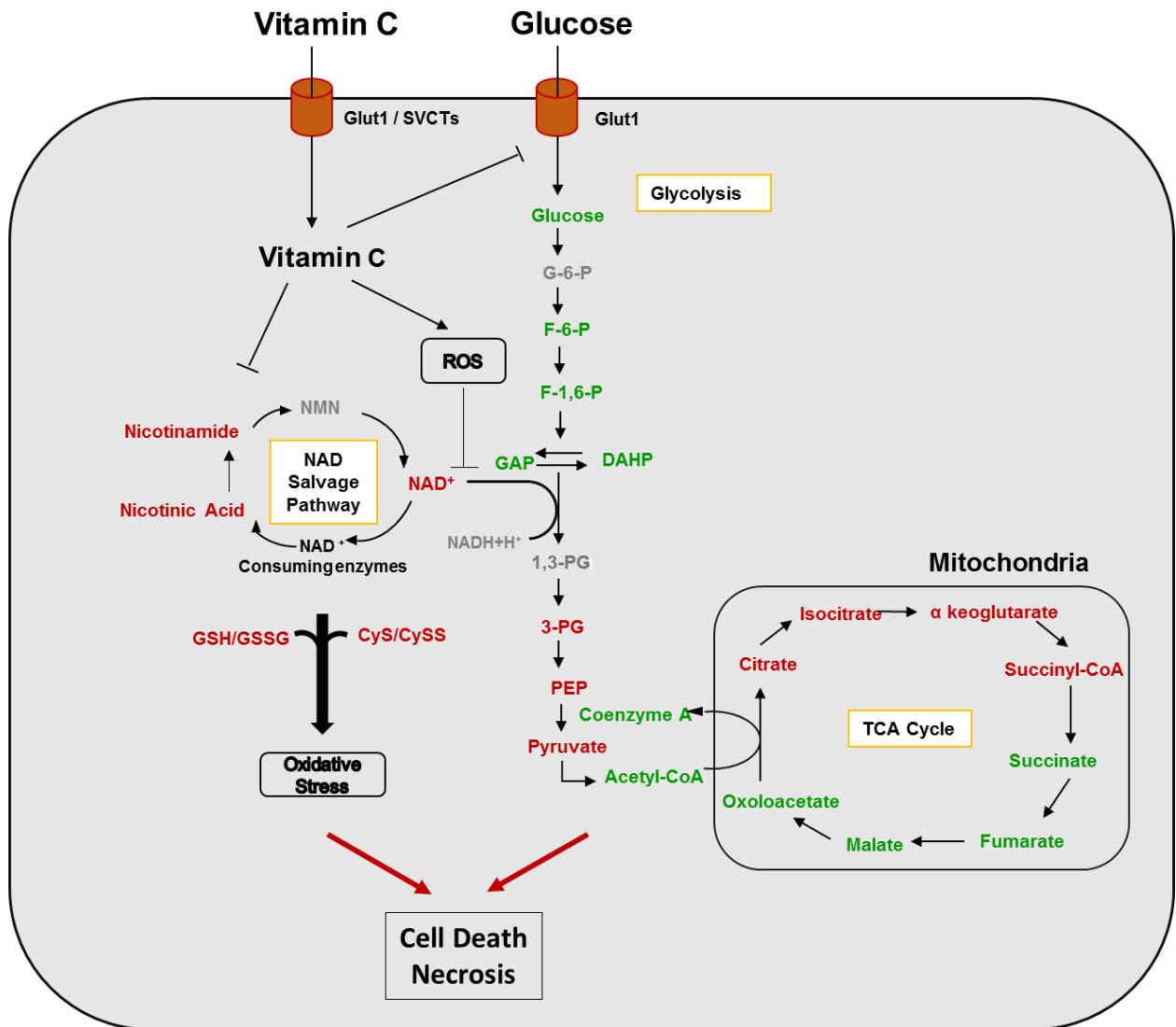


Figure 27. Vitamin C metabolic effects. Summary of vitamin C-effects studied in energetic pathways, such as glycolysis and TCA cycle, Nicotinamide and NAD⁺ availability. Legend: Red=decreased metabolites, Green=increased metabolites, Grey= not detected.

V. Discussion

Metabolic and redox reprogramming in PTC-derived cell lines.

Cancer cells appear to reprogram metabolic pathways to meet bioenergetic, redox and biosynthetic demands (DeBerardinis and Chandel 2016). The elucidation of reprogrammed metabolic activities may provide opportunities to understand tumor development and progression, to predict tumor behavior, and prevent tumor progression by inhibiting essential pathways (Ward and Thompson 2012). Metabolic changes and redox balance are common features in cancer cells and are now considered as fundamental features for the initiation of cancer and for the amplification of the tumor phenotype (Pavlova and Thompson 2016). Several mutated oncogenes and tumor suppressor genes have been associated to different signaling pathways that affect, directly and indirectly, the tumor cell metabolism and redox status (Cairns et al. 2011). The first part of the project aimed to characterize metabolic changes and alterations of redox balance, associated with oncogene pathways, in PTC-derived cell lines, using an immortalized normal thyrocytes cell line Nthy-ori3-1, negative for the PTC genetic mutations, for comparison. Our results revealed that metabolites involved in energy production pathways, including glycolysis, Krebs cycle and glutaminolysis, were found altered in the three studied PTC-derived cell lines. In particular, we found that B-CPAP cell line, with a genetic background reflecting the aggressive behavior of the primary tumor from which it was derived (*TP53*, *BRAF* and *hTERT* mutations), displayed a strong glycolytic phenotype, exemplified by the increase of energetic metabolites such as G6P/F6P, F1,6P, DHAP, GAP, 2PG/3PG, PEP and pyruvate compared to the control line and the other PTC-derived cells line. Particularly, levels of lactic acid were found to be significantly decreased only in B-CPAP, compared to control cells. Based on these results, B-CPAP cell line showed the most perturbed glycolytic phenotype, compared to the control cells and the others PTC-derived cells. These findings are in agreement with the glycolytic phenotype of cancer cells (Lunt et al. 2011). The increase in glycolytic rate allows glycolytic intermediates to fulfill the metabolic demands of proliferating cells, in fact these intermediates, are also used as precursors for macromolecule

synthesis, providing a biosynthetic advantage (Ahn et al. 2015). This high glycolytic rate is regulated by several factors, such as HIF-1 α , which was found to be overexpressed in aggressive types of TC such as ATC (Burrows et al. 2010), and it has been also associated with distant metastasis in PTC (Burrows et al. 2011). Furthermore, also glycolytic enzymes such as the hexokinase II (HKII), phosphoglycerate kinase (PGK), glucose-6-phosphate dehydrogenase (G6PDH), and lactate dehydrogenase A (LDH-A), have also been found overexpressed in TC (Nahm et al. 2017). Moreover, the glycolytic phenotype has been found to be higher in PTCs with *BRAF*^{V600E} mutation compared to wild-type for *BRAF* mutation, which agrees with the results obtained in a previous study (Nagarajah et al. 2015). Overall, our findings support the association of BRAF mutation with the increased glycolysis pathways and suggest PTC-derived cells, with an aggressive phenotype, rely on aerobic glycolysis for energy production, thus exhibiting the Warburg phenotype. Furthermore, the TCA cycle plays a central role for fulfilling bioenergetic, biosynthetic and redox balance requirements and previous studies showed that cancer cells bypass TCA cycle primarily utilizing aerobic glycolysis (Anderson et al. 2018). Moreover, several studies have demonstrated that cancer cells can uncouple glycolysis from TCA cycle, allowing the use of different fuel sources to meet metabolic needs (Chen and Russo 2012; Pavlova and Thompson 2016). Our data displayed that TCA cycle was perturbed in all cell lines as demonstrated by a decrease of acetyl CoA, isocitrate, succinyl CoA, succinate, oxaloacetate and fumarate compared the control cells (although the latter was found to be increased in B-CPAP cells). Interestingly, citrate levels were found to be significantly increased in K1 and B-CPAP cells, probably due to its role in many biochemical pathways. Indeed citrate levels support de novo lipid and sterol biosynthesis in cancer cells (Icard et al. 2012). Several studies have demonstrated that in cancer cells, to promote lipid route through the accumulation of citrate, TCA cycle is slowed down (Icard et al. 2012). In particular, while citrate sustains the lipid production, glutamine fuels TCA cycle with intermediates such as α KG, which are depleted by biosynthetic reactions (Feron 2009). The

increase of glutamine and α KG in PTC-derived cells might further confirmed the role of citrate in the lipid biosynthesis.

An alternative to glucose, as fuel for bioenergetic pathways is glutamine, which feeds the TCA cycle by providing α -ketoglutarate from glutamate (Anderson et al. 2018), by GLS1 activity, showing the characteristics of an oncogene (Maddocks OD and Vousden KH 2011). Hence, we investigated the role of this pathway in PTC-derived cells by measuring glutaminolytic metabolites (glutamine, glutamate and α KG). Our data showed an increase of these metabolites in PTC-derived cells compared to the control cells, particularly in B-CPAP cells. This evidence is in agreement with the importance of glutaminolysis in cancer cells, and it is closely dependent on the marked glycolytic phenotypes. Indeed, due to the high rate of glycolysis, cancer cells usually rely on anaplerotic reactions in order to replenish TCA cycle intermediates through glutaminolysis (DeBerardinis et al. 2007). Consequently, cancer cells displayed an upregulation of glutamine transporters and enzymes involved in its breakdown (Pavlova and Thompson 2016). Metabolites involved in the glutaminolysis were increased in PTC-cells. This metabolic trend supports the idea that glutaminolysis pathway was significantly changed across the several thyroid cancer cell lines. Moreover, previous studies have demonstrated that PTC with *BRAF*^{V600E} mutations, characterized by an aggressive behavior, displayed increased expression of glutamine metabolism-related proteins (Kim et al. 2016). Interestingly, wild-type p53 plays an important role in the regulation of glutamine destiny by activating another glutaminase isoform, GLS2, promoting energy and antioxidant production (Maddocks OD and Vousden KH 2011). The expression of GLS1 rather than GLS2 seem to be closely related to the activity of wild-type p53, which only drives the activation of GLS2 (Maddocks OD and Vousden KH 2011). Considering the fundamental role of GLS1 in glutaminolysis regulation and the role of TP53 mutation in the glutaminolysis regulation, we investigated the expression of Glutaminase 1, usually overexpressed in many cancer types (Choi and Park 2018). Particularly, in some cancer types, increased levels of GLS1 have

been associated with a higher disease stage and poor prognosis (Yu et al. 2015). In our study, GLS1 levels were found to be increased in PTC-cells compared to the non tumoral cells, resulting with its essential role in the bioenergetic state of cancer cells.

We further elucidated fluxes across glycolysis pathway by studying the expression of metabolic carriers (GLUT1 and MCT4), glucose uptake rate, extracellular lactate levels. In order to sustain the energetic demands and compensate for the bioenergetic inefficiency of the glycolytic pathways, cancer cells usually displayed an increased glucose import due to the overexpression of GLUT1 in the plasma membrane (Józwiak et al. 2015). As demonstrated by immunofluorescence, we found an increased expression of GLUT1 mainly in the plasma membrane of B-CPAP cells, while K1, TPC-1 cells showed less expression and the control line was barely positive for the expression of GLUT1. Similarly, cancer cells display also increased production of lactic acid, as result of the increased glucose uptake and consumption, which is then exported in the microenvironment (Jiang 2017; Choi et al. 2016) through the monocarboxylate transporters (MCTs), specifically MCT4 (Choi et al. 2016; Lee et al. 2016). Cancer cells displayed an overspression of this carrier, which contributes to the hyperglycolytic phenotype. In our immunofluorescence data, MCT4 was mostly overexpressed in B-CPAP cells, in accordance with the decreased levels of intracellular lactate which is exportated into the extracellular space. Indeed several studies have underlined that GLUT1 overexpression has been correlated to poor prognosis (Younes et al. 1996) as well as MCT4 being highly expressed level in many tumors (Hao et al. 2010). Glucose addiction for PTC-derived cells was further investigated by exposing cells to four metabolic conditions with different glucose concentrations. Our data showed that the viability of all PTC-derived cells line, particularly B-CPAP and K1 cells, was negatively affected after 48h exposure to low and no glucose concentrations, confirming the glucose dependency of cancer cells. Interestingly, high glucose concentration induced an increase in cell viability in B-CPAP and K1 cells after 48h of incubation, suggesting the glucose addiction of PTC-derived cells harboring *BRAF* mutations.

These findings are in keeping with the already described glucose addiction in cancer (Granja et al. 2015). There is a reciprocal cross talk between metabolic pathways and redox balance of cancer cells, involving pathways such as glycolysis, glutaminolysis, fatty acid oxidation, and the pentose phosphate pathway (Panieri and Santoro 2016). Indeed ROS play a critical role in cancer initiation and in the amplification of the tumor phenotype, and they are considered a byproduct of metabolic processes of highly proliferative cancer cells (Gupta et al. 2012). Alterations in redox balance as well as deregulated redox signaling are now considered common hallmarks of cancer (Kumari et al. 2018). Cancer cells maintain intracellular redox homeostasis and prevent oxidative stress-induced damage by upregulating several antioxidant systems, including glutathione, TrX (Fruehauf and Meyskens 2007) and cysteine/cystine cycle (Lo et al. 2008). The balance between the redox homeostasis, oxidative stress and the antioxidant systems is deeply connected to several metabolic pathways (Cairns et al. 2011). Moreover, recent studies have elucidated the association with deregulated redox signaling and metabolic pathways (Kumari et al. 2018). In our study PTC-derived cells, differing in their genetic background, manifested significant changes in the redox state (viz. decreased ratio of GSH/GSSG and cysteine/cystine). This is in line with the oxidative stress, which previous studies reported has an essential role in the tumorigenesis and in tumor progression (Gupta et al. 2012). To further elucidate the redox homeostasis in PTC, we measured intracellular ROS and electron carriers levels, as key molecules involved in the redox balance and in the antioxidant biosynthesis, respectively (Ying 2008). Particularly, a key molecule produced crucially in quenching ROS production by providing reducing power for the GSH and TRX systems is reduced NADPH, which functions as a cofactor (Cairns et al, 2011). For these reasons NADPH appears to be the limiting factor for oxidative stress management in cancer cells (Nathan and Ding 2010). On the other hand, NAD⁺ is a metabolic co-factor and electron carrier that is crucially involved in both glycolysis and oxidative phosphorylation (Cairns et al. 2011).

PTC-cells showed significant increase of intracellular ROS compared to the control line, as well as NAD^+/NADH and $\text{NADP}^+/\text{NADPH}$ which were found significantly increased in B-CPAP and K1 for the first ratio and only in B-CPAP for the second ratio, supporting previous findings (Cairns et al. 2011). Our findings support the idea of a deregulated redox signaling in cancer cells, resulting from the increased ROS levels and the imbalance of antioxidants and electron carriers. Furthermore, we investigated the expression of a key enzyme in the redox balance: GCL, enzyme responsible for the glutathione biosynthesis. GCL catalyzed the first and rate-limiting step of the glutathione biosynthesis and it is generally overexpressed in cancer cells (Estrela et al. 2006; O'Brien and Tew 1996). In PTC-derived cell lines, the GCL expression was higher in B-CPAP and K1 cells than TPC-1 and the control line, in agreement with the antioxidant demands.

Overall data from the first part of the project reflect the interplay among rewiring tumor metabolism, oncogenic driver mutations and deregulated redox balance. Particularly, PTC cells, with an aggressive genotype (*BRAF*^{V600E}, *hTERT* promoter mutation and *TP53* mutation) showed the most perturbed metabolic and redox phenotype than those harboring wild-type *TP53*. These results are in agreement with previous studies about role of oncogenic mutations, such as *TP53* and *BRAF* mutations, in the reprogramming of the cancer metabolism. Indeed, mutations in *KRAS* or *BRAF* have been demonstrated to play important roles in regulating metabolic alterations, particularly affecting glycolytic and glutaminolysis cancer phenotypes (Hutton et al. 2016). Similarly, p53 is well known to be involved in the regulation of glucose metabolism, TCA cycle and glutaminolysis (Bensaad et al. 2006; Contractor and Harris 2012; Hu et al. 2010).

Metabolomic alterations in CSCs-like in thyrospheres derived from PTC-cell lines.

PTC, similarly to most cancers, shows intracellular tumor heterogeneity, harboring a dynamic population of cells with stem cell-like properties, characterized by a distinct metabolic behavior, invasive potential and different interactions with the tumor microenvironment (Islam et al. 2015). Within this population, CSCs are considered the root cause of metastatic dissemination, therapeutic resistance and tumor recurrence (De Francesco et al. 2018). As differentiated cancer cells adapt their metabolism to support proliferation and survival, CSCs also seem to remodel their metabolism to microenvironmental changes, by shifting toward a glycolytic or a mitochondrial-based metabolism (Peiris-Pegès et al. 2016). The fundamental role of CSCs in carcinogenesis highlights the paramount importance of understanding of the CSCs metabolism, in view of developing combined strategies acting on CSCs metabolism (Wang et al. 2015). Despite the metabolism of CSCs having been the focus of investigation in recent years, it remains far from to be clear whether CSCs are predominately glycolytic or they rely more on OXPHOS. In order to gain therapeutic advantage from the metabolic dynamics of tumors, identifying the metabolic dependencies and alterations that occur within the CSCs might be one of the possible strategies to eradicate these cell population (De Francesco et al. 2018). Although CSC isolations from PTC have been reported by several studies (Mirshahidi et al. 2018), their biological meaning and the metabolic rewiring are still poorly understood. The second part of the project aimed to characterize the metabolic phenotype and dependence of cancer stem cells (CSCs), generated by PTC-derived cell lines through the spheroid-formation assay and an untargeted metabolomic approach.

In our data we found a substantial metabolic alteration between thyrospheres and adherent cells. Particularly, thyrospheres had a significant decreased of metabolites involved in the glycolytic pathways, indicating an highly glycolytic phenotype, which has been reported as important pathways for the maintainance of self-renewing capacity in both CSCs and adult stem cells (Ito

and Suda 2014). Thus, it has been proposed that glycolytic phenotype favours stemness by enhancing also antioxidant capacity (Sancho et al. 2016). According to this finding, cellular metabolism plays an important role in the control of stemness properties. During differentiation, stem cells are also able to adapt their metabolism, to generate the large amounts of energy needed for this process (Jang et al 2015). Subsequently, it has been showed that CSCs from breast, ovarian and colon cancer showed a marked glycolytic phenotype to support energy demands (Bhowmik et al. 2015; Samudio et al. 2010; Ito et al. 2012). Particularly, switching from OXPHOS to aerobic glycolysis was found to be essential for the functionality of CSCs, due to the decreased ROS levels induced by the upregulation of glycolysis (Dong et al. 2013). In our data, tumor thyrospheres, as expected, showed higher consumption of glycolytic metabolites, according to their higher proliferation rate compared to non cancer stem cells. Similarly, our data reported an altered flux of metabolites across the TCA cycle. In particular, levels of succinic and malic acid were found to be increased in tumor thyrospheres, as well as metabolites which might fuel TCA cycle, such as aspartate and glutamate. Particularly, significantly increased level of aminoacids, detected only in tumor thyrospheres, suggests their role in fueling the TCA cycle, determining an anaplerotic flux, a key aspect in proliferating cells (DeBerardinis et al. 2008). Among all the detected aminoacids, levels of glutamate were found to be increased in tumor thyrospheres. Intriguingly, glutamate has been previously reported to be significantly elevated following EMT induction (Bhowmik et al. 2015), a phenomenon observed in TPC-1 and B-CPAP cells (Hardin et al. 2014). On the contrary, several studies indicated that CSCs preferentially use mitochondrial respiration and oxidative metabolism (De Francesco et al. 2018). Moreover, among all the mitochondrial oxidative pathways, some CSCs rely on fatty acid oxidation for ATP and NADPH generation (Samudio et al. 2010). In some cases, FAO appeared to be essential for self-renewal capacity in hematopoietic stem cells (Ito et al. 2012). In our data, we observed a significant increase of fatty acid levels in thyrospheres, such as palmitic and stearic acid, in B-CPAP and palmitic acid in TPC-1. These findings are in line with the fundamental role of FAO pathway in PTC biology and with the

reported overexpression of genes associated with FAO in ovarian CSCs (Pastò et al. 2014). The increased levels of fatty acid oxidation rate are also in agreement with the changes observed in TCA cycle of both B-CPAP and TPC-1 thyrospheres. Indeed, an increase of fatty acid oxidation might result in an increase in concentration of intermediated in the second half of the TCA cycle (Owen et al. 2002). Moreover, our data also showed an increased level of succinic acid in the PTC-derived thyrospheres, confirming a role as oncometabolite and contributing to the CSC phenotype (Tretter et al. 2016; Vinogradov et al. 2012).

This study pin point to the importance of understanding of the CSCs metabolic features involved in survival and functionality, aiming to develop novel therapeutic strategies to eradicate CSCs. Several studies provided information about CSCs metabolism, considering it as a relevant target in anticancer therapy (De Francesco et al. 2018). In this scenario, the second part of this project provided data of the metabolic profiles of two PTC-derived cell lines, which are both representative of the *BRAF*-like PTC subgroup. Although in other tumors the glycolytic and oxidative phenotypes are mutually exclusive (Sancho et al. 2016) in our data, CSCs of PTC-derived cells seem to be characterized by glycolytic and oxidative metabolic features, suggesting a metabolic plasticity. A deeper knowledge on the CSCs ability to switch to different metabolic in response to environmental stimuli, might improve the development of therapeutic strategies.

Anti-tumoral effects and metabolic reprogramming Vitamin C-induced.

Vitamin C has become relevant in cancer research, playing an important role in the regulation of cancer development and growth (Margreet et al. 2018). In the last decades, several studies have reported cytotoxicity toward cancer cells by vitamin C *in vitro* and *in vivo* (Du et al. 2012; Park 2013). Increasing evidences reported that high concentration of vitamin C acts as pro-oxidant in some types of cancer cells, suggesting that doses of vitamin C induce oxidative stress (Bram et al. 1980). The cytotoxic effects of vitamin C have been associated with its ability to produce ROS, which may trigger several effects also in the metabolism of cancer cells (Liu et al. 2008). Indeed previous studies reported that high-dose of vitamin C induced apoptosis in cancer cells through the accumulation of H₂O₂ and, consequently, the oxidation of glutathione (Park et al. 2004). Although the main established mechanism of the cytotoxicity of vitamin C is the induction of oxidative stress in cancer cells, there is an ongoing interest in cellular mechanisms underlying vitamin C effects. Recently, it has been suggested that there is an important relationships between vitamin C pro-oxidant effects and cancer cell metabolism (Park et al. 2018), particularly related to glycolysis, TCA cycle, and pentose phosphate pathway (Uetaki et al. 2015). Furthermore, the biological significance of vitamin C-induced metabolic changes is still far from being clear. In this scenario, the third part of the project aimed to determine the anti-tumoral effects of vitamin C and the modulation of metabolic processes, in PTC-derived cell lines, understanding how vitamin C selectively affects redox balance and energetic pathways. In our data, as expected, PTC-derived cells display a decrease in cell viability due to the high-dose of vitamin C. Particularly, PTC-derived cells and the control cells exhibited different susceptibility to the vitamin C treatment, showing different IC₅₀ at 48 h of incubation. B-CPAP and K1 cells displayed a 50% decrease in cell viability with 5mM of vitamin C, while TPC-1 needed 10mM. The least sensitive cell line for the vitamin C cytotoxicity resulted to be Nthy-ori3-1. These

findings are in agreement with previous studies about the selectively cytotoxic effect of vitamin C in cancer cells harboring *KRAS* or *BRAF* mutations (Yun et al. 2015) as B-CPAP and K1, which shared *BRAF*. As described above, vitamin C stimulates the accumulation of ROS, by H₂O₂ generation, resulting in a deregulation of redox balance (Park et al. 2018). Our data, in keeping with these findings, showed an increase production of ROS, due to vitamin C treatment, particularly in B-CPAP and Nthy-ori cells. TBH was used as positive control, and ROS levels, TBH-induced, was almost 4-fold higher than ROS induction by vitamin C. Interestingly, adding the anti-oxidant compound, NAC significant decreased ROS levels only in PTC-derived cells and not in the control cells. This finding might confirm the different susceptibility to vitamin C between cancer and normal cells (Vissers et al. 2018), and it demonstrated the higher capability of cancer cells to recover the redox homeostasis after the oxidative stimulus vitamin C-induced. Furthermore, ratio of antioxidants, such as GSH/GSSG and Cysteine/Cystine were affected by the vitamin C treatment. Particularly, our data showed a significantly decreased of GSH/GSSG ratio only in B-CPAP, while cysteine/cystine ratio was significant decreased in B-CPAP and K1 and the control cells. In accordance with vitamin C pro-oxidant effects, antioxidant species and their reduced/oxidized ratio appeared to be reduced, probably due to H₂O₂ accumulation (Park 2013). Our data suggested that cysteine/cystine antioxidant system seemed to be more perturbed and involved in the regulation of the oxidative stress vitamin-C induced. Decreased cysteine/cystine ratio induced by vitamin C reflected the increased demands of antioxidants, particularly GSH. Indeed cancer cells exhibited high requirement for cysteine for GSH synthesis, particularly under oxidative stress condition, where cysteine production is insufficient for GSH synthesis (Cramer et al. 2017). Considering the closely relationship between redox balance and metabolism, vitamin C, modulating the redox status, might affects the cancer metabolism, providing an alternative paradigm in cancer therapy, where both redox homeostasis and metabolism will be perturbed. In order to explore metabolic effects, we measured metabolic features, such as glycolytic and TCA cycle metabolites and electron carries involved in redox reaction through metabolomics targeted

analysis by using UHPLC/MS. Our data showed an increase of metabolites upstream the glycolysis, while metabolites from 3PG to pyruvate were decreased in most of the analyzed cells. Additionally, the first part of the TCA cycle was reduced in levels of metabolites from citrate to succinyl-CoA, while succinate, fumarate, malate and oxaloacetate were increased due to the treatment. Interestingly, levels of coenzyme A and acetyl-coA were significantly increased in all PTC-derived cells and in Nthy-ori3-1 and TPC-1 respectively. These results confirmed that vitamin C altered cell metabolism, with a critical reduction of the second half of the glycolysis and the first half of the TCA cycle. These findings are in keeping with previous data about the perturbation of glycolysis, TCA cycle and pentose phosphate shunt vitamin C-induced in breast cancer cells (Uetaki et al. 2015). Moreover, further confirmation of metabolic perturbation vitamin C-induced was obtained by measuring the relative glucose uptake after vitamin C treatment. Exposure to high-dose of vitamin C resulted in a decrease in glucose uptake in PTC-derived and control cells. In particular, B-CPAP and TPC-1 showed a more evident decrease of glucose uptake, suggesting their increase sensitivity to vitamin C treatment compared to the control cells. Indeed the oxidized form of vitamin C, DHA, is similar to glucose in the chemical structure and is uptaken into cells by GLUTs transposters (Rumsey et al. 1997). According to this, entrance of vitamin C into cells might reduce the glucose entrance, perturbing uptake rate of glucose and, consequently, its metabolism. The effects of vitamin C in the PTC-cell metabolism suggested a possible regulation of energetic pathways, particularly glycolysis and TCA cycle. Indeed metabolic effect induced by vitamin C treatment has been already described in breast cancer cells as a consequence of NAD depletion (Uetaki et al. 2015). It has also been hypothesized that NAD depletion was a consequence of oxidative stress H₂O₂-induced (Chen et al. 2005). According with these previous findings, we measured NAD, Nicotinamide and Nicotinic acid levels, involved in the NAD⁺ salvage pathway (Garten et al. 2009). Our data showed a decreased in NAD⁺ (significantly in K1 cells) and its precursors, Nicotinamide (significantly in TPC-1, K1 and B-CPAP cells) and Nicotinic acid (significantly in control cells), due to vitamin C treatment. NAD salvage synthesis,

and the key enzyme of this pathway, Nampt, have been described as potential therapeutic target in cancer (Chini et al. 2014). Overall, we proposed a possible effect of vitamin C on NAD⁺, Nicotinamide and Nicotinic acid viability, mediated by ROS accumulation, which is responsible for NAD⁺ depletion. It has been previously described that vitamin C induces cell cycle arrest in various cancer cells, such as lymphoma cells and leukemia cells (Kao et al. 1993; Yanagisaka-Shiota et al. 1995; Iwasaka et al 1998), melanoma cells (Kang et al. 2005), brain tumor cells (Baader et al.1994; Lee et al. 1994), prostate cancer cells (Maramac et al. 1997; Menon et al. 1998), and stomach cancer cells (Head et al.1996). The cytotoxicity induced by the vitamin C has been linked to the accumulation of hydrogen peroxide, which induces cell growth arrest, apoptosis and/or necrosis (Sakagami et al. 2000). Apoptosis and necrosis may occur simultaneously depending on the stimulus (Elmore et al. 2007). Despite many studies have reported that relatively high concentration of vitamin C induced apoptosis on tumor cells (Kang et al. 2003; Kang et al. 2005), our preliminary data showed that vitamin C treatment induced cell death by necrosis in PTC-cells while in control cells by apoptosis. These findings suggested a different effect in cell death mechanism in cancer and non cancer cells. Normal cells usually activate programmed cell death against toxic stimuli, while cancer cells often avoid this cellular response by disabling the apoptotic pathways (Fernald and Kurokawa 2013). Moreover, accumulating evidences have shown that necrosis can also proceed in a regular manner, by “necroptosis”, which can be induced by several stimuli, including cellular metabolic and genotoxic stresses, or various anti-cancer agents (Su et al 2015).

VI. Conclusion

By examining the alterations in metabolism and redox status, resulting from oncogenic mutations such as *BRAF*, *TP53*, *RET/PTC* and *hTERT* mutations, we provided evidence of the crosstalk among metabolic dependencies, redox modulation and oncogenic features in PTC-derived cells. Particularly, we found that the most perturbed metabolic phenotype, characterized by higher glycolytic rate and altered metabolite flux across TCA cycle and glutaminolysis, was associated with PTC-derived cells harboring the most distinctive genetic background (*BRAF*^{V600E}, *TP53* and *hTERT* mutations). Similarly, considering the heterogenous cancer cell population within tumor mass, we provided evidences about metabolic dependencies and changes in PTC-derived CSCs, pinpointing possible metabolic targets, to eradicate the “beating heart” of tumor.

Overall, our project confirmed the pivotal role of the metabolism and redox state regulation in the cancer development and maintenance, and, consequently, their role as promising therapeutic targets or as diagnostic features. The ongoing investigation and understanding of cancer cell metabolism provide useful information, which can be translated into therapeutic and diagnostic tools. Metabolic differences between normal and malignant tissues are thought to be driven by cancer genes. Nevertheless, it is now becoming increasingly evident that cancer metabolism, as hallmark of cancer, might be considered as root cause of the development, progression and aggressiveness of cancer. Our findings underline this hypothesis, highlighting that the aggressive forms of PTC-derived might be also characterized by marked metabolic alterations.

Hence, the complexity network of oncogenes and metabolic pathways needs to be understood, in order to strategically target cancer cells. In this scenario, we studied the antitumoral effect of vitamin C, according with its ability to affect cell survival and proliferation, mostly by inducing oxidative stress. Interestingly, we report the metabolic effect of Vitamin C in PTC-derived cells, by affecting energy production, inducing oxidative stress, and finally cell death by necrosis. Our data displayed the possible modulation of NAD⁺, Nicotinamide and Nicotinic acid, and, consequently, the arrest of metabolic pathways, by vitamin C treatment.

Despite many studies having focused their attention on cancer cell metabolism and cancer cell metabolic plasticity over the last decade, our study has highlighted the need for a holistic and translational approach of studying cancer, considering the cross talk among oncogenic, metabolic and redox events during tumorigenesis. Overall, we can conclude that understanding and dissecting the metabolic complexity of cancer cells remain a great challenge in this field.

VII. Bibliography

- Acquaviva G, Visani M, Repaci A, Rhoden KJ, de Biase D et al. Molecular pathology of thyroid tumours of follicular cells: a review of genetic alterations and their clinicopathological relevance. *Histopathology* 2018;72:6-31
- Ahn CS, Metallo CM. Mitochondria as biosynthetic factories for cancer proliferation. *Cancer Metab.* 2015;3:1
- Al-Hajj M, Wicha MS, Benito-Hernandez A, Morrison SJ, Clarke MF. Prospective identification of tumorigenic breast cancer cells. *Proc Natl Acad Sci U S A.* 2003;100:3983-8
- Amelio I, Cutruzzolà F, Antonov A, Agostini M, Melino G. Serine and glycine metabolism in cancer. *Trends Biochem Sci.* 2014; 39: 191–198.
- Ames BM, Shigenaga MK, Hagen TM. Oxidants, antioxidants, and the degenerative diseases of aging. *Proc Natl Acad Sci U S A.* 1993;90:7915-22.
- Anderson NN, Mucka P, Kern JS, Feng H. The emerging role and targetability of the TCA cycle in cancer metabolism. *Protein Cell.* 2018;9:216-237.
- Armitage EG, Barbas C. Metabolomics in cancer biomarker discovery: current trends and future perspectives. *J Pharm Biomed Anal.* 2014;87:1-11
- Asa SL. The evolution of differentiated thyroid cancer. *Pathology.* 2017;49:229-237
- Baader S, Bruchelt G, Carmine T, Lode H, Rieth A and Niethammer D: Ascorbic-acid-mediated iron release from cellular ferritin and its relation to the formation of DNA strand breaks in neuroblastoma cells. *J Cancer Res Clin Oncol* 1994;120:415-421.
- Baenke F, Peck B, Miess H, Schulze A. Hooked on fat: the role of lipid synthesis in cancer metabolism and tumour development. *Dis Model Mech.* 2013;6:1353-63.
- Bajad SU, Lu W, Kimball EH, Yuan J, Peterson C, Rabinowitz JD. Separation and quantitation of water soluble cellular metabolites by hydrophilic interaction chromatography-tandem mass spectrometry. *J Chromatogr A.* 2006; 1125:76-88.
- Barker M, Rayens W. Partial least squares for discrimination. *J Chemom.* 2003;17:166–173

- Baysal BE, Ferrell RE, Willett-Brozick JE, Lawrence EC, Myssiorek D, et al. Mutations in SDHD, a mitochondrial complex II gene, in hereditary paraganglioma. *Science*, 2000; 287, 848–851.
- Beckers A, Organe S, Timmermans L, Scheys K, Peeters A, et al.,. Chemical inhibition of acetyl-CoA carboxylase induces growth arrest and cytotoxicity selectively in cancer cells *Cancer Res.* 2007;67:8180-7.
- Beger RD. A review of applications of metabolomics in cancer. *Metabolites*. 2013 Jul 5;3:552-74
- Bensaad A, Tsuruta MA, Selak MN, Vidal K, Nakano R, et al. TIGAR, a p53-inducible regulator of glycolysis and apoptosis. *Cell* 2006;126:107-120
- Bhatia P, Tsumagari K, Abd Elmageed ZY, Friedlander P, Buell JF, et al.,. Stem cell biology in thyroid cancer: Insights for novel therapies. *World J Stem Cells*. 2014; 6: 614–619.
- Bhowmik SK, Ramirez-Peña E, Arnold JM, Putluri V, Sphyris N, et al. EMT-induced metabolite signature identifies poor clinical outcome. *Oncotarget* 2015;6:42651–42660
- Bonnet S, Archer SL, Allalunis-Turner J, Haromy A, Beaulieu C, et al. A mitochondria-K⁺ channel axis is suppressed in cancer and its normalization promotes apoptosis and inhibits cancer growth. *Cancer Cell*. 2007;11:37-51.
- Bos JL, Rehann H, Wittinghofer A. GEFs and GAPs: critical elements in the control of small G proteins. *Cell*. 2007;129:865-77.
- Bradford MM. Rapid and Sensitive Method for the Quantification of Microgram Quantities of Protein Utilizing the Principle of Protein-Dye Binding. *Anal Chemistry*. 1976;72:248-254
- Bram S, Froussard P, Guichard M, Jasmin C, Augery Y. Vitamin C preferential toxicity for malignant melanoma cells. *Nature*. 1980; 284:629-31
- Brand MD. The sites and topology of mitochondrial superoxide production. *Exp Gerontol*. 2010;45:466-72.
- Burrows N, Babur M, Resch J, Williams KJ, Brabant G. Hypoxia-inducible factor in thyroid carcinoma. *J Thyroid Res*. 2011; 2011:762905

- Burrows N, Resch J, Cowen RL, von Wasielewski R, Hoang-Vu C, et al. Expression of hypoxia-inducible factor 1 alpha in thyroid carcinomas. *Endocr Relat Cancer*. 2010; 17:61-72
- Cairns RA, Harris IS, Mak TW. Regulation of cancer cell metabolism. *Nat Rev Cancer*. 2011;11:85-95.
- Cameron E, Pauling L. Supplemental ascorbate in the supportive treatment of cancer: Prolongation of survival times in terminal human cancer. *Proc Natl Acad Sci U S A*. 1976;73:3685-3689
- Cancer Genome Atlas Research Network. Integrated genomic characterization of papillary thyroid carcinoma. *Cell* 2014,159:676–690
- Caria P, Pillai R, Dettori T, Frau DV, Zavattari, et al. Thyrospheres from B-CPAP Cell Line with BRAF and TERT Promoter Mutations have Different Functional and Molecular Features than Parental Cells. *J Cancer*. 2017;8:1629-1639
- Caria P, Tronci L, Dettori T, Murgia F, Santoru ML, et al. Metabolomic Alterations in Thyrospheres and Adherent Parental Cells in Papillary Thyroid Carcinoma Cell Lines: A Pilot Study. *Int J Mol Sci*. 2018;19.
- Carracedo A, Pandolfi PP. The PTEN-PI3K pathway: Of feedbacks and cross-talks. *Oncogene*. 2008;27:5527-41
- Catalano MG¹, Poli R, Pugliese M, Fortunati N, Boccuzzi G. Emerging molecular therapies of advanced thyroid cancer. *Mol Aspects Med*. 2010;31:215-26.
- Chandel NS, Tuveson DA. The promise and perils of antioxidants for cancer patients. *N Engl J Med*. 2014;371:177-8.
- Chen JQ, Russo J. Dysregulation of glucose transport, glycolysis, TCA cycle and glutaminolysis by oncogenes and tumor suppressors in cancer cells. *Biochim Biophys Acta*. 2012;1826:370–384
- Chen M, Shen M, Li Y, Liu C, Zhou K, Hu W, Xu B, Xia Y, Tang W. GC-MS-based metabolomic analysis of human papillary thyroid carcinoma tissue. *Int J Mol Med*. 2015;36:1607-14.

- Chen Q, Espey MG, Krishna MC, Mitchek JB, Corpe CP, et al. Pharmacologic ascorbic acid concentrations selectively kill cancer cells: action as a pro-drug to deliver hydrogen peroxide to tissues. *Proc. Natl. Acad. Sci. USA.* 2005;102:13604–13609
- Chi SL, Wahl ML, Mowery YM, Shan S, Mukhopadhyay S, et al. Angiostatin-like activity of a monoclonal antibody to the catalytic subunit of F1F0 ATP synthase. *Cancer Res.* 2007;67:4716-24.
- Chini CC, Guerrico AM, Nin V, Camacho-Pereira J, Escande C, et al. Targeting of NAD Metabolism in Pancreatic Cancer Cells: Potential Novel Therapy for Pancreatic Tumors. *Clin Cancer Res.* 2014;20:120-30
- Cho ES, Cha YH, Kim HS, Kim NH, Yook JI. The Pentose Phosphate Pathway as a Potential Target for Cancer Therapy. *Biomol Ther.* 2018;26:29-38.
- Choi SY, Xue H, Wu R, Fazli L, Lin D, et al. The MCT4 Gene: A Novel, Potential Target for Therapy of Advanced Prostate Cancer. *Clin Cancer Res.* 2016; 22:2721-33
- Choi YK, Park KG. Targeting Glutamine Metabolism for Cancer Treatment. *Biomol Ther (Seoul).* 2018; 26: 19–28
- Ciavardelli D, Bellomo M, Consalvo A, Crescimanno C, Vella V. Metabolic alterations of thyroid cancer as potential therapeutic targets. *Biomed Res Int.* 2017;2017:2545031.
- Ciavardelli D, Rossi C, Barcaroli D, Volpe S, Consalvo A, et al. Breast cancer stem cells rely on fermentative glycolysis and are sensitive to 2-deoxyglucose treatment. *Cell Death Dis.* 2014;5:e1336
- Clevers H. The cancer stem cell: premises, promises and challenges. *Nat Med.* 2011;17(3):313-9
- Cohen JJ, Duke RC, Fadok VA, Sellins KS. () Apoptosis and cell death in immunity. *Ann. Rev. Immunol.* 1992; 10:267–293.
- Colin IM, Denef JF, Lengelé B, Many MC, Gérard AC. Recent insights into the cell biology of thyroid angiofollicular units. *Endocr Rev.* 2013;34:209-38.

- Contractor T, Harris CR. p53 negatively regulates transcription of the pyruvate dehydrogenase kinase Pdk2. *Cancer Res.* 2012;72:560-567
- Costa AM, Herrero A, Fresno MF et al. BRAF mutation associated with other genetic events identifies a subset of aggressive papillary thyroid carcinoma. *Clin. Endocrinol.* 2008; 68; 618– 634
- Cox AG, Winterbourn CC, Hampton MB. Mitochondrial peroxiredoxin involvement in antioxidant defence and redox signaling. *Biochem J.* 2009;425:313-25.
- Cramer SL, Saha A, Liu J, Tadi S, Tiziani S, et al. Systemic depletion of L-cyst(e)ine with cyst(e)inase increases reactive oxygen species and suppresses tumor growth. *Nat Med.* 2017;23:120-127
- Curry JM, Tassone P, Cotzia P, Sprandio J, Luginbuhl A, Cognetti DM, Mollae M, Domingo M, Pribitkin EA, Keane WM, Zhan TT, Birbe R, Tuluc M, Martinez-Outschoorn U. Multicompartment metabolism in papillary thyroid cancer. *Laryngoscope.* 2016;126:2410-2418.
- Curry JM, Tuluc M, Whitaker-Menezes D, Ames JA, Anantharaman A, et al. Cancer metabolism, stemness and tumor recurrence: MCT1 and MCT4 are functional biomarkers of metabolic symbiosis in head and neck cancer. *Cell Cycle* 2013,12:1371–1384
- Curthoys NP, Watford M. Regulation of glutaminase activity and glutamine metabolism. *Annu Rev Nutr.* 1995;15:133-59.
- Dalerba P, Dylla SJ, Park IK, Liu R, Wang X, et al. Phenotypic characterization of human colorectal cancer stem cells. *Proc Natl Acad Sci U S A.* 2007;104:10158–63
- Davies H, Bignell GR, Cox C, Stephens P, Edkins S, et al. Mutations of the BRAF gene in human cancer. *Nature* 2002; 27;417:949-54
- Davies L, Morris LG, Haymart M, Chen AY, Goldenberg D, et al. 2015. American Association of Clinical Endocrinologists and American College of Endocrinology disease state clinical review: the increasing incidence of thyroid cancer. *Endocr. Pract.* 2015;21:686-96.

- De Francesco EM, Sotgia F, Lisanti MP. Cancer stem cells (CSCs): metabolic strategies for their identification and eradication. *Biochem J.* 2018;475:1611-1634
- De Gonzalo-Calvo D, Lopez-Vilaro L, Nasarre L, Perez-Olabarria M, Vazquez T, Escuin D, Badimon L, Barnadas A, Lerma E, Llorente-Cortés V. Intratumor cholesteryl ester accumulation is associated with human breast cancer proliferation and aggressive potential: a molecular and clinicopathological study. *BMC Cancer.* 2015;15:460.
- DeBerardinis JR, Chandel NS. Fundamental of cancer metabolism. *Sci Adv.*2016; 2(5): e1600200
- DeBerardinis RJ, Cheng T. Q's next: the diverse functions of glutamine in metabolism, cell biology and cancer. *Oncogene.* 2010;29:313-24.
- DeBerardinis RJ, Lum JJ, Hatzivassiliou G, Thompson CB. The Biology of Cancer: Metabolic Reprogramming Fuels Cell Growth and Proliferation Cell Metabolism. *Cell Metab.* 2008;7:11–20
- DeBerardinis RJ, Mancuso A, Daikhin E, Nissim I, Yudkoff M, Wehrli S, Thompson CB. Beyond aerobic glycolysis: transformed cells can engage in glutamine metabolism that exceeds the requirement for protein and nucleotide synthesis. *Proc Natl Acad Sci USA.*2007;104:19345-19350
- Deja S, Dawiskiba T, Balcerzak W, Orczyk-Pawłowicz M, Głód M et al., Follicular adenomas exhibit a unique metabolic profile. ¹H NMR studies of thyroid lesions. *PLoS One.* 2013;8:e84637
- DeNicola GM, Karreth FA, Humpton TJ, Gopinathan A, Wei C, Frese K, Mangal D, Yu KH, Yeo CJ, Calhoun ES, Scrimieri F, Winter JM, Hruban RH, Iacobuzio-Donahue C, Kern SE, Blair IA, Tuveson DA. Oncogene-induced Nrf2 transcription promotes ROS detoxification and tumorigenesis. *Nature.* 2011;475:106-9.
- Denko NC. Hypoxia, HIF1 and glucose metabolism in the solid tumour. *Nat Rev Cancer.* 2008;8:705-13.
- Dhup S, Dadhich RK, Porporato PE, Sonveaux P. Multiple biological activities of lactic acid in cancer: influences on tumor growth, angiogenesis and metastasis. *Curr Pharm Des.* 2012;18:1319-30.

- Di Cristofaro J, Marcy M, Vasko V, Sebag F, Fakhry N, et al. Molecular genetic study comparing follicular variant versus classic papillary thyroid carcinomas: association of N-ras mutation in codon 61 with follicular variant. *Hum. Pathol.* 2006;37:824
- Doherty JR, Cleveland JL. Targeting lactate metabolism for cancer therapeutics. *J Clin Invest.* 2013;123:3685-92.
- Dong C, Yuan T, Wu Y, Wang Y, Fan TW, et al. Loss of FBP1 by Snail-mediated repression provides metabolic advantages in basal-like breast cancer. *Cancer Cell.* 2013;23(3): 316–331
- Du J, Cullen J J, Buettner G R. Ascorbic acid: Chemistry, biology and the treatment of cancer. *Biochim. Biophys. Acta.* 2012; 1826, 443–457.
- Du J, Martin SM, Levine M, Wagner BA, Buettner GR et al. Mechanisms of ascorbate-induced cytotoxicity in pancreatic cancer. *Clin. Cancer Res.* 2010;16, 509–520.
- Dwivedi P, Wu P, Klopsch SJ, Puzon GJ, Xun L, Hill HH. Metabolic profiling by ion mobility mass spectrometry (IMMS). *Metabolomics.* 2008;4:63–80.
- Eagle H. The minimum vitamin requirements of the L and HeLa cells in tissue culture, the production of specific vitamin deficiencies, and their cure. *J Exp Med.* 1955; 102: 595–600.
- El-Naggar CJ, Grandis JR, Takata T and Slootweg PJ. “World Health Organization classification of head and neck tumours,” in *World Health Organization Classification of Tumours.* 2017, vol. 9, 4th edition.
- Elmore S. Apoptosis: A review of programmed cell death. *Toxicol Pathol.* 2007;35:495–516.
- Emmink BL, Verheem A, Van Houdt WJ, Steller EJ, Govaert KM et al. The secretome of colon cancer stem cells contains drug-metabolizing enzymes. *J Proteomics.* 2013 Oct 8;91:84-96
- Erler JT, Bennewith KL, Nicolau M, Dornhöfer N, Kong C, et al. Lysyl oxidase is essential for hypoxia-induced metastasis. *Nature* 2006;440
- Eruslanov E, Kusmartsev S. Identification of ROS Using Oxidized DCFDA and Flow-Cytometry. *Methods Mol Biol.* 2010;594:57-72.

- Estrela JM, Ortega A, Obrador E. Glutathione in cancer biology and therapy. *Crit Rev Clin Lab Sci.* 2006; 43:143-81
- Fang YZ, Yang S, Wu G. Free radicals, antioxidants, and nutrition. *Nutrition.* 2002;18(10):872-9.
- Feng C, Gao Y, Wang C, Yu X, Zhang W, Guan H, Shan Z, Teng W. Aberrant Overexpression of Pyruvate Kinase m2 is associated with aggressive tumor features and the BRAF mutation in papillary thyroid cancer. *J Clin Endocrinol Metab.* 2013;98:E1524-33
- Fernald K, Kurokawa M. Evading apoptosis in cancer. *Trends Cell Biol.* 2013 Dec; 23: 620–633.
- Feron O. Pyruvate into lactate and back: from the Warburg effect to symbiotic energy fuel exchange in cancer cells. *Radiother Oncol.*2009;92:329-333
- Fiehn O, Kopka J, Dörmann P, Altmann T, Trethewey RN, Willmitzer L. Metabolite profiling for plant functional genomics. *Nature Biotechnology.* 2000;18:1157–1161
- Fiehn O. Metabolomics--the link between genotypes and phenotype. *Plant Mol. Biol.*2002;48, 155-71.
- Finkel T. From sulfenylation to sulphydration: What a thiolate needs to tolerate. *Sci Signal.* 2012;5:pe10.
- Fredriksson NJ, Ny L, Nilsson JA, Larsson E. Systematic analysis of noncoding somatic mutations and gene expression alterations across 14 tumor types. *Nat. Genet.* 2014;46:1258–63
- Frilling A, Tecklenborg K, Görges R, Weber F, Clausen M, Broelsch EC. Preoperative diagnostic value of [(18)F] fluorodeoxyglucose positron emission tomography in patients with radioiodine-negative recurrent well-differentiated thyroid carcinoma. *Ann Surg.* 2001;234:804-11.
- Fruehauf JP, Meyskens FL Jr. Reactive oxygen species: a breath of life or death?. *Clin Cancer Res.* 2007;13:789-94
- Fujinaga S, Sakagami H. Possible role of hydrogen peroxide in apoptosis induction by ascorbic acid in human myelogenous leukemic cell lines. *Showa Univ. Med. Sci.* 1994;6:135–144

- Furuta E, Okuda H, Kobayashi A, Watabe K. Metabolic genes in cancer: their roles in tumor progression and clinical implications. *Biochim Biophys Acta*. 2010;1805:141- 152
- Gambhir SS. Molecular imaging of cancer with positron emission tomography. *Nature Rev. Cancer* 2002;1:683–693
- Gao P, Tchernyshyov I, Chang T, Lee Y, Kita K, Ochi T, Zeller KI, De Marzo AM, Van Eyk JE, Mendell JT, Dang CV. c-Myc suppression of miR-23a/b enhances mitochondrial glutaminase expression and glutamine metabolism. *Nature*. 2009;458:762-5.
- Garcia A, Barbas C. Gas chromatography–mass spectrometry (GC–MS)-based metabolomics. *Methods Mol Biol*. 2011;708:191-204
- Garten A, Petzold S, Korner A, Imai S, Kiess W. Nampt: linking NAD biology, metabolism and cancer. *Trends Endocrinol Metab* 2009;20: 130–38
- Ghossein R and Livolsi VA. Papillary thyroid carcinoma tall cell variant. *Thyroid*. 2008;18:1179-81.
- Gill KS, Tassone P, Hamilton J, Hjelm N, Luginbuhl A et al., Thyroid cancer metabolism: a review. *Thyroid Disorders Ther* 2016, 5:200.
- Giordano TJ, Kuick R, Thomas DG, Misek DE, Vinco M, et al. Molecular classification of papillary thyroid carcinoma: distinct BRAF, RAS, and RET/PTC mutation-specific gene expression profiles discovered by DNA microarray analysis. *Oncogene* 2005 24:6646–56
- Giordano TJ. Follicular cell thyroid neoplasia: insights from genomics and The Cancer Genome Atlas research network. *Curr Opin Oncol*. 2016; 28:1-4
- Giordano TJ. Genomic Hallmarks of Thyroid Neoplasia. *Annu Rev Pathol*. 2018 Jan 24;13:141-162.
- Goodwin ML, Gladden LB, Nijsten MW, Jones KB. Lactate and cancer: revisiting the warburg effect in an era of lactate shuttling. *Front Nutr*. 2014; 1: 27.
- Gottlieb E and Tomlinson IP. Mitochondrial tumour suppressors: A genetic and biochemical

update. *Nature Reviews. Cancer* 2005;5:857–866.

- Gowda GA, Djukovic D. Overview of Mass Spectrometry-Based Metabolomics: Opportunities and Challenges. *Methods Mol Biol.* 2014;1198:3-12
- Grabellus F, Nagarajah J, Bockisch A, Schmid KW, Sheu SY. Glucose transporter 1 expression, tumor proliferation, and iodine/glucose uptake in thyroid cancer with emphasis on poorly differentiated thyroid carcinoma. *Clin Nucl Med.* 2012;37:121-7.
- Granja S, Pinheiro C, Reis RM, Martinho O, Baltazar F. Glucose Addiction in Cancer Therapy: Advances and Drawbacks. *Curr Drug Metab.* 2015;16:221-42
- Grieco M, Santoro M, Berlingieri MT, Melillo RM, Donghi R et al. PTC is a novel rearranged form of the ret proto-oncogene and its frequently detected in vivo human thyroid papillary carcinomas. *Cell* 1990; 23;60:557-63.
- Guha M, Srinivasan S, Ruthel G, Kashina AK, Carstens RP, Mendoza A, et al. Mitochondrial retrograde signaling induces epithelial-mesenchymal transition and generates breast cancer stem cells. *Oncogene.* 2014;33:5238-50.
- Guo S, Qiu L, Wang Y, Qin X, Liu H, et al. Tissue imaging and serum lipidomic profiling for screening potential biomarkers of thyroid tumors by matrix-assisted laser desorption/ionization-Fourier transform ion cyclotron resonance mass spectrometry. *Anal Bioanal Chem.* 2014 Jul;406:4357-70
- Guo S, Wang Y, Zhou D, Li Z. Significantly increased monounsaturated lipids relative to polyunsaturated lipids in six types of cancer microenvironment are observed by mass spectrometry imaging. *Sci Rep.* 2014;4:5959
- Gupta N, Goswami B, Chowdhury V, Ravishankar L, Kakar A. Evaluation of the role of magnetic resonance spectroscopy in the diagnosis of follicular malignancies of thyroid. *Arch Surg.* 2011;146:179-82

- Gupta SC, Hevia D, Patchva S, Park B, Koh W, Aggarwal BB. Upsides and downsides of reactive oxygen species for cancer: the roles of reactive oxygen species in tumorigenesis, prevention, and therapy. *Antioxid Redox Signal*. 2012;16:1295-322
- Halket JM, Waterman D, Przyborowska AM, Patel RK, Fraser PD, Bramley PM. Chemical derivatization and mass spectral libraries in metabolic profiling by GC/MS and LC/MS/MS. *J Exp Bot*. 2005;56:219-43
- Halliwell B, Clement MV, Long LH. Hydrogen peroxide in the human body. *FEBS Lett*. 2000;486:10-3.
- Hamanaka RB, Chandel NS. Targeting glucose metabolism for cancer therapy. *J Exp Med*. 2012; 209:211–5
- Hanahan D and Weinberg RA. The Hallmarks of Cancer: The next generation. *Cell*, 2011;144, 646-674
- Hao J, Chen H, Madigan MC, Cozzi PJ, Beretov J, et al. Co-expression of CD147 (EMMPRIN), CD44v3-10, MDR1 and monocarboxylate transporters is associated with prostate cancer drug resistance and progression. *Br J Cancer*. 2010;103:1008–18
- Hardin H, Guo Z, Shan W, Montemayor-Garcia C, Asioli S, et al. The roles of the epithelial-mesenchymal transition marker PRRX1 and miR-146b-5p in papillary thyroid carcinoma progression. *Am. J. Pathol*. 2014;184:2342–2354
- Hatzivassiliou F, Zhao DE, Bauer C, Andreadis AN, Shaw D, et al.,. ATP citrate lyase inhibition can suppress tumor cell growth. *Cancer Cell*. 2005;8:311-321
- Head KA. Ascorbic acid in the prevention and treatment of cancer. *Altern Med Rev*; 1996 3: 174-186.
- Hemminki K and Li X. Familial risk of cancer by site and histopathology. *Int J Cancer*. 2003;103:105-9.

- Hirota K, Semenza GL. Regulation of hypoxia-inducible factor 1 by prolyl and asparaginyl hydroxylases. *Biochem Biophys Res Commun.* 2005;338:610-6
- Holmes E, Wilson ID, Nicholson JK. Metabolic phenotyping in health and disease. *Cell* 2008;134:714-717.
- Hu W, Zhang C, Wu R, Sun Y, Levine A, Feng Z. Glutaminase 2, a novel p53 target gene regulating energy metabolism and antioxidant function. *Proc. Natl. Acad. Sci. U. S. A.*2010;107:7455-7460
- Hutton JE, Wang X, Zimmerman LJ, Slebos R, Trenary IA et al. Oncogenic KRAS and BRAF Drive Metabolic Reprogramming in Colorectal Cancer. *Mol Cell Proteomics.* 2016;15(9):2924-38
- Icard P, Poulain L, Licet H. Understanding the central role of citrate in the metabolism of cancer cells. *Biochim Biophys Acta.* 2012 Jan;1825:111-6
- Islam F, Qiao B, Smith RA, Gopalan V, Lam AK. Cancer stem cell: Fundamental experimental pathological concepts and updates. *Exp. Mol. Pathol.* 2015;98:184-91.
- Ito K, Carracedo A, Weiss D, Arai F, Ala U et al. A PML-PPAR-delta pathway for fatty acid oxidation regulates hematopoietic stem cell maintenance. *Nat Med.* 2012,18, 1350-8
- Ito K, Suda T. Metabolic requirements for the maintenance of self-renewing stem cells . *Nat Rev Mol Cell Biol.* 2014;15: 243–256
- Iwasaka K, Koyama N, Nogaki A, Maruyama S, Tamura A, Takano H, et al. Role of hydrogen peroxide in cytotoxicity induction by ascorbates
- and other redox compounds. *Anticancer Res* 1998;18: 4333-4337.
- Jackson AL, Loeb LA. The contribution of endogenous sources of DNA damage to the multiple mutations in cancer. *Mutat Res.* 2001;477:7-21.
- Jang H, Yang J, Lee E, Cheong JH. Metabolism in embryonic and cancer stemness. *Arch Pharm Res.* 2015;38:381–8

- Jang H, Yang J, Lee E, Cheong JH. Metabolism in embryonic and cancer stemness. *Arch Pharm Res.* 2015;38:381–8
- Jang YY, Sharkis SJ. A low level of reactive oxygen species selects for primitive hematopoietic stem cells that may reside in the low-oxygenic niche. *Blood.* 2007;110:3056–63
- Jaramillo MC, Zhang DD. The emerging role of the Nrf2-Keap1 signaling pathway in cancer. *Genes Dev.* 2013;27:2179-91.
- Jiang B. Aerobic glycolysis and high level of lactate in cancer metabolism and microenvironment. *Genes & Diseases* 2017;4:25-27
- Jiang P, Du W, Wu M. Regulation of the pentose phosphate pathway in cancer. *Protein Cell.* 2014; 5: 592–602.
- Jolliffe IT. *Principal Component Analysis.* 2. Springer; 2002
- Józwiak P, Krześlak A, Bryś M, Lipińska A. Glucose-dependent glucose transporter 1 expression and its impact on viability of thyroid cancer cells. *Oncol Rep.* 2015; 33:913-20
- Kaelig WG. The von Hippel-Lindau tumour suppressor protein. *Nat Rev Cancer.* 2008;8(11):865-73.
- Kanani H, Chrysanthopoulos PK, Klapa MI. Standardizing GC–MS metabolomics. *J Chromatogr B Analyt Technol Biomed Life Sci.* 2008;871, 191–201
- Kang JS, Cho D, Kim YI, Hahm E, Yang Y, Kim D, Hur D, Park H, Bang S, Hwang YI, Lee WJ. L-ascorbic acid (vitamin C) induces the apoptosis of B16 murine melanoma cells via a caspase-8-independent pathway. *Cancer Immunol Immunother.* 2003;52:693–698
- Kang JS, Cho D, Kim YI, Hahm E, Kim YS, et al. Sodium ascorbate (vitamin C) induces apoptosis in melanoma cells via the down-regulation of transferrin receptor dependent iron uptake. *J Cell Physiol* 2005;204: 192-197.
- Kao T, Meyers W and Post F: Inhibitory effects of ascorbic acid on growth of leukemic and lymphoma cell lines. *Cancer Lett* 1993;70: 101-106.

- Khan A1, Khan MI, Iqbal Z, Shah Y, Ahmad L et al. A new HPLC method for the simultaneous determination of ascorbic acid and aminothiols in human plasma and erythrocytes using electrochemical detection. *Talanta*. 2011;84:789-801
- Khanafshar E and Lloyd RV. The spectrum of papillary thyroid carcinoma variants. *Adv. Anat. Pathol.* 2011; 18; 90–97
- Kim HM, Kim H. Oncogenes and Tumor Suppressors Regulate Glutamine Metabolism in Cancer Cells. *J Cancer Prev.* 2013; 18: 221–226.
- Kim HM, Lee YK, Koo JS. Expression of glutamine metabolism-related proteins in thyroid cancer. *Oncotarget*. 2016;7:53628-53641.
- Kim JW, Gao P, Liu YC, Semenza GL, Dang CV. Hypoxia-inducible factor 1 and dysregulated c-Myc cooperatively induce vascular endothelial growth factor and metabolic switches hexokinase 2 and pyruvate dehydrogenase kinase 1. *Mol. Cell. Biol.* 2007;27:7381-93
- Kim SJ, Kwon MC, Ryu MJ, Chung HK, Tadi S, Kim YK, Kim JM, Lee SH, Park JH, Kweon GR, Ryu SW, Jo YS, Lee CH, Hatakeyama H, Goto Y, Yim YH, Chung J, Kong YY, Shong M. CRIF1 is essential for the synthesis and insertion of oxidative phosphorylation polypeptides in the mammalian mitochondrial membrane. *Cell Metab.* 2012;16:274-83.
- Kimura ET, Nikiforova MN, Zhu Z, Knauf JA, Nikiforov YE, Fagin JA. High prevalence of BRAF mutations in TC: genetic evidence for constitutive activation of the RET(RAS/RAF) signaling pathway in papillary thyroid carcinoma. *Cancer Res.* 2003;63:1454-7.
- King A, Selak MA, Gottlieb E. Succinate dehydrogenase and fumarate hydratase: linking mitochondrial dysfunction and cancer. *Oncogene.* 2006;25(34):4675-82.
- King AD, Yeung DK, Ahuja AT, Tse GM, Chan AB, et al.,. In vivo ¹H MR spectroscopy of thyroid carcinoma. *Eur J Radiol.* 2005;54:112-7.
- Klupczyńska A, Dereziński P, Kokot ZJ. Metabolomics in medical sciences – trends, challenges and perspectives. *Acta Pol Pharm.* 2015;72:629-41.

- Koek MM, Muilwijk B, van der Werf MJ, Hankemeier T. Microbial metabolomics with gas chromatography/mass spectrometry. *Anal Chem.* 2006;78, 1272–1281.
- Krause K, Jessnitzer B, Fuhrer D. Proteomics in thyroid tumor research. *J Clin Endocrinol Metab.* 2009;94:2717-24
- Kroemer G, Pouyssegur J. Tumor Cell Metabolism: Cancer’s Achilles’ Heel. *Cancer Cell.* 2008;13:472-82
- Kumari S, Badana AK , Murali Mohan G, Shailender G, Malla R. Reactive Oxygen Species: A Key Constituent in Cancer Survival. *Biomark Insights.* 2018;13: 1177271918755391
- Landa I, Ganly I, Chan TA, Mitsutake N, Matsuse M, et al.. Frequent somatic TERT promoter mutations in thyroid cancer: higher prevalence in advanced forms of the disease. *J. Clin. Endocrinol. Metab.* 2013;98:E1562–66
- Lapidot T, Sirard C, Vormoor J, Murdoch B, Hoang T, et al.,. A cell initiating human acute myeloid leukaemia after transplantation into SCID mice. *Nature.* 1994 Feb 1;367:645-8.
- Lee JY, Lee I, Chang WJ, Ahn SM, Lim SH, et al. MCT4 as a potential therapeutic target for metastatic gastric cancer with peritoneal carcinomatosis. *Oncotarget* 2016;7:43492-43503
- Lee YS and Wurster RD. Potentiation of anti-proliferative effect of nitroprusside by ascorbate in human brain tumor cells. *Cancer Lett* 1994;78: 19-23.
- Li C, Heidt DG, Dalerba P, Burant CF, Zhang L, Adsay V, Wicha M, Clarke MF, Simeone DM. Identification of pancreatic cancer stem cells. *Cancer Res.* 2007 Feb 1;67:1030-7
- Li C, Zhang G, Zhao L, Ma Z, Chen H. Metabolic reprogramming in cancer cells: glycolysis, glutaminolysis, and Bcl-2 proteins as novel therapeutic targets for cancer. *World J Surg Oncol.* 2016;14:15.
- Li XF, Chen C, Xiang DM, Qu L, Sun W, et al. Chronic inflammation-elicited liver progenitor cell conversion to liver cancer stem cell with clinical significance. *Hepatology.* 2017;66:1934-1951.

- Liao J, Qian F, Tchabo N, Mhawech-Fauceglia P, Beck A et al. Ovarian cancer spheroid cells with stem cell-like properties contribute to tumor generation, metastasis and chemotherapy resistance through hypoxia-resistant metabolism. *PLoS One*. 2014;9:e84941.
- Liesenfeld DB, Habermann N, Owen RW, Scalbert A, Ulrich CM. Review of Mass Spectrometry-Based Metabolomics in Cancer Research. *Cancer Epidemiol Biomarkers Prev*. 2013;22:2182-201
- Liggi S, Hinz C, Hall Z, Santoru ML, Poddighe S, Fjeldsted J, Atzori L, Griffin. KniMet: a pipeline for the processing of chromatography-mass spectrometry metabolomics data. *Metabolomics*. 2018;14:52.
- Liou GY, Storz P. Reactive oxygen species in cancer. *Free Radic Res*. 2010;44:479-96.
- Liu B, Chen Y, St Clair DK. ROS and p53: versatile partnership. *Free Radic. Biol. Med.*2008;44:1529–1535
- Liu X, Bishop J, Shan Y, Pai S, Liu D et al. Highly prevalent TERT promoter mutations in aggressive thyroid cancers. *Endocr Relat Cancer*. 2013;20:603-610
- Liu Y, Hyde AS, Simpson MA, Barycki JJ. Barycky JJ. “Emerging regulatory paradigms in glutathione metabolism. *Adv Cancer Res*. 2014;122:69-101.
- Liu Y, Zuckier LS, Ghesani NV. Dominant uptake of fatty acid over glucose by prostate cells: a potential new diagnostic and therapeutic approach. *Anticancer Res*. 2010;30:369-74.
- Lo M, Wang YZ, Gout PW. The x(c)- cystine/glutamate antiporter: a potential target for therapy of cancer and other diseases. *J Cell Physiol*. 2008;215:593-602
- Locasale JW and Cantley LC. Altered metabolism in cancer. *BMC Biol*. 2010 Jun 25;8:88.
- Locasale JW, Cantley LC, Vander Heiden MG. Cancer’s insatiable appetite. *Nat Biotechnol* 2009;27:916-7.
- Locasale JW. Serine, glycine and one-carbon units: cancer metabolism in full circle. *Nat Rev Cancer*. 2013;13:572-83

- Lubitz CC, Sosa JA. The changing landscape of papillary thyroid cancer: Epidemiology, management, and the implications for patients. *Cancer*. 2016 Dec 15;122:3754-3759.
- Lucarelli G, Galleggiante V, Rutigliano M, Sanguedolce F, Cagiano S, Bufo P, Lastilla G, Maiorano E, Ribatti D, Giglio A, Serino G, Vavallo A, Bettocchi C, Selvaggi FP, Battaglia M, Ditonno P. Metabolomic profile of glycolysis and the pentose phosphate pathway identifies the central role of glucose-6-phosphate dehydrogenase in clear cell-renal cell carcinoma. *Oncotarget*. 2015;6:13371-86.
- Luengo A, Gui DY, Vander Heiden MG. Targeting Metabolism for Cancer Therapy. *Cell Chem Biol*. 2017;24:1161-1180
- Lunt SY, Vander Heiden MG. Aerobic glycolysis: meeting the metabolic requirements of cell proliferation. *Annu Rev Cell Dev Biol*. 2011;27:441-64
- Luo X, Cheng C, Tan Z, Li N, Tang M, Yang L, Cao Y7. Emerging roles of lipid metabolism in cancer metastasis. *Mol Cancer*. 2017;16 :76.
- Maddocks OD, Vousden KH. Metabolic Regulation by p53. *J Mol Med*.2011;89:237-45
- Malaguarnera R, Vella V, Vigneri R, Frasca F. p53 family proteins in thyroid cancer. *Endocr Relat Cancer*. 2007;14:43-60.
- Mani SA, Guo W, Liao MJ, Eaton EN, Ayyanan A, et al,. The epithelial–mesenchymal transition generates cells with properties of stem cells. *Cell*, 2008;133,704-715
- Manzella L, Stella S, Pennisi MS, Tirrò E, Massimino M, et al. New Insights in Thyroid Cancer and p53 Family Proteins. *Int J Mol Sci*. 2017; 18: 1325.
- Maramag C, Menon M, Balaji KC, Reddy PG and Laxmanan S. Effect of vitamin C on prostate cancer cells in vitro: effect on cell number, viability, and DNA synthesis. *Prostate* 1997;32: 188-195.

- Maric I, Viaggi S, Caria P, Frau DV, Degan P, Vanni R. Centrosomal and mitotic abnormalities in cell lines derived from papillary thyroid cancer harboring specific gene alterations. *Mol Cytogenet.* 2011;4:26.
- Marín-Hernández A, Gallardo-Pérez JC, Ralph SJ, Rodríguez-Enríquez S, Moreno-Sánchez R. HIF-1alpha modulates energy metabolism in cancer cells by inducing over-expression of specific glycolytic isoforms. *Mini Rev Med Chem.* 2009;9:1084-101.
- Meireles AM, Preto A, Rocha AS, Rebocho AS, Mximo V, et al. Molecular and genotypic characterization of human thyroid follicular cell carcinoma-derived cell lines. *Thyroid.* 2007;17:705-715.
- Menendez JA, Lupu R. Fatty acid synthase and the lipogenic phenotype in cancer pathogenesis. *Nat Rev Cancer.* 2007;7:763-77.
- Menon M, Maramag C, Malhotra RK and Seethalakshmi L. Effect of vitamin C on androgen independent prostate cancer cells (PC3 and Mat-Ly-Lu) in vitro: involvement of reactive oxygen species-effect on cell number, viability and DNA synthesis. *Cancer Biochem Biophys* 1998;16: 17-30.
- Miccoli P, Torregrossa L, Shintu L, Magalhaes A, Chandran J et al. Metabolomics approach to thyroid nodules: a high-resolution magic-angle spinning nuclear magnetic resonance-based study. *Surgery,* 2012;152:1118-24
- Migita T, Narita T, Nomura K, Miyagi E, Inazuka F, Matsuura M, Ushijima M, Mashima T, Seimiya H, Satoh Y, Okumura S, Nakagawa K, Ishikawa Y. ATP citrate lyase: activation and therapeutic implications in non-small cell lung cancer. *Cancer Res.* 2008;68:8547-54.
- Mirshahidi S, Simental A, Lee SC, De Andrare Filho PA, Peterson NE et al.,. Subpopulations of cancer stem cells found in papillary thyroid carcinoma. *Exp Cell Res.* 2018;362:515-524

- Morani F, Phadngam S, Follo C, Titone R, Thongrakard V, et al., PTEN deficiency and mutant p53 confer glucose-addiction to thyroid cancer cells: Impact of glucose depletion on cell proliferation, cell survival, autophagy and cell migration. *Genes Cancer*, 2014 Jul;5:226-39.
- Mosmann T. Rapid colorimetric assay for cellular growth and survival: application to proliferation and cytotoxicity assays. *J Immunol Methods*. 1983;65:55-63.
- Murphy MP. How mitochondria produce reactive oxygen species. *Biochem J*. 2009;417:1-13.
- Murphy MP. Mitochondrial thiols in antioxidant protection and redox signaling: Distinct roles for glutathionylation and other thiol modifications. *Antioxid Redox Signal*. 2012;16:476-95.
- Nagarajah J, Ho AL, Tuttle RM, Webwe WA, Grewal RK. Correlation of BRAFV600E mutation and glucose metabolism in thyroid cancer patients: an ¹⁸F-FDG PET study. *J Nucl Med* 2015; 56: 662–667
- Nahm J. H., Kim H. M., Koo J. S. Glycolysis-related protein expression in thyroid cancer. *Tumor Biology*. 2017;39: 1010428317695922
- Nahm JH, Kim HM, Koo JS. “Glycolysis-related protein expression in thyroid cancer. *Tumour Biol*. 2017;39:1010428317695922.
- Nakajima EC, Van Houten B. Metabolic symbiosis in cancer: refocusing the Warburg lens. *Mol Carcinog*. 2013 May;52:329-37
- Nathan C, Ding A. SnapShot: Reactive Oxygen Intermediates (ROI). *Cell*. 2010;140(6):951-951.
- Nicholson JK, Lindon JC, Holmes E. 'Metabonomics': understanding the metabolic responses of living systems to pathophysiological stimuli via multivariate statistical analysis of biological NMR spectroscopic data. *Xenobiotica*. 1999; 29:1181-9
- Nicholson JK, Lindon JC. Systems biology: metabonomics. *Nature*. 2008; 455:1054-6
- Nikiforov YE and Nikiforova MN.. Molecular genetics and diagnosis of thyroid cancer. *Nat. Rev.Endocrinol* 2011, 30;7:569-80.

- O'Brien CA, Pollett A, Gallinger S, Dick JE. A human colon cancer cell capable of initiating tumour growth in immunodeficient mice. *Nature*. 2007; 445:106–10
- O'Brien ML, Tew KD. Glutathione and related enzymes in multidrug resistance. *Eur J Cancer*. 1996; 32A:967-78
- Omabe M, Ezeani M, Omabe KN. Lipid metabolism and cancer progression: The missing target in metastatic cancer treatment. *Journal of applied biomedicine*. 2015; 13:47-59.
- Owen OE, Kalhan SC, Hanson RW. The key role of anaplerosis and cataplerosis for citric acid cycle function. *J. Biol. Chem*. 2002;27:30409–30412
- Palorini R, Votta G, Balestrieri C, Monestiroli A, Olivieri S, et al. Energy metabolism characterization of a novel cancer stem cell-like line 3AB-OS. *J Cell Biochem*. 2014;115:368-79
- Panieri E, Santoro MM. ROS homeostasis and metabolism: a dangerous liason in cancer cells. *Cell Death Dis*. 2016; 7: e2253
- Papke B, Der CJ. Drugging RAS: Know the enemy. *Science* 2017;355:1158–63
- Park S, Ahn S, Shin Y, Yang Y, Yeom CH. Vitamin C in Cancer: A Metabolomics Perspective. *Front Physiol*. 2018; 9:762
- Park S, Han SS, Park CH, Hahm ER, Lee SJ, et al. L-Ascorbic acid induces apoptosis in acute myeloid leukemia cells via hydrogen peroxide-mediated mechanisms. *Int. J. Biochem. Cell Biol*. 2004;36:2180–2195
- Park S. The Effects of High Concentrations of Vitamin C on Cancer Cells. *Nutrients* 2013;5:3496-3505
- Pastò A, Bellio C, Pilotto G, Ciminale V, Silic-Benussi M, et al. Cancer stem cells from epithelial ovarian cancer patients privilege oxidative phosphorylation, and resist glucose deprivation. *Oncotarget* 2014;5:4305–4319
- Patra KC, Hay N. The pentose phosphate pathway and cancer. *Trends Biochem Sci*. 2014; 39: 347–354.

- Pavlides S, Whitaker-Menezes D, Castello-Cros R, Flomenberg N, Witkiewicz AK, Frank PG, Casimiro MC, Wang C, Fortina P, Addya S, Pestell RG, Martinez-Outschoorn UE, Sotgia F, Lisanti MP. The reverse Warburg effect: aerobic glycolysis in cancer associated fibroblasts and the tumor stroma. *Cell Cycle*. 2009;8:3984-4001.
- Pavlova NN and Thompson CB. The emerging hallmarks of cancer metabolism. *Cell Metab*. 2016; 23: 27–47
- Peiris-Pegès M, Martinez-Outschoorn U, Pestell RG, Sotgia F, Lisanti MP. Cancer stem cell metabolism. *Breast Cancer Res*.2016;18:55
- Perez-Gomez C, Campos-Sandoval JA, Alonso FJ, Segura JA, Manzanares E, Ruiz-Sanchez P, González ME, Márquez J, Matés JM. Co-expression of glutaminase K and L isoenzymes in human tumour cells. *Biochem J*. 2005;386:535-42.
- Petros JA, Baumann AK, Ruiz-Pesini E, Amin MB, Sun CQ, et al. mtDNA mutations increase tumorigenicity in prostate cancer. *Proc Natl Acad Sci U S A*. 2005 Jan;102:719-24
- Plaks V, Kong N, Werb Z. The Cancer Stem Cell Niche: How Essential Is the Niche in Regulating Stemness of Tumor Cells?. *Cell Stem Cell*. 2015;16:225-38.
- Plas DR and Thompson CB. Akt-dependent transformation: there is more to growth than just surviving. *Oncogene*. 2005;24:7435-42.
- Pouyssegur J, Dayan F, Mazure NM. Hypoxia signalling in cancer and approaches to enforce tumour regression. *Nature*. 2006;441:437-43.
- Prigione A, Fauler B, Lurz R, Lehrach H, Adjaye J. The senescence-related mitochondrial/oxidative stress pathway is repressed in human induced pluripotent stem cells. *Stem Cells*. 2010; 28:721-33
- Pylayeva-Gupta Y, Grabocka E, Bar-Sagi D. RAS oncogenes: weaving a tumorigenic web. *Nat. Rev. Cancer* 2011;11:761–74

- Quiros RM, Ding HG, Gattuso P, Prinz RA, Xu X. Evidence that one subset of anaplastic thyroid carcinomas are derived from papillary carcinomas due to BRAF and p53 mutations. *Cancer* 2005; 103; 2261–2268
- Ramautar R, Somsen GW, de Jong GJ. CE-MS for metabolomics: developments and applications in the period 2010-2012. *Electrophoresis*. 2013; 34:86-98
- Rankin EB, Giaccia AJ. The role of hypoxia-inducible factors in tumorigenesis. *Cell Death Differ*. 2008;15:678-85.
- Rempel A, Mathupala SP, Griffin CA, Hawkins AL, Pedersen PL. Glucose catabolism in cancer cells: amplification of the gene encoding type II hexokinase. *Cancer Res*. 1996;56:2468-74
- Renshaw AA. Accuracy of thyroid fine-needle aspiration using receiver operator characteristic curves. *Am J Clin Pathol* 2001; 116:477–482
- Rhee SG, Woo HA, Kil IS, Bae SH. Peroxiredoxin functions as a peroxidase and a regulator and sensor of local peroxides. *J Biol Chem*. 2012;287:4403-10.
- Roberts LD, Souza AL, Gerszten RE, Clish CB. Targeted metabolomics. *Curr Protoc Mol Biol*. 2012 ;Chapter 30:Unit 30.2.1-24
- Roomi M W, House D, Eckert-Maksic M, Maksic Z B, Tsao CS. Growth suppression of malignant leukemia cell line in vitro by ascorbic acid (vitamin C) and its derivatives. *Cancer Lett*.1998;122, 93–99.
- Rumsey SC, Kwon O, Xu GW, Burant CF, Simpson I, Levine M. Glucose transporter isoforms GLUT1 and GLUT3 transport dehydroascorbic acid. *J Biol Chem*. 1997;272:18982-9
- Ryoo I, Kwon H, Kim SC, Jung SC, Yeom JA et al., Metabolomic analysis of percutaneous fine-needle aspiration specimens of thyroid nodules: Potential application for the preoperative diagnosis of thyroid cancer. *Sci Rep*. 2016;6:30075
- Sakagami H, Satoh K, Hakeda Y, Kumegawa M. Apoptosis-inducing activity of vitamin and vitamin K. *Cell Molec Biol*. 2000;46:129–43

- Salem AF, Whitaker-Menezes D, Howell A, Sotgia F, Lisanti M. Mitochondrial biogenesis in epithelial cancer cells promotes breast cancer tumor growth and confers autophagy resistance. *Cell Cycle*. 2012; 11: 4174–4180.
- Samudio I, Harmancey R, Fiegl M, Kantarjian H, Konopleva M, et al. Pharmacologic inhibition of fatty acid oxidation sensitizes human leukemia cells to apoptosis induction. *J Clin Invest*. 2010;120, 142-56
- Sancho P, Barneda D, Heeschen C. Hallmarks of cancer stem cell metabolism. *Br J Cancer*.2016;114:1305-12
- Savini I, Rossi A, Pierro C, Avigliano L, Catani MV. SVCT1 and SVCT2: key proteins for vitamin C uptake. *Amino Acids*. 2008;34:347-55
- Schafer ZT, Grassian AR, Song L, Jiang Z, Gerhart-Hines Z, Irie HY, Gao S, Puigserver P, Brugge JS. Antioxidant and oncogene rescue of metabolic defects caused by loss of matrix attachment. *Nature*. 2009;461:109-13.
- Sciacovelli M, Gaude E, Hilvo M, Frezza C. The metabolic alterations of cancer cells. *Methods Enzymol*. 2014;542:1-23.
- Selak MA, Armour SM, MacKenzie ED, Boulahbel H, Watson DG. Succinate links TCA cycle dysfunction to oncogenesis by inhibiting HIF- α prolyl hydroxylase. *Cancer Cell*. 2005;7:77-85.
- Semenza GL. HIF-1: upstream and downstream of cancer metabolism. *Curr Opin Genet Dev*. 2010;20:51-6
- Shukla S, Khan S, Sinha S, Meeran SM. Lung cancer stem cells: an epigenetic perspective. *Curr Cancer Drug Targets*. 2018;18:16–31
- Simons AL, Ahmad IM, Mattson DM, Dornfeld KJ, Spitz DR. 2-Deoxy-D-glucose combined with cisplatin enhances cytotoxicity via metabolic oxidative stress in human head and neck cancer cells. *Cancer Res*. 2007;67:3364-3370.

- Singh SK, Hawkins C, Clarke ID, Squire JA, Bayani J, et al., Identification of human brain tumour initiating cells. *Nature*. 2004;432:396-401.
- Skvortzov DA, Rubzova MP, Zvereva ME, Kiselev FL, Donzova OA. The regulation of telomerase in oncogenesis. *Acta Naturae*. 2009;1: 51–67.
- Smalley M, Ashworth A. Stem cells and breast cancer: a field in transit. *Nat.Rev.Cancer*,2003;832-844
- Smith B, Schafer XL, Ambeskovic A, Spencer CM, Land H, Munger J. Addiction to Coupling of the Warburg Effect with Glutamine Catabolism in Cancer Cells. *Cell Rep*. 2016; 17: 821–836.
- Snyder NW, Mesaros C, Blair IA. Translational metabolomics in cancer research. *Biomark Med*. 2015;9:821-34.
- Son J, Lyssiotis CA, Ying H, Wang X, Hua S, Ligorio M, Perera RM, Ferrone CR, Mullarky E, Shyh-Chang N, Kang Y, Fleming JB, Bardeesy N, Asara JM, Haigis MC, DePinho RA, Cantley LC, Kimmelman AC. Glutamine supports pancreatic cancer growth through a KRAS-regulated metabolic pathway. *Nature*. 2013; 496:101–105.
- Sporn MB, Liby KT. NRF2 and cancer: the good, the bad and the importance of context. *Nat Rev Cancer*. 2012;12:564-71.
- Spratlin JL, Serkova NJ, Eckhardt SG. Clinical applications of metabolomics in oncology: a review. *Clin. Cancer Res*.2009;15:431-40
- Su Z, Yang Z, Xu Y, Chen Y, Yu Q. Apoptosis, autophagy, necroptosis, and cancer metastasis. *Mol Cancer*. 2015; 14: 48.
- Sun WY, Kim HM, Jung WH, Koo JS. Expression of serine/glycine metabolism-related proteins is different according to the thyroid cancer subtype. *J Transl Med*. 2016; 14: 168.
- Suzuki S, Tanaka T, Poyurovsky MV, Nagano H, Mayama T, Ohkubo S, Lokshin M, Hosokawa H, Nakayama T, Suzuki Y, Sugano S, Sato E, Nagao T, Yokote K, Tatsuno I, Prives C. Phosphate-

activated glutaminase (GLS2), a p53-inducible regulator of glutamine metabolism and reactive oxygen species. *Proc Natl Acad Sci USA*. 2010;107:7461-6.

- Szeliga M, Matyja E, Obara M, Grajkowska W, Czernicki T, Albrecht J. Relative expression of mRNAs coding for glutaminase isoforms in CNS tissues and CNS tumors. *Neurochem Res*. 2008;33:808-13.
- Szeliga M, Sidoryk M, Matyja E, Kowalczyk P, Albrecht J. Lack of expression of the liver-type glutaminase (LGA) mRNA in human malignant gliomas. *Neurosci Lett*. 2005;374:171-3.
- Takahashi K, Yamanaka S. Induction of pluripotent stem cells from mouse embryonic and adult fibroblast cultures by defined factors. *Cell*, 2006;126, 663-676
- Takemura Y, Satoh M, Satoh K, Hamada H, Sekido Y, Kubota S. High dose of ascorbic acid induces cell death in mesothelioma cells. *Biochem. Biophys. Res. Commun.* 2010;394, 249–253
- Tallini G, Tuttle RM, Ghossein RA. The history of the follicular variant of papillary thyroid carcinoma. *J. Clin. Endocrinol. Metab.* 2017; 102:15–22
- Teicher BA, Linehan WM, Helman LJ. Targeting Cancer Metabolism. *Clin Cancer Res*. 2012; 18: 5537–5545.
- Tian Y, Nie X, Xu S, Li Y, Huang T et al. Integrative metabolomics as potential method for diagnosis of thyroid malignancy. *Sci Rep* 2015;5:14869.
- Tomlinson IP, Alam NA, Rowan AJ, Barclay E, Jaeger EEM, et al. Germline mutations in FH predispose to dominantly inherited uterine fibroids, skin leiomyomata and papillary renal cell cancer. *Nat. Genetics* 2002;30:406–410.
- Torregrossa L, Shintu L, Nambiath Chandran J, Tintaru A, Ugolini C, et al., Toward the reliable diagnosis of indeterminate thyroid lesions: a HRMAS NMR-based metabolomics case of study. *J Proteome Res*. 2012 ;11:3317-25.
- Tretter L, Patocs A, Chinopoulos C. Succinate, an intermediate in metabolism, signal transduction, ROS, hypoxia, and tumorigenesis. *Biochim. Biophys. Acta* 2016;1857:1086–1101

- Turner A, McGivan JD. Glutaminase isoform expression in cell lines derived from human colorectal adenomas and carcinomas. *Biochem J.* 2003;370:403-8.
- Uetaki M, Tabata S, Nakasuka F, Soga T, Tomita M. Metabolomic alterations in human cancer cells by vitamin C-induced oxidative stress, *Sci. Rep.*2015;5:13896.
- Uetaki M, Tabata S, Nakasuka F, Soga T, Tomita M. Metabolomic alterations in human cancer cells by vitamin C-induced oxidative stress. *Sci Rep.* 2015; 5:13896
- Valent P, Bonnet D, Wohrer S, Andreeff M, Copland M, Chomienne C, Eaves C. Heterogeneity of neoplastic stem cells: theoretical, functional, and clinical implications. *Cancer Res.* 2013;73:1037–45
- Valko M, Rhodes CJ, Moncol J, Izakovic M, Mazur M. Free radicals, metals and antioxidants in oxidative stress-induced cancer. *Chem Biol Interact.* 2006;160:1-40.
- Vander Heiden MG, Cantley LC, Thompson CB. Understanding the Warburg Effect: The Metabolic Requirements of Cell Proliferation. *Science.* 2009;324:1029-33
- Vegran F, Boidot R, Michiels C, Sonveaux P, Feron O. Lactate influx through the endothelial cell monocarboxylate transporter MCT1 supports an NF- κ B/IL-8 pathway that drives tumor angiogenesis. *Cancer Res.* 2011 Apr 1;71:2550-60.
- Vera JC, Rivas CI, Velasquez FV, Zhang RH, Concha II, Golde DW. Resolution of the facilitated transport of dehydroascorbic acid from its intracellular accumulation as ascorbic acid. *J Biol Chem.* 1995; 270:23706–23712.
- Vinagre J, Almeida A, Populo H, Batista R, Lyra J, et al. Frequency of TERT promoter mutations in human cancers. *Nat. Commun* 2013;4:2185. doi: 10.1038/ncomms3185.
- Vinogradov S, Wei X. Cancer stem cells and drug resistance: The potential of nanomedicine. *Nanomedicine* 2012;7:597–615
- Vissers CMM, Das AB. Potential Mechanisms of Action for Vitamin C in Cancer: Reviewing the Evidence. *Front Physiol.* 2018;9: 809

- Wagle A, Jivraj S, Garlock GL, Stapleton SR. Insulin regulation of glucose-6-phosphate dehydrogenase gene expression is rapamycin-sensitive and requires phosphatidylinositol 3-kinase. *J Biol Chem.* 1998;273:14968-74.
- Walenta S, Voelxen NF, Mueller-Klieser W. Lactate-An Integrative Mirror of Cancer Metabolism. *Recent Results Cancer Res.* 2016; 207:23-37
- Wang A, Chen L, Li C, Zhu Y. Heterogeneity in cancer stem cells. *Cancer Lett.* 2015;357:63-68
- Wang HQ, Altomare DA, Skele KL, Poulikakos PI, Kuhajda FP, et al. Positive feedback regulation between AKT activation and fatty acid synthase expression in ovarian carcinoma cells. *Oncogene.* 2005;24:3574-82.
- Wang W, Yi M, Chen S, Li J, Zhang H, et al.,. NOR1 suppresses Cancer stem-like cells properties of tumor cells via the inhibition of the AKT-GSK-3 β -Wnt/ β -catenin-ALDH1A1 signal circuit. *J Cell Physiol.* 2017;232:2829–40
- Warburg O, Wind F, Negelein E. The Metabolism Of Tumors In The Body. *J Gen Physiol.* 1927 Mar 7;8:519-30.
- Warburg O. On the origin of cancer cells. *Science.* 1956; 123:309–314
- Ward PS, Thompson CB. Metabolic Reprogramming: A Cancer Hallmark Even Warburg Did Not Anticipate. *Cancer Cell* 2012; 21: 297–308
- Weir B, Zhao X, Meyerson M. Somatic alterations in the human cancer genome. *Cancer Cell* 2004;6:433-8.
- Welch RW, Wang Y, Crossman AJ, Park JB, Kirk KL, Levine M. Accumulation of vitamin C (ascorbate) and its oxidized metabolite dehydroascorbic acid occurs by separate mechanisms. *J Biol Chem.* 1995; 270:12584–12592.
- Wise RW, Thompson CB. Glutamine addiction: a new therapeutic target in cancer. *Trends Biochem Sci.* 2010; 35: 427–433.

- Wojakowska A, Chekan M, Widlak P, Pietrowska M. Application of Metabolomics in Thyroid Cancer Research. *Int Journ Endocrinology*. 2015;258763.
- Xing M, Haugen BR, Schlumberger M. Progress in molecular-based management of differentiated thyroid cancer. *Lancet*.2013; 381:1058–1069
- Xing M. BRAF mutation in thyroid cancer. *Endocr Relat Cancer*.2005;12: 245–62
- Xing M. Molecular pathogenesis and mechanisms of thyroid cancer. *Nat Rev Cancer*. 2013; 13: 184–199.
- Xing M. Prognostic utility of BRAF mutation in papillary thyroid cancer. *Mol.Cell Endocrinol*.2010;321,86-93
- Xu Y, Zheng X, Qiu Y, Jia W, Wang J, Yin S. Distinct Metabolomic Profiles of Papillary Thyroid Carcinoma and Benign Thyroid Adenoma. *J Proteome Res*. 2015;14:3315-21
- Yanagisawa-Shiota F, Sakagami H, Kuribayashi N, Lida M and Sakagami T: Endonuclease activity and induction of DNA fragmentation in human myelogenous leukemic cell lines. *Anticancer Res* 1995;15:259-265.
- Yang L, Venneti S, Nagrath D. Glutaminolysis: A Hallmark of Cancer Metabolism. *Annu Rev Biomed Eng*. 2017;19:163-194.
- Yi M, Li J, Chen S, Cai J, Ban Y, et al,. Emerging role of lipid metabolism alterations in Cancer stem cells. *J Exp Clin Cancer Res*. 2018;37:118.
- Yi M, Yang J, Li W, Li X, Xiong W, et al,. The NOR1/ OSCP1 proteins in cancer: from epigenetic silencing to functional characterization of a novel tumor suppressor. *J Cancer*. 2017;8:626–35
- Ying H, Kimmelman AC, Lyssiotis CA, Hua S, Chu GC, Fletcher-Sananikone E, et al. Oncogenic Kras maintains pancreatic tumors through regulation of anabolic glucose metabolism. *Cell*. 2012;149:656-70.
- Ying W. NAD⁺/NADH and NADP⁺/NADPH in cellular functions and cell death: regulation and biological consequences. *Antioxid Redox Signal*. 2008;10:179-206.

- Younes M, Lechago LV, Somoano JR, Mosharaf M, Lechago J. Wide expression of the human erythrocyte glucose transporter Glut1 in human cancers. *Cancer Res.* 1996;56:1164–7
- Yu D, Shi X, Meng G, Chen J, Yan C, et al. Kidney-type glutaminase (GLS1) is a biomarker for pathologic diagnosis and prognosis of hepatocellular carcinoma. *Oncotarget.* 2015; 6:7619-31
- Yun J, Mullarky E, Lu C, Bosch KN, Kavalier A, et al. Vitamin C selectively kills KRAS and BRAF mutant colorectal cancer cells by targeting GAPDH. *Science.* 2015 Dec 11;350:1391-6
- Yun J, Mullarky E, Lu C, Bosch KN, Kavalier A, et al. Vitamin C selectively kills KRAS and BRAF mutant colorectal cancer cells by targeting GAPDH. *Science* 2015;350:1391-1396
- Zaidi N, Swinnen JV, Smans K. ATP-citrate lyase: a key player in cancer metabolism. *Cancer Res.* 2012;72:3709–3714
- Zhang S, Balch C, Chan MW, Lai HC, Matei D, et al. Identification and characterization of ovarian cancer-initiating cells from primary human tumors. *Cancer Res.* 2008;68:4311–20
- Zhou W, Choi M, Margineantu D, Margaretha L, Hesson J, et al. HIF1alpha induced switch from bivalent to exclusively glycolytic metabolism during ESC-to-EpiSC/hESC transition. *EMBO J.* 2012; 31: 2103–2116.
- Zou C, Wang Y, Shen Z. 2-NBDG as a fluorescent indicator for direct glucose uptake measurement. *J Biochem Biophys Methods.* 2005;64:207-15

Appendix: Publications and Presentations

Publications

- Caria P, Tronci L, Dettori T, Murgia F, Santoru ML, et al. **Metabolomic Alterations in Thyrospheres and Adherent Parental Cells in Papillary Thyroid Carcinoma Cell Lines: A Pilot Study**. Int J Mol Sci. 2018;19(10).
- Murgia F, Iuculano A, Peddes C, Santoru ML, Tronci L, Deiana M, Atzori L, Monni G. **Metabolic fingerprinting of chorionic villi samples in normal pregnancy and chromosomal disorders**. Placenta Journal. 2018 (in press).
- Iuculano A, Murgia F, Peddes C, Santoru ML, Tronci L, Deiana M, Balsamo A, Euser A, Atzori L, Monni G. **Metaboli characterization of amniotic fluids of fetusis with large nuchal translucency**. Journal of Perinatal Medicina. 2018 (in press).
- Murgia F, Angioni S, Pirarba S, Noto A, Santoru ML, Tronci L, Fanos V, Atzori L, Congiu F. **Metabolomic profile of endometriosis patients: a case control study**. Reproductive Sciences. 2018 (in press)

Conference presentations

- Laura Tronci, Marta Kowalik, Cristina Piras, Sonia Liggi, Andrea Perra, Amedeo Columbano, Luigi Atzori. **Metabolomic Profiles In Different Models Of Hepatocytes Proliferation: Partial Hepatectomy And Mitogen-Induced Hyperplasia**. 12th Annual Conference Of The Metabolomics Society, June 27-30 2016, Dublin (Oral communication).
- Laura Tronci, Marta Kowalik, Cristina Piras, Sonia Liggi, Andrea Perra, Amedeo Columbano, Luigi Atzori. **Comprehensive Metabolomic Analysis Of Hepatocytes Proliferation After**

Partial Hepatectomy And Lead nitrate Administration. Scientific Dianzani School Meeting, 8-9 July 2016, Siena, Italy. (Oral communication).

- Laura Tronci, Paola Caria, Monica Pibiri, Sonia Liggi, Daniela Frau, James West, Monica Deiana, Julian Griffin, Paola Vanni, Luigi Atzori. **Correlation between different genotypes, metabolic alterations and redox state in different thyroid cancer cell lines pre and post Vitamin C treatment.** Scientific Dianzani School Meeting 17-18 November 2017, Novara, Italy. (Oral communication)
- Laura Tronci, Marta Kowalik, Cristina Piras, Sonia Liggi, Andrea Perra, Amedeo Columbano, Luigi Atzori. **Comprehensive Metabolomic Analysis Of Hepatocytes Proliferation After Partial Hepatectomy And Lead Nitrate Administration.** International Scientific School “How to bridge metabolomics and genomics”. 12-16 September, 2016. Pula, Sardinia, Italy. (Poster presentation).
- Laura Tronci, Paola Caria, Cristina Piras, Monica Deiana, Roberta Vanni, Luigi Atzori. **Correlation between Different Genotypes, Metabolic Alterations and Redox State in Different Thyroid Cancer Cell Lines.** Oxidative Stress and Disease. Gordon Research Conference. 19-24 Marzo, 2017. Lucca, Italy. (Poster presentation)